

**DEVELOPMENT OF NOVEL CHITOSAN  
NANOCOMPOSITES AS A CONTROLLED DRUG  
RELEASE SYSTEM FOR *HELICOBACTER PYLORI*  
TREATMENT**

**A Thesis Submitted to  
The Graduate School of Engineering and Sciences of  
İzmir Institute of Technology  
in Partial Fulfillment of the Requirements for the Degree of**

**DOCTOR OF PHILOSOPHY**

**in Bioengineering**

**by  
Suna Seda GÜNEŞ**

**January, 2016  
İZMİR**

We approve the thesis of **Suna Seda GÜNEŞ**

**Examining Committee Members:**

---

**Prof. Dr. Funda TIHMINLIOĞLU**

Department of Chemical Engineering, İzmir Institute of Technology

---

**Prof. Dr. Serdar ÖZÇELİK**

Department of Chemistry, İzmir Institute of Technology

---

**Assoc. Prof. Dr. Mehmet ATEŞ**

Institute of Health Sciences, Dokuz Eylül University

---

**Prof. Dr Volga BULMUŞ**

Department of Bioengineering, İzmir Institute of Technology

---

**Assist. Prof. Dr. Evren ATLIHAN GÜNDOĞDU**

Department of Pharmaceutical Technology, Radiopharmacy, Ege University

**15 January 2016**

---

**Prof. Dr. Funda TIHMINLIOĞLU**

Supervisor,  
Department of Chemical Engineering,  
İzmir Institute of Technology

---

**Prof. Dr. Özlem YILMAZ**

Co- Supervisor,  
Faculty of Medicine, Department of  
Medical Microbiology, Dokuz Eylül  
University

---

**Prof. Dr. Volga BULMUŞ**

Head of the Department of Biotechnology  
and Bioengineering

---

**Prof. Dr. Bilge KARAÇALI**

Dean of the Graduate School of  
Engineering and Sciences

## ACKNOWLEDGMENTS

Firstly, I would like to express my deep and sincere gratitude to my advisor Prof. Dr. Funda TIHMINLIOĞLU for her suggestions, guidance, encouragement and support throughout my Ph.D. study. I would like to thank to Prof. Dr. Özlem YILMAZ as my co-advisor for her support and contributions during my thesis. I also would like to thank to Assoc. Prof. Dr. Ali ÇAĞIR for his discussions and contributions.

I would like to express my appreciation to Dr. INÊS de Castro GONÇALVES de Almada Lobo from INEB (Instituto de Engenharia Biomédica) for providing MKN45 cell line. I also would like to thank to my lab-mates Dr. Ebru DEMİRAY GÜRBÜZ and Tuba BECERİKLİ for their friendship, help and discussions in accomplishing the antimicrobial tests. I am grateful to Assist. Prof. Dr. Duygu ALTIOK for her support and contributions. I would also thank to Assist. Prof. Dr. Evren ATLIHAN GÜNDOĞDU and Assist. Prof. Dr. Derya İLEM ÖZDEMİR for their kindly help and contributions in radiolabelling studies.

I would like to thank to the staff of Biotechnology and Bioengineering Research and Application Centre

I would like to thank to my co-workers, Sedef TAMBURACI, İpek ERDOĞAN, Çağla SAYILGAN, Gülşah KÜRKÇÜ, Serkan KANGAL, Esra AYDINLIOĞLU, Damla TAYKOZ, Aykut ZELÇAK for their support, help, patience and friendship. I also want to express special thanks to my family for their endless support, encouragement and patience during my education and dedicated my thesis to my lovely family.

## ABSTRACT

### DEVELOPMENT OF NOVEL CHITOSAN NANOCOMPOSITES AS A CONTROLLED DRUG RELEASE SYSTEM FOR *HELICOBACTER PYLORI* TREATMENT

*Helicobacter pylori* is one of the most common bacterial infection and responsible for gastroduodenal diseases in humans. Due to increasing failure rate of currently used antibiotic therapies, newer drugs and therapeutic approaches are needed. Therefore the use of encapsulated cinnamon bark oil is a promising approach for *H. pylori* eradication. The main objective of this dissertation was to develop a novel drug delivery system using chitosan and nanoclay containing cinnamon bark oil to be released in a controlled manner in gastrointestinal system for *H. pylori* eradication as an alternative or complementary to conventional antibiotic treatment.

Minimum inhibition concentration (MIC) value of cinnamon bark oil was determined. Cinnamon bark oil loaded chitosan nanocomposite microspheres were produced by spray drying. The prepared microspheres were characterized for particle size & morphology, encapsulation efficiency, surface charge, mucoadhesion, degradation, swelling and drug release. Antimicrobial activity of the microspheres against *H. pylori* were investigated. *In vitro* cell viability of fibroblast and gastric epithelial cells were evaluated. *In vitro* cellular uptake and binding studies of microspheres were investigated by using gastric epithelial cells.

MIC value of cinnamon bark oil was found as 8 µg/mL. Nanoclay incorporation decreased the biodegradation of nanocomposite microspheres and improved the release of cinnamon bark oil. Drug release mechanism was anomalous diffusion which refers to combination of diffusion and erosion controlled. The prepared microspheres showed strong mucoadhesive property. Oil released from prepared microspheres inhibited *H. pylori* growth. Although cinnamon oil showed cytotoxic effect above 31 µg/mL, the oil encapsulated chitosan microspheres did not show any cytotoxic effect on NIH3T3 and MKN45 cells. The prepared microspheres were able to get internalized into MKN45 cells and had great incorporation activity. The results of this study demonstrated that cinnamon bark oil loaded chitosan nanocomposites may serve as biocompatible and effective gastroretentive drug carrier for the treatment of *H. pylori* infection.

# ÖZET

## *HELICOBACTER PYLORI* TEDAVİSİNE YÖNELİK KONTROLLÜ İLAÇ SALIM SİSTEMİ OLARAK YENİLİKÇİ KİTOSAN NANOKOMPOZİTLERİN GELİŞTİRİLMESİ

*Helicobacter pylori* (*H. pylori*) enfeksiyonu, en yaygın bakteriyel enfeksiyonlardan biri olup insanlarda gastroduodenal rahatsızlıkların nedenidir. Mevcut antibiyotik tedavisinde tamamen bir eradikasyon sağlanamadığı için yeni ilaç ve tedavi yaklaşımlarına ihtiyaç vardır. Bu nedenle enkapsule edilmiş tarçın yağının kullanımı, *H. pylori* eradikasyonunda umut vaad etmektedir. Bu çalışmanın amacı, *H. pylori* eradikasyonu için geleneksel antibiyotik tedavilerine alternatif veya yardımcı olabilecek, gastrointestinal sistemde kontrollü salımını sağlayan tarçın yağı içeren kitosan nanokil temelli yenilikçi ilaç salım sistemlerinin geliştirilmesidir.

Tarçın yağının *H.pylori* için MİK değeri belirlenmiştir. Tarçın yağı yüklü kitosan nanokompozit mikroküreler püskürtmeli kurutma ile üretilmiştir. Hazırlanan mikroküreler, partikül boyutu, morfoloji, enkapsulasyon verimi, mukoadezyon, şişme, biyodegradasyon açısından karakterize edilmiş ve ilaç salım çalışmaları yürütülmüştür. Kürelerden salınan tarçın yağının *H.pylori* üzerine inhibisyon etkisi araştırılmıştır. Tarçın yağı ve kitosan nanokompozitlerin üzerinde *in vitro* sitotoksik etkileri araştırılmış ve kürelerin MKN45 hücreleri tarafından hücre sel alımları belirlenmiştir.

Tarçın yağının MİK değeri 8 µg/mL olarak belirlenmiştir. Nanokil katkısı, küre degradasyonunu azaltmış ve salım profilinde iyileştirmiştir. İlaç salım mekanizması, difüzyon ve erozyon kontrolünün kombinasyonu olan “anomalous” difüzyon olarak belirlenmiştir. Hazırlanan mikrokürelerin mukoadeziv olduğu saptanmıştır. Mikrokürelerden salınan tarçın yağının *H. pylori* üremesini inhibe etmektedir. Tarçın yağı 31 µg/mL konsantrasyonun üzerinde toksik etki gösterirken, yağ yüklü mikroküreler, NIH3T3 ve MKN45 hücreleri üzerinde herhangi bir toksik etki göstermemiştir. Kitosan mikrokürelerin, MKN45 hücreleri tarafından alındığı, yüksek bağlanma aktivitesi gösterdiği ve gastrointestinal sistem için biyouyumlu olduğu belirlenmiştir. Böylece tarçın yağı yüklü mikrokürelerin *H. pylori* enfeksiyonu tedavisinde kontrollü ilaç salım sistemi olarak potansiyel bir aday olduğu belirlenmiştir.

# TABLE OF CONTENTS

LIST OF FIGURES .....	ix
LIST OF TABLES.....	xii
CHAPTER 1. INTRODUCTION .....	1
CHAPTER 2. CONTROLLED DELIVERY SYSTEMS.....	4
2.1. General Aspects .....	4
2.1.1. Desirable Characteristics of Delivery Systems.....	5
2.1.2. Factors Affecting Release .....	6
2.2. Types of Drug Delivery Systems .....	8
2.3. Release Mechanisms and Mathematical Models .....	10
2.4. Gastroretentive Drug Delivery Systems .....	16
2.4.1. Chitosan in Drug Delivery System .....	19
2.5. Controlled Drug Delivery systems for Eradication of <i>H. pylori</i> .....	28
2.6. Nanocomposites in Drug Delivery.....	32
2.6.1. Structure and Properties .....	34
2.6.2. Pharmaceutical Applications.....	38
CHAPTER 3. MICROENCAPSULATION OF ESSENTIAL OILS FOR PHARMACEUTICAL APPLICATION.....	41
3.1. General Aspects .....	41
3.1.1. Advantages and Limitations of Encapsulation.....	43
3.2. Production Techniques.....	43
3.2.1. Spray Drying .....	44
3.2.2. Encapsulation by Supercritical Fluids.....	46
3.2.3. Ionotropic Gelation .....	47

3.2.4. Emulsification-Solvent Evaporation .....	47
3.2.5. Coacervation .....	48
3.3. Pharmaceutical Applications of Essential Oils .....	48
3.3.1. Encapsulated Essential Oils .....	52
3.3.2. Essential Oils for <i>H.pylori</i> Eradication Treatment.....	55
CHAPTER 4. MATERIALS AND METHODS .....	57
4.1. Materials .....	57
4.2. Methods.....	58
4.2.1. Determination of Minimum Inhibitory Concentration (MIC) of Cinnamon Bark Oil .....	58
4.2.2. Production of Chitosan Microspheres .....	64
4.2.3. Characterization of Chitosan Microspheres .....	68
4.2.4. <i>In vitro</i> Release .....	72
4.2.5. The Study of Released Cinnamon Bark oil on <i>H. pylori</i> .....	73
4.2.6. <i>In vitro</i> Cell Viability and Proliferation of Chitosan Microspheres and Cinnamon Bark Oil .....	75
4.2.7. <i>In Vitro</i> Cellular Uptake.....	77
4.2.8. <i>In Vitro</i> Cell Binding Studies .....	77
4.9. Statistical Analysis.....	79
CHAPTER 5. RESULTS AND DISCUSSIONS .....	80
5.1. Determination of Minimum Inhibitory Concentration (MIC) of Cinnamon Bark Oil .....	80
5.1.1. Minimum Inhibitory Concentration (MIC) of Clarithromycin .....	80
5.1.2. Minimum Inhibitory Concentration (MIC) of Cinnamon Bark Oil...	80
5.2. Effects of Spray Drying Parameters on Microsphere Characteristic ....	83
5.3. Characterization of Chitosan Microspheres.....	86
5.3.1. Particle Size and Morphology .....	86
5.3.2. Encapsulation Efficiency (EE) .....	90

5.3.3. Surface Charge .....	91
5.3.4. Nanocomposite Structure .....	95
5.3.5. Chemical Characterization .....	100
5.3.6. <i>In Vitro</i> Mucoadhesion.....	106
5.3.7. Swelling Degree .....	109
5.3.8. Biodegradation Study.....	111
5.4. <i>In Vitro</i> Release Study .....	113
5.5. The Effects of Released Cinnamon Bark oil on <i>H.pylori</i> .....	122
5.6. <i>In vitro</i> Cytotoxicity and Biocompatibility of Chitosan Microspheres and Cinnamon bark oil.....	124
5.7. <i>In vitro</i> Cell Viability and Interaction of MKN45 Cells with Chitosan Microspheres and Cinnamon bark oil .....	126
5.8. <i>In Vitro</i> Cellular Uptake.....	129
5.9. Radiolabeling and <i>In vitro</i> Cell Binding Study.....	132
5.9.1. Radiolabeling Studies.....	132
5.9.2. <i>In vitro</i> Cell Binding Study .....	133
 CHAPTER 6. CONCLUSIONS .....	 135
 REFERENCES .....	 139



## LIST OF FIGURES

<b><u>Figure</u></b>	<b><u>Page</u></b>
Figure 2. 1. External stimuli and responses .....	10
Figure 2. 2. Chemical structure of chitosan .....	20
Figure 2. 3. Interaction of chitosan based systems with mucus layer.....	22
Figure 2. 4. Chemical structure of genipin .....	26
Figure 2. 5. Chitosan-genipin crosslinking mechanism.....	27
Figure 2. 6. Schematic illustration of <i>H.pylori</i> infection and virulence factors .....	29
Figure 2. 7. Mucoadhesive delivery system for <i>H. pylori</i> eradication.....	32
Figure 2. 8. Scheme of the mechanism of barrier improvement by the addition of clay platelets .....	34
Figure 2. 9. Swelling and cation exchange of clays.....	35
Figure 2. 10. Sandwich structure of 2:1 layered silicate.....	36
Figure 2. 11. Dispersion of clay platelet in a polymeric matrix .....	38
Figure 3. 1. Schematic illustration of microsphere formation by spray drying .....	46
Figure 3. 2. Formation by ionotropic gelation .....	47
Figure 3. 3. Mechanisms of carriers enhanced absorption by enteric mucosa .....	53
Figure 4. 1. Schematic illustration of agar plates for inoculation of bacterial suspension .....	64
Figure 4. 2. Flow diagram of chitosan microsphere production.....	67
Figure 4. 3. Spray drying apparatus used in this study .....	67
Figure 5. 1. Morphological characterization of chitosan nanocomposite microspheres; a. 6 mL/s, b. 7 mL/s, c. 8 mL/s at 180 °C; d. 6 mL/s, e. 7 mL/s, f. 8 mL/s at 190 °C; g. 6 mL/s, h. 7 mL/s, i. 8 mL/s at 200 °C. ....	86
Figure 5. 2. SEM images of the chitosan microspheres a. Chitosan b. CO c. COM1 d. COM3 e. COM5 microspheres .....	88
Figure 5. 3. SEM images of a. CM1 b. CM3 c. CM5 microspheres.....	89
Figure 5. 4. TEM images of oil loaded COM5 microspheres.....	90
Figure 5. 5. Calibration curve of cinnamon bark oil.....	91
Figure 5. 6. Schematic representation of layered silicate structure .....	92
Figure 5. 7. The effect of pH on surface charge of montmorillonite (Cloisite 10A).....	93
Figure 5. 8. XRD patterns of neat chitosan microspheres .....	96

Figure 5. 9. XRD pattern of oil loaded chitosan (CO) microsphere.....	97
Figure 5. 10. XRD patterns of cinnamon oil loaded chitosan/MMT nanocomposite microspheres (COM1, COM3, COM5) .....	98
Figure 5. 11. TEM images of oil loaded chitosan/5%MMT microspheres with different magnifications (COM5) .....	99
Figure 5. 12. Organic-inorganic interaction of chitosan/MMT nanocomposite .....	99
Figure 5. 13. FTIR spectra of chitosan nanocomposite microspheres. Vertical line 1 characteristic band of MMT (Si-O stretching), 2 belongs to -NH <sub>2</sub> bending of chitosan (amine II), 3 refers to imine formation and 4 refers to characteristic band of chitosan amide I.....	101
Figure 5. 14. FTIR spectra of cinnamon bark oil.....	101
Figure 5. 15. <sup>1</sup> H-NMR spectra: a. control chitosan microspheres, b. cinnamon bark oil .....	102
Figure 5. 16. <sup>1</sup> H-NMR spectra of oil loaded chitosan microspheres (CO) and schiff base reaction between chitosan and cinnamaldehyde .....	103
Figure 5. 17. <sup>1</sup> H-NMR spectra: a. chitosan/oil/3MMT (COM3) microspheres, b. chitosan/3MMT microspheres .....	103
Figure 5. 18. Raman spectra of chitosan microspheres .....	104
Figure 5. 19. Raman spectra of nanoclay (MMT) .....	104
Figure 5. 20. Effects of oil and clay loading on Raman spectra of chitosan microspheres .....	105
Figure 5. 21. Raman spectra of cinnamon bark oil.....	106
Figure 5. 22. Schematic diagram showing influence of contact angle between device and mucous membrane on bioadhesion (Source: Carvalho et al., 2011)	107
Figure 5. 23. Contact angle images of chitosan microspheres a. Neat chitosan; b. C0; c. COM1; d. COM3; e. COM5 nanocomposites.....	107
Figure 5. 24. Contact angle values of chitosan microspheres.....	107
Figure 5. 25. Mucoadhesion (%) of oil loaded and unloaded chitosan microspheres ..	109
Figure 5. 26. Swelling degree of microspheres in SGF .....	110
Figure 5. 27. Swelling degree of microspheres in pH 4.5 .....	111
Figure 5. 28. Biodegradation results of oil loaded and unloaded chitosan microspheres in SGF at 37 °C.....	112
Figure 5. 29. <i>In vitro</i> release profile of cinnamon bark oil loaded chitosan microspheres in SGF .....	115

Figure 5. 30. <i>In vitro</i> release profile of cinnamon bark oil loaded chitosan microspheres in pH 4.5.....	115
Figure 5. 31. First-order release kinetic model of cinnamon bark oil loaded chitosan microspheres .....	116
Figure 5. 32. Higuchi release kinetic model for chitosan microspheres.....	117
Figure 5. 33. Korsmeyer-Peppas release kinetic model for chitosan microspheres .....	117
Figure 5. 34. Fit of model to experimental data, cinnamon bark oil release from CO microspheres .....	121
Figure 5. 35. Fit of model to experimental data, cinnamon bark oil release from COM1 microspheres .....	121
Figure 5. 36. Fit of model to experimental data, cinnamon bark oil release from COM3 microspheres .....	122
Figure 5. 37. Fit of model to experimental data, cinnamon bark oil release from COM5 microspheres .....	122
Figure 5. 38. <i>In vitro</i> cytotoxicity of chitosan microspheres on NIH3T3 cell line.....	125
Figure 5. 39. <i>In vitro</i> cytotoxicity of cinnamon bark oil on NIH3T3 cell line .....	126
Figure 5. 40. <i>In vitro</i> in direct cytotoxicity of chitosan microspheres on MKN45 cell line.....	128
Figure 5. 41. <i>In vitro</i> cell viability of chitosan microspheres treated MKN45 cells ...	128
Figure 5. 42. <i>In vitro</i> cell viability of MKN45 cells treated with cinnamon bark oil...	129
Figure 5. 43. Flourescent images of MKN45 cells incubated with chitosan microspheres for 2 and 4 hours; Chi; CO; COM1; COM3; COM5 treated cells (red color shows internalized microspheres and blue color shows nucleus stained with DAPI) .....	131
Figure 5. 44. <i>In vitro</i> cell binding of chitosan microspheres to MKN45 gastric cells..	134

## LIST OF TABLES

<b><u>Table</u></b>	<b><u>Page</u></b>
Table 2. 1. Factors effecting drug release .....	7
Table 2. 2. Types of controlled release .....	9
Table 2. 3. Release exponent n of the Peppas equation and drug release mechanism from polymeric controlled delivery systems of different geometry .....	15
Table 2. 4. Physicochemical and biological properties of chitosan.....	21
Table 2. 5. Pharmaceutical and biomedical applications of chitosan .....	24
Table 2. 6. <i>H.pylori</i> treatment regimens based on clarithromycin resistance.....	30
Table 2. 7. Alternative drug delivery systems for <i>H. pylori</i> treatment.....	32
Table 2. 8. Crystal structure and properties of three kinds of clay minerals .....	35
Table 2. 9. Use of clay minerals as excipients in solid dosage forms .....	38
Table 2. 10. Interactions between clay minerals and organic compounds .....	40
Table 3. 1. Main considerations in microencapsulation parameters.....	42
Table 3. 2. Different techniques for microencapsulation.....	44
Table 3. 3. Comparison of different techniques.....	44
Table 3. 4.Examples of encapsulated EOS for different polymer-active agent systems	54
Table 3. 5. Effects of essential oils on <i>H. pylori</i> growth; GI, partial growth inhibition; ND, not determined .....	56
Table 4. 1. Formulation codes and content of microspheres produced by spray drying	66
Table 4. 2. Release parameters and conditions .....	73
Table 5. 1. Effects of spray drying parameters on product humidity, yield and size of microsphere.....	83
Table 5. 2. Encapsulation efficiency of microspheres .....	91
Table 5. 3. Surface charge of chitosan and oil loaded chitosan nanocomposite microspheres in SGF.....	94
Table 5. 4. Surface charge of chitosan and oil loaded chitosan nanocomposite microspheres at pH 4.5 phosphate buffer (n=6) .....	95
Table 5. 5. FTIR data of chitosan nanocomposite microspheres.....	102
Table 5. 6. Release kinetic coefficients for chitosan microspheres .....	119
Table 5. 7. Diffusion and erosion coefficient values of chitosan microspheres using Kopcha equation .....	120

Table 5. 8. Diffusion coefficients by using Crank equation .....	121
Table 5. 9. Viable colony counts of <i>H.pylori</i> (CFU) treated with different cinnamon bark oil chitosan microspheres and chitosan nanocomposite microspheres .....	124
Table 5. 10. Percentage of radioactivity of microsphere formulations after labeling ..	132
Table 5. 11. Radiochemical purity of labeled microspheres.....	132
Table 5. 12. Cell binding of chitosan microspheres during 2 h and 4 h exposure .....	134

# CHAPTER 1

## INTRODUCTION

Recently, there are growing interest to site-specific drug delivery systems (DDS), because they provide effective and targeted drug delivery and minimize the side effects in contrary to the traditional drug-dosage form in the pharmaceutical field. A large number of drug delivery systems have been developed. Gastroretentive drug delivery systems which can prolong gastric residence time and provide a high drug concentration in the stomach promise an option for increasing the effectiveness of *H. pylori* treatment with better microbial eradication.

*Helicobacter pylori* (*H. pylori*) which is a Gram-negative, microaerophilic ubiquitous gastric pathogen, infected more than 50% of the world's population and 90% of population in developing countries. It is directly associated with dyspepsia, gastritis, peptic ulcer and risk factor in mucus-associated lymphoid tissue lymphoma (MALT). This chronic bacterial infection has significant morbidity and mortality with economic impact. However, current therapies are not effective enough to eradicate *H. pylori*. The main problems in eradication therapy are: poor permeability to mucus layer, instability in gastric conditions and antibiotic resistance of *H. pylori*. In regions of high clarithromycin resistance (>20%), alternative therapies should be recommended (Malfertheiner et al., 2012). Due to the resistance to currently recommended antibiotics, there is a need to seek alternative compounds from other sources with proven antimicrobial activity to overcome problems related with eradication therapy. Newer drugs and therapeutic approaches with enhanced action and reduced side effects are needed for better eradication of the organism (Shasis, 2014). Potentially useful active ingredients from natural products can serve as template for the synthesis of new antimicrobial drugs (Samie et al., 2014). Therefore, it is required to develop novel drug delivery systems carrying bioactive substances which have higher biological activity and which can be alternative to conventional antibiotic treatment for patients having antibiotic allergy and for eradication of antibiotic resistant strains.

In recent years, essential oils have growing interest in medicinal applications. Since the middle ages, essential oils have been widely used for bactericidal, viriucidal,

fungicidal, antiparasitical, insecticidal, medicinal and cosmetic applications and it was shown that some essential oils have antimicrobial activity against *H. pylori* (Bakkali, Averbeck, Averbeck, and Idaomar, 2008). The antimicrobial activity of essential oils from plants have been reported before. It was found that cinnamon bark oil has antimicrobial activity against *H. pylori* and the MIC value of cinnamon bark oil was determined as 8µg/mL (Altiok, 2011). Cinnamon bark oil was encapsulated in chitosan microspheres. Although Altiok (2011) found that oil releasing from microspheres inhibited the *H. pylori* growth *in vitro*, controlled drug release was required because of the burst release effect of cinnamon bark oil in gastric conditions. In the light of the related studies, in this study, it is expected that chitosan based nanoclay composite drug carrier system would alleviate the problems of burst release by controlling the release rate and enhancing stability of the microspheres. Polymer-nanoclay composites are particular interest in the literature because of enhancement of some physical properties of polymer and also provides tortuous pathway for drug delivery. Polymer-nanoclay based microsphere may increase the life span of active constituents and control the release of bioactive agents (Suresh et al., 2010).

The aim of this dissertation is to develop a novel drug delivery system containing cinnamon bark oil which has the potential to be used in gastrointestinal (GI) systems. In this study, nanoclay was introduced into chitosan matrix to improve stability, mucoadhesive and release properties of cinnamon bark oil. Oil loaded chitosan microspheres and nanocomposite microspheres were developed and produced by spray drying. After production, the prepared microspheres were characterized in terms of particle size, encapsulation efficiency, surface charge properties, *in vitro* mucoadhesion and swelling. The morphological and chemical characterization of the microspheres were investigated by scanning electron microscopy, FT-IR, Raman and NMR spectroscopies. Swelling degree was determined in SGF and pH 4.5. Biodegradation studies were performed in order to investigate stability in SGF and pH 4.5 to mimic the gastric conditions. *In vitro* drug release studies in simulated gastric fluid (SGF) and pH 4.5 were performed. Minimum inhibition concentration (MIC) of cinnamon bark oil against *H. pylori* was determined by agar dilution method. Based on these studies, *in vitro* antimicrobial effect of released cinnamon bark oil from chitosan nanoclay microspheres against *H. pylori* was investigated. *In vitro* cytotoxicity and cell proliferation assays of cinnamon bark oil and chitosan nanocomposites on NIH3T3 fibroblast and MKN45 gastric epithelial cells were performed. *In vitro* cellular uptake of nanocomposites was

investigated on MKN45 cell line. Microspheres were radiolabelled with  $^{99m}\text{Tc}$  and cell binding affinity of prepared microspheres to gastric epithelial cells was evaluated by cell culture incorporation studies.

The organization of the dissertation is as follows: Chapter 1 gives a brief information about this dissertation. Chapter 2 reviews the control drug delivery systems including different drug delivery systems and release mechanisms as well as nanocomposite systems. Chapter 3 gives background on the microencapsulation studies and essential oils. In Chapter 4 information about material-methods used in experiments is presented. In Chapter 5, the results of the study are discussed. Finally, Chapter 6 offers the conclusions of this work and the suggestions for future works.



## CHAPTER 2

### CONTROLLED DELIVERY SYSTEMS

#### 2.1. General Aspects

Controlled drug delivery systems, which include encapsulation of active pharmaceutical ingredients (API), or bioactive molecules, have been developed in order to control the delivery of an active agent in targeted site maintaining a desired concentration for a given period to enhance drug therapy as well as increase patient compliance. Drug needs to be delivered and it acts at the diseased site. Several mechanisms could operate simultaneously and/or different release mechanisms could dominate at different stages of the drug delivery process at a given period. These systems can reduce patient expenses, risks of toxicity, while increasing the drug efficacy, specificity, tolerability and therapeutic indices of drugs. Both natural and synthetic materials have been tested and proposed as components of controlled drug delivery and many efforts have been made to synthesize materials with the biological and mechanical properties (Kevadiya and Bajaj, 2013).

There are some advantages of controlled released systems over conventional systems:

- Maintenance of optimum therapeutic drug concentration in the blood or in a cell
- Control release of drug/active agent to give a sustained therapeutic effect and site-specific delivery
- Enhancement of activity duration for short half-life drugs
- The elimination of side effects, frequent dosing, waste of drug, optimized therapy
- Better patient compliance
- Enhancement pharmacological potency, solubility and bioavailability
- Protection from physical and chemical degradation

In general, the ideal drug delivery system should be inert, biocompatible, mechanically strong, comfortable for the patient, capable of achieving high drug loading,

safe from accidental release, simple to administer and remove, and easy to fabricate and sterilize (Lai et al. 2009).

### **2.1.1. Desirable Characteristics of Delivery Systems**

Numerous drug delivery systems have been developed that could be used to deliver pharmaceutical components. The specific requirements of the encapsulant material and the delivery system should be taken into account. The development of a successful encapsulation system for a target application requires knowledge about the stability of the chosen bioactive (core); the properties of the materials used for encapsulation (encapsulant) and the suitability of the delivery system for its final application (Augustin and Sanguansri, 2008). Therefore, there are some useful selection criteria that can be used to distinguish between different delivery systems for a particular application. The most important criteria could be summarized as:

- Loading capacity and efficiency: The loading capacity (LC) is the quantity of encapsulated bioactive agent per unit carrier material. An ideal delivery system should have a high loading capacity. The loading efficiency (LE) is the total amount of loaded bioactive agent over the initial amount of bioactive agent.

- Delivery mechanism: The delivery system should be designed so that it carries and releases bioactive agents to a particular site-of-action. The release should be at a controlled rate or in response to a specific environmental stimuli (e.g., pH, ionic strength, enzyme activity or temperature).

- Protection against degradation: The delivery system may have to be designed to protect an encapsulated material against some form of chemical degradation and biodegradation mechanism. The rate of these chemical degradation reactions may be promoted by certain factors that need to be controlled, such as heat, light, oxygen or specific chemicals.

- Economic Production: The delivery system could be economically manufactured using inexpensive ingredients and processes. Also it should be easy to fabricate and sterilize. Ultimately, the benefits gained from encapsulating the material (API or bioactive agent) should outweigh any additional costs arising from encapsulation.

- **Bioactivity:** A delivery system should be biocompatible, improve or at least not adversely affect the bioavailability of the encapsulated component and achieve desired biological response (McClements et al., 2009).

The selection of a biomaterial for a specific application depends on the physicochemical properties and durability of the material, the nature of the physiological environment at the organ or tissue, adverse effects in case of failure, cost and production ease, biocompatibility, mechanical strength, sterilization requirement, etc. Typically, inorganic (metals, ceramics, and glasses) and polymeric (synthetic and natural) materials have been used for such items as artificial heart-valves, (polymeric or carbon-based), synthetic blood-vessels, artificial hips (metallic or ceramic), medical adhesives, sutures, dental composites, and polymers for controlled slow drug delivery. There are several polymers, which are both synthetic and natural for controlled drug delivery applications. Among them, the biodegradable polymers, which are broken down into biologically acceptable molecules that are metabolized and removed from the body via normal metabolic pathways have been widely used for sutures, controlled drug delivery and tissue engineering. During the last two decades, significant advances were taken place in the development of biocompatible and biodegradable materials for biomedical applications (Sinha et al., 2004).

### **2.1.2. Factors Affecting Release**

The main factors that affect drug release mechanism and kinetics include physicochemical properties of drugs and polymer, drug:polymer ratio, degradation rate of polymers, swelling of polymer, erosion of polymer, dissolution or diffusion characteristics of drug, drug distribution inside the matrix and geometry (cylinder or sphere) of the system, crystallinity of polymer, molecular weight of polymer, the morphology and size of particle. Significant parameters that affect drug release are tabulated in Table 2.1.

Table 2. 1. Factors effecting drug release  
(Source: Fu and Kao, 2010; Raval et al., 2010)

<b>Polymer matrix</b>	<b>Release media</b>	<b>Active agent</b>	<b>Formulation and Processing</b>
Composition	pH	Solubility	Processing technique
Structure	Temperature	Stability	Properties of solvent
Swelling	Ionic strength	Charge	Formulation geometry and size
Degradation	Enzyme	Drug/polymer ratio (interaction)	Excipients
Thermal properties		Molecular weight and size	
Degree of crystallinity			

Drug:polymer ratio affects encapsulation efficiency and drug release. Decreasing the polymer concentration leads to reduction in loading efficiency due to maximum drug:polymer ratio (Dhakar et al., 2010). Several researchers showed that the encapsulation efficiency increase as drug:polymer ratio decrease. Since the quantity of polymer is insufficient to cover and encapsulate the drug completely, at high drug:polymer ratio, encapsulation efficiency is very low. The interaction between drug and polymer contributes to increasing encapsulation efficiency. At lower drug loading conditions, drug-polymer interaction would be weak and release rate increases. Also large pore formations could increase water uptake and drug release (Desai and Park, 2005). Also, interactions between protein and polymer can limit protein release from the microparticles and release rate decreases (Dhakar et al., 2010). Desai and Park (2005) found that the encapsulation efficiency of the spray-dried chitosan–TPP microspheres increased as the amount of chitosan increased. This situation may be explained on the basis that an increase in viscosity of the chitosan solution with increase in concentration prevents drug crystals from leaving the droplet.

The drug release is also dependent on particle size. In general, release rate of a molecule decreases with increasing particle size due to the decreased surface area/volume ratio of the particle. According to Fick's laws of diffusion, increased length of the diffusion pathways leads to decrease drug concentration gradients (which are the driving forces for diffusion) resulting in decreasing drug release rates with increasing microparticle size. However, since drug release is influenced by physical and chemical processes, the effects of particle size on drug release rate are not obvious. For instance, it

was reported that particle size of PLGA-based particles affects polymer degradation kinetics due to autocatalytic effect (Freiberg and Zhu, 2004; Klose et al., 2006; Siepmann et al., 2004; Xia and Pack, 2014). Also the porosity of particles plays an important role as well as particle size. Siepmann et al. (2004) indicated that drug release rate increased with increasing particle size of 5-FU loaded PLGA microparticles. In addition, water penetration into smaller particles may be quicker due to the shorter distance from the surface to the center of the particle.

Physical state of the drug in polymeric matrix is another important parameter while investigating the drug release kinetics microspheres. The physical state of the drug may vary from molecular dispersion (amorphous) to well-defined crystalline structures (Raval et al., 2010). Generally it is known that polymer degradation and drug release rate could be increased by greater hydrophilicity in the backbone or end groups, greater reactivity among hydrolytic groups in the backbone, and less crystallinity in the polymer structure (Alexis, 2005).

## **2.2. Types of Drug Delivery Systems**

Depending on the parameters listed in Table 2.1, one or more different phenomena might be taken part in controlled release of an active agent. These phenomena are explained below and Table 2.2 summarizes the types of controlled release mechanisms commonly used in the currently available controlled release dosage forms. The controlled release mechanisms can be broadly classified into physical and chemical mechanisms.

- Wetting of surface and water transport into the polymeric system by pores and/or through polymeric networks)
- Phase transitions of polymers (glassy to rubbery phase)
- Dissolution
- Degradation
- Swelling
- Diffusion of active agents and/or excipients
- Changes in drug and/or polymer solubility depending on micro environmental conditions
- Physical-active agent-excipient (polymer) interaction (ionic interactions, Van der Waals forces)

- Chemical reactions between active agent and excipient (polymer) and/or water (Siepmann and Siepmann, 2008).

Table 2. 2. Types of controlled release

1. Diffusion Controlled - Reservoir Systems - Matrix Systems (Monolithic)
2. Osmotically Controlled ( Water Penetration )
3. Swelling Controlled
4. Dissolution Controlled
5. Chemically Controlled (Degradation)
6. External Stimuli

**In diffusion controlled systems**, the diffusion can occur through pores in the polymer matrix or by passing between polymer chains. Drug release by diffusion involves three steps. Firstly, the penetration of water into drug delivery system resulted in swelling of the matrix; secondly, changing of glassy polymer into rubbery matrix and the third step is the diffusion of drug from the swollen matrix (Mitra and Dey, 2011).

In reservoir systems, drug is surrounded by a very thin polymer membrane and drug release is controlled by diffusion through the membrane. In monolithic systems, drug is dissolved uniformly in a polymer matrix. The matrix should be inert and non-degradable so that drug can be released by diffusion through matrix. It can be non-swelling or fully swollen.

**In osmotically controlled (water penetration) systems**, drug release is controlled by the rate of water diffusion into the device. For example, osmotically controlled delivery devices.

Another controlled drug delivery mechanism could be achieved by using biodegradable polymers in the system. Drug is loaded into a biodegradable or bioerodible reservoir or matrix system. These materials degrade within the body, eliminating the need to remove a drug delivery system after the release of the active agent has been completed. One design criteria is that significant bioerosion cannot take place until drug delivery has been completed.

**In external stimuli systems** as seen in Figure 2.1, depending upon the polymer, the environmental change can involve pH, temperature, or ionic strength, and the system can either shrink or swell upon a change in any of these environmental factors. “Smart” polymers undergo conformational changes and phase transition under external stimuli such as ionic strength, pH, light, electric field, irradiation, and temperature. For most of these polymers, the structural changes are reversible and repeatable upon additional changes in the external environment.

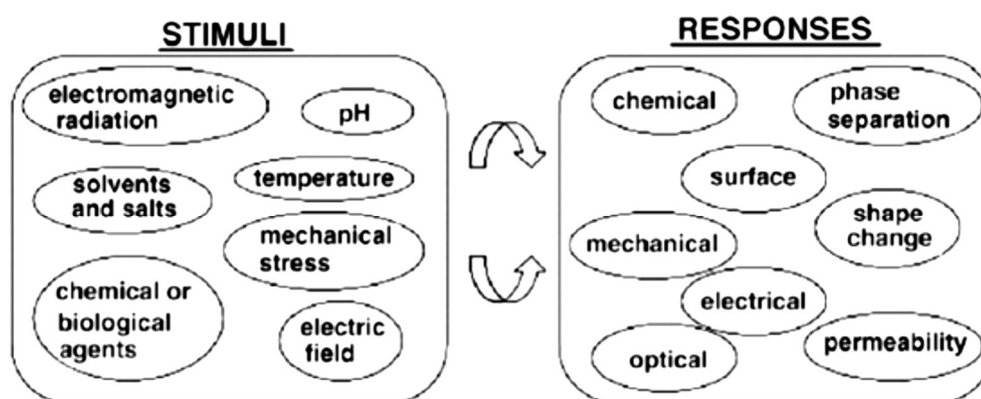


Figure 2. 1. External stimuli and responses  
(Source: Schmaljohann, 2006)

### 2.3. Release Mechanisms and Mathematical Models

Drug release kinetics and mechanism should be understood by generating a drug release profile as a function of time and applying transport equations and time dependent kinetic expressions to characterize the release rate from the dosage form. Ideally, physiological conditions at the site of administration should be taken into account when selecting the *in vitro* dissolution/release test conditions. The complexity of the release mechanism of some novel/special dosage forms and the lack of knowledge about the conditions under which release occurs *in vivo* make it difficult to design physiologically based tests in all cases, but it should be possible to conceive a test that can detect the influence of critical manufacturing variables, differentiate between degrees of product performance, and to some extent characterize the biopharmaceutical quality of the dosage form (Siewert et al., 2003).

## ***In Vitro* Release Methods**

In recent years, the use of surfactants for *in vitro* release testing of water-insoluble drugs has increased because of the similarities to *in vivo* release. In general, SLS (SDS) as an anionic surfactant, cetyltrimethylammonium bromide (CTAB) for a cationic surfactant and the polysorbate 80 and Tweens for a non-ionic surfactant are used to enhance the solubility. *In vitro* release studies are generally performed in order to accomplish one or more of the aims listed below:

1. As an indirect measurement of drug availability, especially in preliminary stages of product development
2. Quality control to support batch release and to comply with specifications of batches proven to be clinically and biologically effective
3. Assess formulation factors and manufacturing methods that are likely to influence bioavailability
4. Substantiation of label claim of the product
5. As a compendial requirement (D'Souza and DeLuca, 2006).

An *in vitro* release profile reveals fundamental information on the structure (e.g., porosity) and behaviour of the formulation on a molecular level, possible interactions between drug and polymer, and their influence on the rate and mechanism of drug release and model release data. Over the past decade, there have been attempts to compare *in vitro* test methods to study drug release from parenteral biodegradable microspheres. The following test conditions were employed to assess *in vitro* release in buffer:

1. USP XII paddle dissolution test apparatus: 1000 ml buffer at 100 and 200 rpm
2. Rotating bottle apparatus
3. Shaker incubator: 100-ml buffer at 60 and 120 strokes/min
4. Recycling flow-through cell:

For lipophilic substances, a modified basket method, a paddle method with a wired screen and a sinker and a modified flow-through cell with a specific dual chamber have all been recommended (D'Souza and DeLuca, 2006).

The flexibility in polymer processing plays an important role in the development of controlled delivery devices for a range of applications related to drugs, food-related bioactive ingredients, and genes. The release of bioactive agents from a delivery system may be either diffusion-controlled (diffusion of drug through a rate-controlling barrier/matrix), degradation controlled (chemical or physical breakdown of the matrix



leads to bioactive agent release), or via an environmental trigger (change in pH, ionic strength, or pressure tailors the release of the bioactive agent) (Averous, 2013).

There are several controlled-release mechanisms, including:

- dissolution,
- diffusion,
- swelling,
- erosion, and targeting.

Each drug delivery system have characteristic release properties depending on the physicochemical characteristics and structural conditions.

Several realistic as well as empirical mathematical models have been established to study and elucidate the water and drug transport processes. Realistic mathematical theories were based on the equations that describe the real phenomena by solving partial differential equations using initial and final boundary conditions. Mathematical theories based on diffusion, swelling, dissolution, and erosion mechanisms were developed and extensively explained in the Siepmann and Siepmann (2008).

If drug release occurs by diffusion controlled with constant diffusion coefficients, Fick's law of diffusion can be used to describe the transport of a bioactive agent from polymeric system. Fick's law in one dimension is explained by the following equation;

Fick's Law of Diffusion:

$$J = -D \frac{dC_i}{dx} \quad (2.1)$$

Fick's law is related with the diffusive flux,  $J$  ( $\text{mol}\cdot\text{m}^{-2}\cdot\text{s}^{-1}$ ) to concentration gradient under steady state conditions. It explains that flux,  $J$  ( $\text{mol}\cdot\text{m}^{-2}\cdot\text{s}^{-1}$ ), is proportional to the concentration gradient ( $dC_i/dx$ ).  $D$  is the diffusivity coefficient of the drug. The Fick's second law of diffusivity for one-dimensional drug release can be described as follow:

$$\frac{\partial C_i}{\partial t} = D \frac{\partial^2 C_i}{\partial x^2} \quad (2.2)$$

where  $C_i$  is drug concentration and  $D$  is diffusivity coefficient. The surface resistance is assumed to be negligible and perfect sink condition is considered. During the experiment, the release medium temperature is considered constant. Also, viscosity

does not change, implying that the diffusion coefficient is constant and it is assumed that there is no matrix erosion and chemical reactions take place. The geometry of the system affects drug release kinetics. So, in the case of spherical drug delivery systems, by rearranging (Crank, 1975):

$$\frac{M_t}{M_0} = 1 - \frac{6}{\pi^2} \sum_{n=1}^{\infty} \frac{1}{n^2} \exp\left(-\frac{Dn^2\pi^2t}{R^2}\right) \quad (2.3)$$

$M_t$  is the cumulative released drug from the particulate system at time,  $t$ ,  $M_0$  is the initial loading,  $D$  is the diffusion coefficient of drug within matrix and  $R$  is the radius of the sphere. The summation in Eq. 2.3 converges slowly when  $t$  is small, so a simplified expression for initial region of release, the short term [ $M_t/M_0 < 0.3$ ], is given by:

$$\frac{M_t}{M_0} = \frac{6}{\sqrt{\pi}} \sqrt{\frac{Dt}{r^2}} \quad (2.4)$$

In the long term region, the release curve approaches the asymptotic form and Eq. 2.3 is rearranged by:

$$\frac{M_t}{M_0} = 1 - \frac{6}{\pi^2} \exp\left(-\frac{Dn^2\pi^2t}{R^2}\right) \quad (2.5)$$

By taking Ln of both sides, a plot of  $\ln [1-M_t/M_0]$  versus  $t$  will approach a straight line with slope  $(-\frac{D\pi^2}{R^2})$  and intercept  $\ln (6/\pi^2)$  (Crank, 1975; Karger and Ruthven, 1992).

There is no general mathematical model which can be applied to all drug delivery systems. Certain models could be applied to limited number of DDS. Therefore empirical /semi empirical models are useful for comparison of different drug release profiles. They can give an indication of mechanism of drug release under specific conditions. Mathematical models are:

**1) Zero order release model:** It describes the systems where the drug release rate is independent of its concentration of the dissolved substance.

$$M_t = M_0 - k_0 t \quad (2.6)$$

where;  $M_t$ : Amount of drug released or dissolved at time  $t$ ;  $M_0$ : Initial amount of drug;  $k_0$ : Zero-order rate constant;  $t$ : time. Cumulative percentage drug release versus time plot is drawn to study the release kinetic.

**2) First order release model:** Drug release rate depends on its concentration. This model has been used for dissolution of pharmaceutical dosage forms such as containing water soluble drugs in porous matrices.

$$\ln M_t = \ln M_0 \pm kt \quad (2.7)$$

$$\log M_t = \log M_0 - \frac{kt}{2.303} \quad (2.8)$$

The data are plotted as log cumulative percentage drug remained versus time. Slope of the plot gives  $(k/2.303)$ .

**3) Higuchi release model:** Most of drug release data fits Higuchi model, therefore the most widely used equation. The Higuchi equation suggests that the drug release by diffusion. This model could be applied to several types of modified release, transdermal systems and matrix tables.

$$\frac{M_t}{M_0} = k_H \sqrt{t} \quad (2.9)$$

The data are plotted as cumulative percentage of drug release versus square root of time and it gives a straight line. Slope gives  $k$  value which is Higuchi release constant.

An important advantage of this model is its simplicity. However, when applying it to controlled drug delivery systems, the assumptions should carefully be taken in consideration: (i) the initial drug concentration in the system is much higher than the soluble amount of the drug at time  $t$  (which explained by the initial short time solution of the Crank equation), (ii) Mathematical analysis is based on one-dimensional diffusion, (iii) Swelling or dissolution of the polymer carrier is negligible, (iv) The diffusivity of the drug is constant.

**4) Korsmeyer – Peppas release model:** To find out the drug release mechanism, first 60% cumulative drug release data were generally fitted in Korsmeyer-Peppas model. This model is a simple relationship that describes drug release from a polymeric system.

$$\frac{M_t}{M_\infty} = kt^n \quad (2.10)$$

where; k = Release constant incorporating structural and geometric characteristics of the device; n = Diffusion or release exponent, which can indicate drug release mechanism.  $M_t$  and  $M_\infty$  represent the amount of drug released at time t and at infinite time (equilibrium state) (Drużyńska and Czubenko, 2012).  $M_t/M_\infty$  is the fraction of drug release at time t. Log fraction of drug released versus log time is plotted. From the slope, n is estimated and different n values indicate release mechanism for different geometries (Table 2.3).

Table 2. 3. Release exponent n of the Peppas equation and drug release mechanism from polymeric controlled delivery systems of different geometry (Source: Siepmann, 2008)

Release or diffusion exponent, n			Release mechanism
Thin film	Sphere	Cylinder	
$n \leq 0.5$	$n \leq 0.45$	$n \leq 0.43$	Fickian diffusion
$0.5 < n < 0.1$	$0.45 < n < 0.89$	$0.43 < n < 0.85$	Anomalous diffusion or non-Fickian diffusion
$n \geq 1$	$n \geq 0.89$	$n \geq 0.85$	Case-2 relaxation or super case transport-2

Fickian diffusional release is controlled by molecular diffusion of active agent due to chemical potential gradient. Anomalous diffusion or non-Fickian diffusion refers to overlapping of different phenomena such as; combination of both diffusion and erosion controlled rate release or swelling. Case-2 relaxation or super case transport-2 refers to polymer swelling and chain relaxation in water or biological fluids. This term also includes polymer disentanglement and erosion (Singhvi and Singh, 2011).

**5) Hixson-Crowell model:** This model explains the release of drug from the system where there is a change in surface area and diameter of particle and therefore assumes erosion based release terms.

$$M_0^{\frac{1}{3}} - M_t^{\frac{1}{3}} = k_{hc} t \quad (2.11)$$

**6) Kopcha Model:** The Kopcha model can be used to quantify the relative contributions of diffusion (A) and erosion (B) contributions to drug release. To quantify (A) and (B) release data can be fitted to the Kopcha's empirical equation:

$$M = A\sqrt{t+Bt} \quad (2.12)$$

where, M: Cumulative released drug at time, t; A: Diffusional constant; B: Erosion constant. According to this equation, if diffusion/erosion ratio  $A/B=1$ , release mechanism is equally controlled by both diffusion and erosion mechanism. If  $A/B > 1$ , diffusion prevails and if  $A/B < 1$  erosion predominates. To determine the coefficients, A and B, The data can be drawn as  $M/t$  versus  $1/\sqrt{t}$  graph. Slope gives A value and the intercept gives B value (Chevalier et al., 2009). The correlation coefficient  $r^2$  expressed the goodness of the model fit.

## 2.4. Gastroretentive Drug Delivery Systems

The oral route is the most common and preferable route for the delivery of drugs. During past few decades, number of oral controlled drug delivery systems have been developed for release of drugs over a defined period of time at a controlled rate. The major challenge in the development of an oral controlled-release drug delivery system is not only sustain the drug release but also to prolong the presence of the dosage form within the gastrointestinal tract (GIT) until all the drug is completely released at the desired time (Hooda et al., 2012).

The development of controlled release systems for drug delivery to mucosal surfaces, such as lung airways, GI tract, female reproductive tract, nose and eye, is of widespread interest. These mucosal surfaces are coated with the viscous, elastic and sticky mucus layer that lines all mucosal tissues which protect the body by rapidly trapping and removing foreign particles and hydrophobic molecules. The limited permeability of drug delivery particles and many hydrophobic drugs through the mucus barrier leads to their rapid clearance from the delivery site, often precluding effective drug

therapies at non-toxic dosages. In order to avoid rapid mucus clearance and/or reach the underlying epithelia, drug carrier systems such as micro/nanoparticles can be designed that overcome the the mucus barrier and and thereby provide targeted or sustained drug delivery for localized therapies in mucosal tissue. Therefore, various gastroretentive systems have been designed to provide controlled release of drugs with low absorption in the GI tract or for local treatment of gastric diseases. Several approaches were developed to retain the dosage form in the stomach. Typically, gastric residence time is depending on size and density of the formulation and the stomach state (fed or fasted). These gastroretentive dosage forms could be classified as: (1) floating systems, (2) high-density systems, (3) mucoadhesive systems, (4) magnetic systems, (5) extendible or swellable systems. Drugs that act locally in the stomach, e.g. antacids and antibiotics; drugs that are absorbed primarily in the stomach, e.g. metronidazole; drugs that are poorly soluble at alkaline pH, e.g. diazepam; drugs that have a narrow absorption window in the stomach (riboflavin); drugs that are absorbed rapidly from the GI tract (amoxicillin); drugs that degrade or are unstable in the colonic (metoprolol) (Lai et al., 2009; Devrim and Canefe 2006).

**Floating delivery systems** generally have a bulk density, that is less than the density of the gastric contents and thus remain buoyant in the stomach, without affecting the gastric emptying rate for a prolonged period of time. A common feature of floating dosage forms is their density of  $<1.0$  g/mL (Touitou and Barry, 2007). A floating system could lead to high drug levels in the fundal area of stomach. Therefore floating dosage forms could be a useful delivery systems for narrow spectrum antibiotics for peptic ulcer disease. The drug content should be released slowly as the dosage form remains floating on the gastric contents. At the end of the release period, the DDS should exit from the stomach. This system has been shown to increase gastroretention and reduce fluctuations in drug plasma concentrations (Adebisi and Conway, 2011). Patel et al., developed a multiple-unit floating beads provide sustained release of Famotidine with a view to providing an effective and safe therapy for stomach ulcer with a reduced frequency of dose with prolonged therapeutic effect. This alginate based floating-type gastroretentive dosage form of famotidine would be better for treating gastric ulcers (Patel et al., 2009).

**High-density systems** are dosage forms that have a density greater than the density of normal stomach contents which is  $1.004$  g/cm<sup>3</sup>. The density of the formulation should be close to  $2.5$  g/cm<sup>3</sup>. It has been reported that for the above densities of the range

2.4–2.8 g/cm<sup>3</sup>, formulations can be retained in the lower part of the stomach. There is no formulation utilising this strategy currently on the market (Adebisi and Conway, 2011).

Another approach is the **swellable or expandable systems** that delay passage through pyloric sphincter opening. Dosage forms could be designed in size to enhance retention in the stomach. Important property of these formulations are that the dosage form must be small enough for it to be easily swallowed. The increase in size of the formulation is normally achieved by swelling in stomach. Another key parameter is that this system should be strong enough to withstand the contractions and forces of stomach.

Although most common way to deliver pharmaceutical active ingredients (API) is oral route, generally orally administered particles undergo direct transit through the GIT (gastrointestinal tract). Therefore in recent years, mucoadhesion has been commonly employed in controlled delivery systems to improve the residence time of particles in the GIT as well as improve the bioavailability of bioactives.

**Mucoadhesive systems** provide the absorption of API and bioactives through the mucosal lining of the GIT. Besides main function of mucus in digestion system, mucus protects epithelial cells from pathogens and acidic environment. Mucus is secreted to remove pathogens and lubricate the epithelium. Mucus is a complex hydrogel composed of proteins, carbohydrates, lipids, salts, antibodies, bacteria, and cellular debris. Mucus is mainly composed of mucins, which can be either secreted or cell-bound. They are both highly glycosylated consisting of 80% carbohydrates primarily N-acetylgalactosamine, N-acetylglucosamine, fucose, galactose, and sialic acid. Mucoadhesive microspheres/microparticles provide efficient absorption and enhanced bioavailability of drugs due to a high surface/volume ratio, higher intimate contact with the mucus layer, and specific targeting of drugs to the absorption site (Raval et al., 2010).

Advantages of mucoadhesive microspheres drug delivery system:

- As a result of adhesion and intimate contact, prolongs the residence time at the delivery site, improves API bioavailability and therapeutic efficacy for disease treatment.
- Controlled API release and increased residence time lower administration frequency and improve patient compliance.
- High loading of active ingredients (water & lipid soluble drugs)
- Economic impact; significant cost reductions due to lower dose frequency.
- Maintenance of therapeutic plasma drug concentration.

- Better processability (improving solubility, dispersibility, flowability) (Mythri et al., 2011; Kharia and Singhai, 2013).

Characteristics of an ideal mucoadhesive polymer:

1. The polymer and its degradation products should be nontoxic and should be nonabsorbable from the GI tract.
2. It should be non-irritant to the mucus membrane.
3. It should be preferably mucoadhesive.
4. It should adhere quickly to most tissue and should possess some site specificity.
5. The polymers must not decompose on storage or during the shelf life of the dosage form.
6. It should be economical (Kharia and Singhai, 2013).

### **2.4.1. Chitosan in Drug Delivery System**

Mucoadhesive polymers improve intimate contact with the mucosa of the GIT and hence enhance bioavailability especially poorly absorbed drugs. In recent years, chitosan, therefore, takes attention as gastroretentive drug carrier due to its mucoadhesive property. This biopolymer has many advantages in drug delivery applications. The free amino groups of the glucosamine units allow different chemical modifications of the backbone in order to functionalize and improve the properties of chitosan. Chitosan shows antimicrobial activity, it has been reported that pretreatment with this polymer could prevent ulcerogenic effects in rats. These antacid and antiulcer activities may also be helpful in preventing or weakening drug irritation in the stomach. Chitosan and its derivatives are able to easily be fabricated as nano/micro particle formulation. Besides its mucoadhesive properties, chitosan has the ability to gradually swell and float in an acidic medium which makes it an ideal candidate for controlled drug delivery applications (Bruno and Neves, 2012).

#### **2.4.1.1. Structure, Physicochemical and Biological Properties**

Chitin, which is the second most abundant biopolymer after cellulose, is a primary component of exoskeletons of crustaceans such as crabs and shrimp and insects as well as



of cell walls of some bacteria and fungi. Chitosan is derived from of the chitin and is produced by partial alkaline deacetylation of chitin to form the polymer of acetyl glucosamine. The primary unit of chitosan is 2-amino-2-deoxy-D-glucose and with  $\beta\rightarrow 1-4$  glucosidic linkages polymer chain is formed. Depending on its degree of deacetylation, the structure of chitosan includes 2-acetamido-2-deoxy-D-glucose. The molar fraction of residual acetyl groups in chitosan is expressed as a degree of acetylation (DA), where the molar fraction of deacetylated residues is regarded as the deacetylation degree (DD). DD is a key factor that effects the physicochemical and biological properties of chitosan. Properties of chitosan such as size (average molecular weight; MW), DD, solubility, crystallinity or the pattern of acetylation may differ depending on the source and manufacturing conditions (Kumirska et al., 2011). The chemical structure of chitosan is given in Figure 2.2.

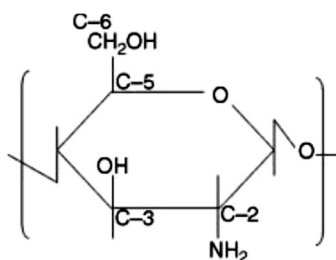


Figure 2. 2. Chemical structure of chitosan  
(Source: Bruno and Neves, 2012)

Chitosan is a polycationic polysaccharide which has a pKa value of 6.5. Below pH 6.0 the amino groups ( $-\text{NH}_2$  function) on the C-2 position of the D-glucosamine repeat unit become protonated and makes chitosan soluble in diluted acids. The positively charged amino groups on the chitosan molecule bind to the negatively charged carboxylic groups of free fatty acids. These amino groups of chitosan are responsible for the differences in their structures and physicochemical properties and its distribution is random, which generates intra- and inter-molecular hydrogen bonds. In addition, chitosan has primary and secondary hydroxyl groups at the C-3 and C-6 positions. All three groups allow chemical modifications of chitosan that include acylation, alkylation, Schiff base formation, carboxymethylation, and silylation which provides number of derivatives for different application (Rinaudo 2006; Zhang et al. 2010; Bruno and Neves, 2012). Among several biomaterials, chitosan has drawn increasing attention as a gastroretentive drug delivery system. Chitosan has several pharmaceutical and biomedical applications due to its abundant availability, mucoadhesivity, inherent pharmacological properties, and other

beneficial biological properties such as biocompatibility, biodegradability, nontoxicity and low-immunogenicity (Table 2.4).

Table 2. 4. Physicochemical and biological properties of chitosan  
(Source: Hejazi and Amiji 2003)

<b>Chemical Properties of Chitosan</b>	<b>Biological Properties of Chitosan</b>
Cationic polyamine	Natural biopolymer
High charge density at pH <6.5	Biocompatible
Mucoadhesive to negatively charges surfaces	Biodegradable
Forms gel with polyanions	Safe and non-toxic
High molecular weight with linear polyelectrolyte	Hemostatic, bacteriostatic and fungistatic
Viscosity, high to low	Anticancerogen
Chelates certain transitional metals	Antihypercholesteremic (reduces LDL cholesterol)
Able to chemical modification	Reasonable cost
Reactive amino/hydroxyl groups	Promotes weight loss
	Regenerative effect on connective tissue
	Wound healing

Biocompatibility of chitosan is related to biodegradation rate of chitosan microspheres. The biodegradability of chitosan leads to the release of nontoxic oligosaccharides of variable length that can be subsequently incorporated into glycosaminoglycans and glycoproteins or into metabolic pathways or be excreted. Rapid degradation can cause accumulation of amino sugars, inducing an inflammatory response. It was reported that chitosan with low DD degrade more rapidly and may cause an acute inflammation and as DD increases, inflammatory response decreases (Bruno and Neves, 2012).

Chitosan has antimicrobial property and absorbs toxic metals like mercury, cadmium, lead, etc. and antimicrobial property is attributed to the polycationic structure of chitosan. As environmental pH is below the pKa of the chitosan, electrostatic interactions between the polycationic structure of the chitosan and anionic components of the microorganisms' surface plays a primary role (Kong et al., 2010).

Another important aspect of chitosan is that it possesses mucoadhesive properties due to molecular attractive forces formed by electrostatic interaction between positively charged amino groups of chitosan and negatively charged sialic acid of mucosal surfaces. This property may be attributed to:

- (a) strong hydrogen bonding groups like  $-OH$ ,  $-COOH$
- (b) strong charges and ionic interactions
- (c) high molecular weight
- (d) sufficient chain flexibility
- (e) surface energy properties providing spreading into mucus (Sinha et al., 2004).

Mucoadhesive property of chitosan enables interaction of the drug with the mucus layer covering epithelial surfaces. Rapid drug transit is one of the limitation of mucosal deliver. Chitosan–mucus interaction forms a viscous gel that may reduce the clearance and increase the residence time of the drug which makes chitosan very useful carrier for mucosal drug delivery (Figure 2.3) (Bruno and Neves, 2012).

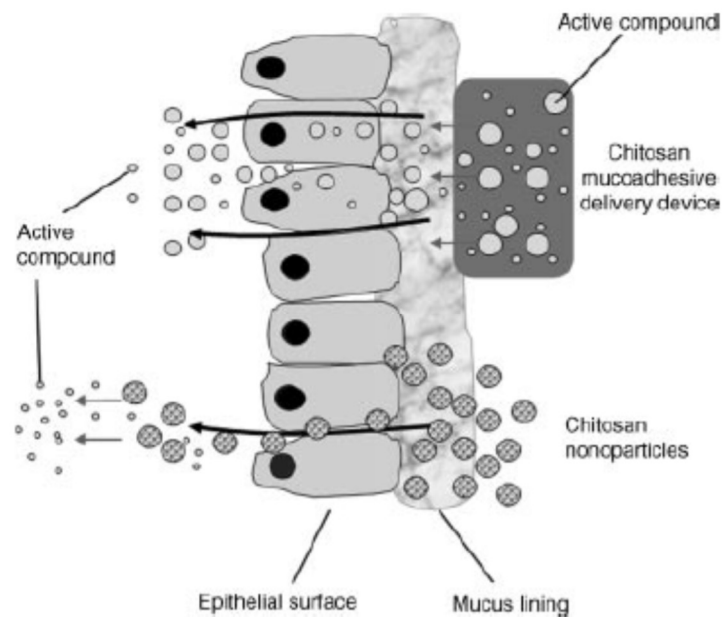


Figure 2. 3. Interaction of chitosan based systems with mucus layer  
(Source: Bruno and Neves, 2012)

Several factors affect chitosan mucoadhesion, such as physiological variables and the physicochemical properties of chitosan. Mucoadhesive drug delivery systems have several advantages:

- Significant retention time in stomach

- High loading of active ingredients (water & lipid soluble drugs)
- Controlled release of such drugs over a period of time that is clinical need.

#### **2.4.1.2. Pharmaceutical Usage of Chitosan**

Several pharmaceutical applications of chitosan have been reported as tablet excipients. It was used as vehicle for sustained release preparations for enhancement of dissolution rate and bioavailability of water insoluble drugs and directly compressed tablets as disintegrant, binder, granulating agent, in ground mixtures, as a drug carrier for sustained release preparations (Sinha et al., 2004; Nunthanid et al., 2004). Also number of spray dried chitosan powder and granule studies have been reported in the literature. Degree of deacetylation degree and molecular weight effect physicochemical and biological properties of chitosan. Chitosan is available in different forms depending on the molecular weight and degree of deacetylation. High deacetylation degree (>85%) is required for biomedical applications. The pharmaceutical requirements of chitosan could be summarized as: particle size <30  $\mu\text{m}$ , 1.35-1.4  $\text{g}/\text{cm}^3$  density, pH 6.5-7.5, insoluble in water and soluble in weak acids (Hejazi and Amiji 2003).

Chitosan is able to bind to cell membranes due to its positive surface charge. It is reported that chitosan and its several derivatives decrease the trans-epithelial resistance (TEER) of cell monolayers and also increase paracellular permeability. Chitosan has been shown to increase both trans- and paracellular permeability in a reversible and dose-dependent manner by opening tight junctions between epithelial cells. A combination of mucoadhesion and transient opening of tight junction in the mucosal membrane explain the enhanced absorption ability of chitosan. For instance, chitosan-EDTA has strong affinity toward divalent cations, such as  $\text{Ca}^{+2}$ , could open tight junctions in mucosal tissues leading to an improved peroral absorption of peptide and protein drugs (Davis Samuel, 2011; Bruno and Neves, 2012). Chitosan also shows antimicrobial activity against both Gram negative and Gram positive bacteria. The mechanisms responsible for the antibacterial and antifungal activity of chitosan are attributed to the ionic interaction of its amino groups with the negatively charged microbial surface, leading to structural and permeability changes. Chitosan leads to disruption of barrier properties of the outer membrane of Gram-negative bacteria. Different forms of chitosan in pharmaceutical and biomedical applications were represented in Table 2.5.

Table 2. 5. Pharmaceutical and biomedical applications of chitosan

<b>Form</b>	<b>Application</b>
Directly compressible excipients for tablets	Binder, coating, disintegrant, wet granulation
Controlled/sustained release tablet	
Gels	Bioadhesive systems, drug delivery, transdermal transport, tissue engineering
Films	
Fiber	
Micro/nanoparticle	
Scaffold	

### **Drug Delivery**

Among the several drug delivery systems, microsphere-based therapy allows the drug to be released to the specific target through the choice and formulation of different drug/polymer combinations. By using innovative microencapsulation technologies and by varying the drug-polymer ratio, the molecular weight of the polymer, microspheres can provide the optimal release profile. Microspheres may increase the life of active drugs and control the release of bioactive agents. As they are small in size, they have a large surface: volume ratio and can be used for the controlled release of insoluble drugs.

An important application of chitosan in industry is the development of drug delivery systems such as nanoparticles, hydrogels, microspheres, films and tablets. If degree of deacetylation and molecular weight of chitosan can be controlled, then it would be a material of choice for developing micro/nanoparticles. Chitosan has many advantages, particularly for developing micro/nanoparticles.

The use of chitosan in drug delivery has been focused on production of carrier system which improves the effectiveness and stability of encapsulated agents. Chitosan based carriers have been developed as microspheres (Berthold et al., 1996; Harris et al., 2010; Wang et al., 2010; Zhou et al., 2014), nanoparticles (Hosseini et al., 2013; Lin et al., 2013; Qi et al., 2005; Yuan et al., 2010) encapsulating different bioactive agent. Chitosan has been also used for coating agent (Luo et al., 2015; Sahasathian et al., 2010). Due to gel forming property, chitosan based hydrogels have been reported in the literature (Baysal et al., 2013; Bhattarai et al., 2010; Cojocariu et al., 2012; Muzzarelli, 2009). Up

to date several chitosan based gastroretentive dosage forms have been developed for the eradication of *H.pylori* and treatment of gastric diseases (Sahasathian et al., 2010; Adebisi and Conway 2014; Chang et al. 2011; Hejazi and Amiji 2004; Patel and Patel 2007; Shah et al. 1999). Chitosan based carriers prolong the gastric residence time with the help of mucoadhesive property and provide better effectiveness.

#### **2.4.1.3. Crosslinking of Chitosan**

A great number of chitosan derivatives have been studied by grafting new functional groups on the chitosan backbone. Modification does not change the fundamental skeleton of chitosan but improved its properties such as mucoadhesion and permeation enhancement. The crosslinking may be achieved in acidic, neutral or basic environments depending on the method. Crosslinking is divided into two main groups: physical and chemical. Chemical crosslinking is the most preferred method to produce permanent networks using covalent bonding between the polymer chains (Shweta and Sonia, 2013).

The crosslinking reaction is mainly influenced by the size and type of crosslinker agent and the functional groups of chitosan. The smaller the molecular size of the crosslinker, the faster the crosslinking reaction, since its diffusion is easier. Depending on the nature of the crosslinker, the main interactions forming the network are covalent or ionic bonds. Covalently crosslinked hydrogels present the crosslinking degree as the main parameter influencing important properties such as mechanical strength, swelling and drug release. Crosslinked chitosan is useful in pharmaceutical technology for formulation of various novel DDS like microspheres, nanoparticles, hydrogels and film/membranes. The release of drug from chitosan microspheres is depend on the molecular weight of chitosan, drug loading and crosslinking degree. Various therapeutic agents such as anticancer, anti-inflammatory, antibiotics, steroids, proteins, vitamins have been encapsulated in crosslinked chitosan microspheres to improve bioavailability, drug targeting to specific site and controlled drug delivery. Crosslinking is an efficient method to overcome some limitations such as degradation, instability and provides narrow size distributions, good morphology and controlled release of bioactive agents (Zhang et al., 2013).

Amino groups of the chitosan backbone can interact with different crosslinker agents such as glutaraldehyde, sodium sulphate, tripolyphosphate (TPP), genipin, vanillin etc. The crosslinking may be achieved in acidic, neutral or basic environments depending on the method. Although there are several chemical crosslinker agent, they have some disadvantages such as cytotoxicity and physiological incompatibility. Genipin (GP) shown in Figure 2.4, is one of the natural crosslinker agent extracted from the plant *Gardenial jasminoides* Ellis, and approximately 10,000 times less cytotoxic than glutaraldehyde and an ideal crosslinker for clinical usage (Yuan et al., 2007).

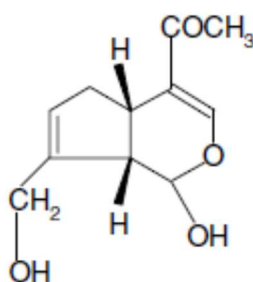


Figure 2. 4. Chemical structure of genipin  
(Source: Yuan et al., 2007)

Genipin reacts under mild conditions with its primary amine groups and crosslinking reaction occurs between chitosan as well as other biomaterials containing amino groups. Inherent blue colour indicates a successful crosslinking reaction (Arteche Pujana et al., 2013). The crosslinking reaction mechanisms for chitosan with genipin depend on pH values of medium. Under acidic and neutral conditions, a nucleophilic attack by the amino groups of chitosan on the olefinic carbon atom at C-3 occurs, followed by opening the dihydropyran ring and attacked by the secondary amino group on the newly formed aldehyde group (Figure 2.5). In other words, genipin acts as a dialdehyde but its condensation products are much more stable compared to glutaraldehyde. In the product, short chains of condensed genipin act as crosslinking bridges. Under basic conditions, nucleophilic attack by hydroxyl ions in aqueous solution leads to ring-opening of genipin and as a result intermediate aldehyde groups, which subsequently undergo aldol condensation are formed. The terminal aldehyde groups on the polymerized genipin undergoes a Schiff reaction with the amino groups on chitosan to form crosslinked networks. Therefore, the pH condition plays an important role in influencing the crosslinking reactions (Muzzarelli, 2009).

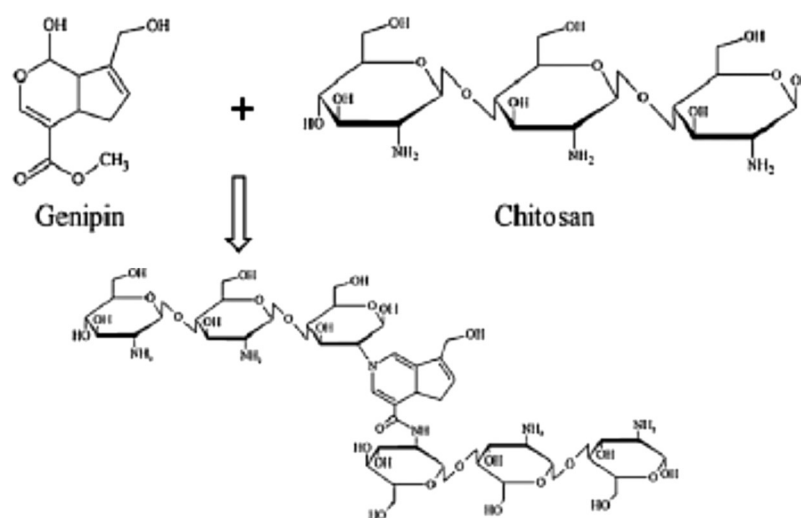


Figure 2. 5. Chitosan-genipin crosslinking mechanism  
(Source: Gao et al. 2014)

TPP is a nontoxic crosslinker and multivalent anions. It can form gel by ionic interaction between positively charged amino groups of chitosan and negatively charged of TPP. Ko et al. (2002) investigated the effect of TPP concentration and crosslinking time on drug content and drug release properties. Felodipine was used as model drug. They found that as the MW and concentration of chitosan solution and crosslinking time increased, the release of felodipine decreased significantly. Also, higher concentration of TPP solution resulted in slower felodipine release from chitosan microparticles. As the crosslinking time increased it was observed that drug release decreased (Ko et al., 2002). It could be inferred that short crosslinking time might not give the sufficient interaction time for the TPP-chitosan matrix.

Harris et al. (2010) investigated the effect of crosslinking time and polymer/genipin concentration on chitosan genipin crosslinking and developed crosslinked drug loaded microspheres by spray drying process for controlled release. They found that genipin crosslinking improved release profiles (Harris et al., 2010). Zhang et al. (2013) studied that preparation of genipin crosslinked chitosan microspheres for release of resveratrol (RES). RES has burst release effect while genipin crosslinked microspheres decreased burst effect and provided controlled release (Zhang et al., 2013). Also, crosslinking time effects swelling property of biomaterials. It was shown that the swelling degree of the crosslinked chitosan microspheres increased with the decrease of reaction time (Mi et al., 2000). This can be explained by the required time for achieving crosslinked genipin-chitosan structure. The lower swelling degree of chitosan



microspheres could be attributed to the increased intermolecular or intramolecular linkage of the  $-NH_2$  sites in chitosan, which could be achieved by a more complete crosslinking reaction.

## **2.5. Controlled Drug Delivery systems for Eradication of *H. pylori***

*Helicobacter pylori* (*H. pylori*) is a Gram-negative spiral-shaped bacterium that was first isolated by Barry Marshall and J. Robin Warren. Since its discovery in 1983, the microorganism has been associated with the etiopathogenesis of several diseases of the digestive system, such as gastritis, peptic ulcer disease and gastric cancer (Cogo et al., 2010).

*H. pylori* resides exclusively in the gastric mucus layer and the intracellular junctions of the mucus-secreting cells with significant colonization of the gastric antral region. Although *H. pylori* is very sensitive to acidic pH, the organism survive in the stomach by its urease activity which converts urea into bicarbonate and ammonia, which are strong bases and neutralizes the acidic zone around *H. pylori* (Shah et al.,1999). Gastric colonization is facilitated by cell wall associated lectins which permit the bacterium to bind to gastric mucus and the gastric epithelial cell. Once, *H. pylori* produces several enzymes which may harm the gastric epithelium, particularly urease (through ammonia generation) and phospholipases A and C. *H. pylori* also weakens the gastric mucous layer by digesting its glycoproteins and lipids, making the mucus less hydrophobic and more water soluble. *H. pylori* attracts phagocytic cells, inducing both acute and chronic inflammation as well as an antibody response (Marshall, 1991). There are several pathogenity mechanisms of *H. pylori* infection as represented Figure 2.6. *H. pylori* has flagella which is responsible for motility in viscous mucus medium. It passes through the mucus layer by mucus disrupting enzymes such as proteases, phospholipases. It is not an acidophilic bacteria; it neutralizes the acidic media of stomach by its urease activity and protects itself from the acidic conditions of stomach. Disease outcome is the result of the complex interplay between the host and the bacterium. Host immune gene polymorphisms and gastric acid secretion largely determine the bacterium's ability to colonize a specific gastric niche. Bacterial virulence factors such as the cytotoxin-associated gene CagA pathogenicity island-encoded protein and the vacuolating cytotoxin VacA aid in this colonization of the gastric mucosa. vacA is responsible for the

formation of acidic vacuoles in epithelial cells and leads to their death following infection and colonization of an *H. pylori*. Adhesion factors such as SabA, OipA, AlpA, and AlpB, enable binding of the bacterium to the gastric cells. Many different molecules such as SabA, OipA, AlpA, AlpB and BabA2 have adhesion activity (Tanih et al., 2010).

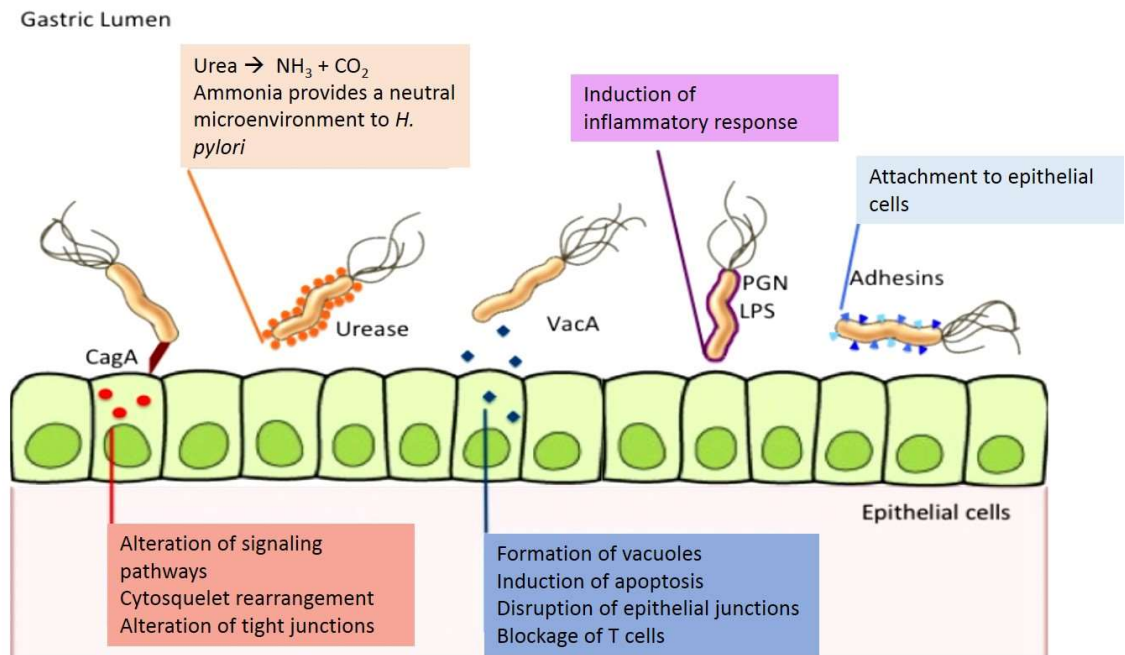


Figure 2. 6. Schematic illustration of *H.pylori* infection and virulence factors (Source: Guerrero et al., 2013)

Amoxicillin, clarithromycin, tetracycline and metronidazole are commonly used antibiotics in *H. pylori* treatment. However, the use of antibiotics in the *H. pylori* eradication has resulted in the formation of resistance to these antibiotics. Although the microorganism is highly susceptible to many antimicrobial agents *in vitro*, clinical trials with a single antimicrobial agent have resulted in a low eradication rate of *H. pylori*. Triple therapies over a period of two weeks is usually required for effective in clinical application. The Maastricht Consensus Report (2012) have been introduced for the therapeutic management and eradication of *H. pylori* infection. According to this consensus report, the triple therapy eradication a combination of clarithromycin containing (amoxicillin or metronidazole) and proton pump inhibitor (PPI) is used in areas where clarithromycin resistance is low (<20%). Current recommended therapies (Table 2.6) could not eradicate infection in all treated cases and at least 20% post-treatment patients continue to suffer. However, none of these drugs is effective enough

to eradicate *H. pylori* in monotherapy, and such a combination of treatments does not always offer a complete cure and undesirable side effects are often observed.

Table 2. 6. *H.pylori* treatment regimens based on clarithromycin resistance

	<b>1<sup>st</sup> line therapy</b>	<b>2<sup>nd</sup> line therapy</b>	<b>3<sup>rd</sup> therapy</b>
<b>With low clarithromycin resistance (&lt;20%)</b>	PPI+Clarithromycin +Amoxicillin/ Metronidazole	Bi quadruple or PPI+Levofloxacin+ Amoxicillin	Should be determined based on antibiotic susceptibility testing
<b>With high clarithromycin resistance (&gt;20%)</b>	Bi quadruple (Bi containing treatment)	PPI+Levofloxacin+ Amoxicillin	

Antibiotic resistance and noncompliance due to secondary effects are the major causes of eradication treatment failure. However, some other reports and clinical trials indicate that the therapies cannot achieve complete eradication of *H. pylori* and suggest that the therapeutic effect needs more investigation. There are some problems in current eradication therapy of *H. pylori*:

- poor diffusion of antibiotics to mucus layer,
- low stability & rapid destruction of the antibiotic in the gastric conditions,
- difficulty of reaching MICs for *H. pylori*,
- insufficient duration (residence) time of the antibiotic in the stomach,
- side effects,
- antibiotic resistance of *H. pylori*,
- allergy of patients against antibiotics.

In regions of high clarithromycin resistance (>20%), alternative therapies should be recommended (Malfertheiner et al., 2012). Therefore, the identification of a non antibiotic agent, which is both effective and free from these side-effects, is required for the eradication of *H. pylori*. Newer drugs and therapeutic approaches with enhanced action and reduced side effects are needed for better eradication of the organism. For effective *H. pylori* eradication, antibiotics need to penetrate through the gastric mucus

layer and maintain a sufficient concentration and residence time for antibacterial activity in the infected site. There are several ways to improve the effectiveness of the treatment (or decrease treatment failure): by finding new and more potent drugs to kill the bacteria, by developing a vaccine approach to stimulate the host immune defenses or by developing new nutritional approaches to the management of the infection.

Bioadhesive systems are to target specifically a site in the gastrointestinal tract. GRDRS is one of the specific application for eradication of *H. pylori*. Recently, the gastroretentive systems for treatment of *H. pylori* have shown special interest. Mucoadhesive system approach for a better *H. pylori* eradication was explained schematically in Figure 2.7. The prolongation of the local availability of the antibacterial agents has been reported to be an important factor to increase the effectiveness of *H. pylori* treatment. Alternative chitosan based drug delivery systems developed in the literature have been listed in Table 2.7. This drug delivery systems will ensure a high drug concentration in the gastric mucosa for better microbial eradication. Amoxicillin containing mucoadhesive floating microspheres was prepared by Liu et al. (2005) and reported much better *H. pylori* eradication compared to powder drug. Umamaheshwari et al. reported that receptor-mediated targeting of lectin-conjugated gliadin nanoparticles of acetohydroxamic acid for *H. pylori* treatment. They also developed floating bioadhesive microspheres and mucoadhesive nanoparticles of amoxicillin and a new gastroretentive drug delivery system using cholestyramine containing acetohydroxamic acid for the treatment of *H. pylori* (Ramteke, Ganesh, Bhattacharya, and Jain, 2009). The amoxicillin incorporated microspheres provided 10 times greater anti-*H. pylori* activity than the amoxicillin suspension. Moreover, adhesion of microspheres on the stomach wall was well observed (47% and 20% remained in the stomach after 2 and 4 h, respectively). The authors concluded that these mucoadhesive microspheres with an appropriate antimicrobial agent could be used for the eradication of *H. pylori*. In the particular case of *H. pylori* eradication, the ideal dosage form should, to be effective, not only stay in the stomach, but also target the bacterium (Bardonnet, Faivre, Pugh, Piffaretti, and Falson, 2006).

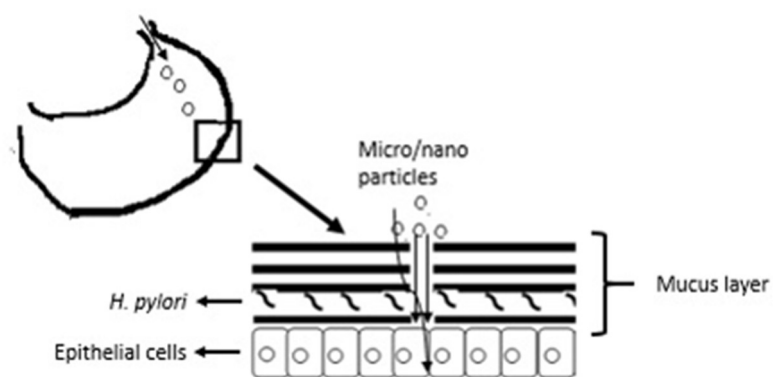


Figure 2. 7. Mucoadhesive delivery system for *H. pylori* eradication

Table 2. 7. Alternative drug delivery systems for *H. pylori* treatment

Polymer	System	Used Technique	Crosslinking Agent	Drug	Source
Chitosan Polyacrylic Acid	Hydrogel	Spray drying	-	Amoxicillin	(Torre et al., 2003)
Chitosan	Microsphere	Emulsification	Glutaraldehyde	Amoxicillin	(Patel and Patel, 2007)
Chitosan	Microsphere	Emulsification	Glutaraldehyde	Clarithromycin	(Majithiya and Murthy, 2005)
Chitosan Polyacrylic Acid	Hydrogel	Spray drying	-	Amoxicillin	(Torre et al., 2005)
Chitosan	Microsphere	Ionic crosslinking/ Precipitation	-	Tetracycline	(Hejazi and Amiji, 2002)
Chitosan	Microsphere	Chemical crosslinking/ Precipitation	Glyoxal	Tetracycline	(Hejazi and Amiji, 2004)
Chitosan Polyethylene oxide	Hydrogel	Spray drying	Glyoxal	Amoxicillin metranidazole	(Patel and Amiji, 1996)
Chitosan Polyacrylic Acid	Hydrogel	Spray drying	-	Amoxicillin	(Torrado et al., 2004)

## 2.6. Nanocomposites in Drug Delivery

Microsphere is one of the most promising forms as drug delivery system because it can be easily injected or administrated orally into body easily, targeted to the desired

site, prolong the half-life and improve the bioavailability of the encapsulated drug. It is known that as the particle size decreases from micro to nanoscale, the properties of polymer composites increases remarkably. Especially chitosan microspheres when brought in contact with acidic media tend to release the active agent rapidly resulting a burst effect and degrade easily. Initial burst effect is a common problem encountered with chitosan based delivery systems when loaded with water-soluble drug, and hence, their utility for the controlled delivery of drugs in gastrointestinal tract is questionable. To overcome initial burst problems, considerable attempts have been made to improve the preparation method of chitosan microspheres by coating or grafting with other polymers.

Nanocomposites generally consist of a polymer matrix and a discontinuous phase or filler. To improve properties of biomaterials or modify polymers, inorganic fillers at nanoscale are incorporated into polymer matrix (Aguzzi et al., 2010). Polymer/clay based nanocomposites have been also proposed for drug delivery/release applications in biomedical and pharmaceutical applications (Hua et al., 2010). Layered silicates are used as inorganic filler and polymer/nanoclay microspheres are nomenclatured as chitosan nanocomposite microsphere in this study. The addition of nanoparticles provides tortuous pathway to allow slower drug release and more controlled release and reduced swelling and improved mechanical properties of polymer nanocomposites (Figure 2.8) (Paul and Robeson, 2008). It has been reported that nanocomposites such as polymer layered silicate composites have the ability to protect drugs from the degradation and improve stability in gastrointestinal tract as well as providing targeted delivery of drugs to various areas of the body. This technology enables the delivery of poorly soluble drugs and preventing the first pass metabolism. The challenges with use of large size materials in drug delivery are poor bioavailability, *in vivo* stability, solubility, intestinal absorption, sustained and targeted delivery to site of action, therapeutic effectiveness, generalized side effects, and plasma fluctuations of drugs (Maniruzzaman et al., 2012). The extent of clay:polymer interaction is influenced by the degree of dispersion, the size and shape, and the surface properties of the clay particles and level of dispersion affects nanocomposite properties such as diffusion pathway, mechanical properties and also release behaviour (Theng 1970). Therefore, the effect of nanoclay intercalation on microsphere properties and drug release profiles were discussed in this dissertation. The next section explains the importance of nanocomposite structure.

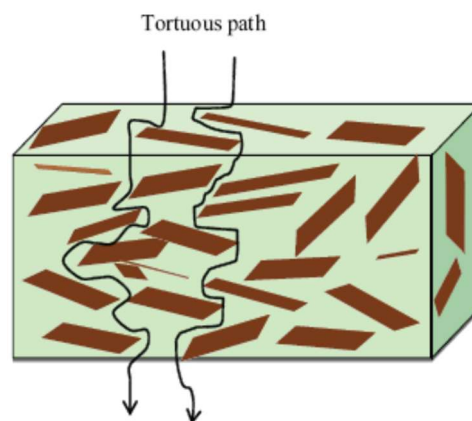


Figure 2. 8. Scheme of the mechanism of barrier improvement by the addition of clay platelets

### 2.6.1. Structure and Properties

Layered silicates are classified according to types and unit crystal lamellae. The layered silicates are divided into main 3 categories: 1:1 type, 2:1 type and 2:2 type.

- **1:1 type:** Its unit lamellar crystal is composed of one crystal sheet of silica tetrahedron combined with one-crystal lamellae of alumina octahedron.
- **2:1 type:** Its unit lamellar crystal is composed of two crystal sheets of silica tetrahedron combined with one crystal sheet of alumina octahedron between them.
- **2:2 type:** Its unit lamellar crystal is composed of four crystal sheets, in which crystal sheets of silica tetrahedron and alumina or magnesium octahedron are alternately arranged.

One of the mostly used layered silicates for the preparation of polymer/layered silicate nanocomposites (PLSN) belong to the 2:1 layered- or phyllosilicates. The layer thickness is about 1 nm, while the lateral dimensions of these layers may range from a few nanometers to several microns or several hundreds of microns, depending on the layered silicate, the source of the clay and the preparation method. Therefore, clays have high aspect ratio. The layers of the silicates form self-organized stacks with a regular Van der Waals gap in between layers named as interlayer or the gallery. Intermolecular forces between layers and Van der Waals interaction energy hold stacks together depending on interlamellar spacing. Small molecules including water, solvents, and monomer as well as polymer, can enter into these galleries and causes the expansion of the lattice (Figure 2.9). The d-spacing is the repeat unit in the crystalline structure including the 1 nm thick

platelet and the spacing in between the platelet sheets and characteristic value for each type of layered silicate (Cossio et al. 2012; Utracki, 2004).

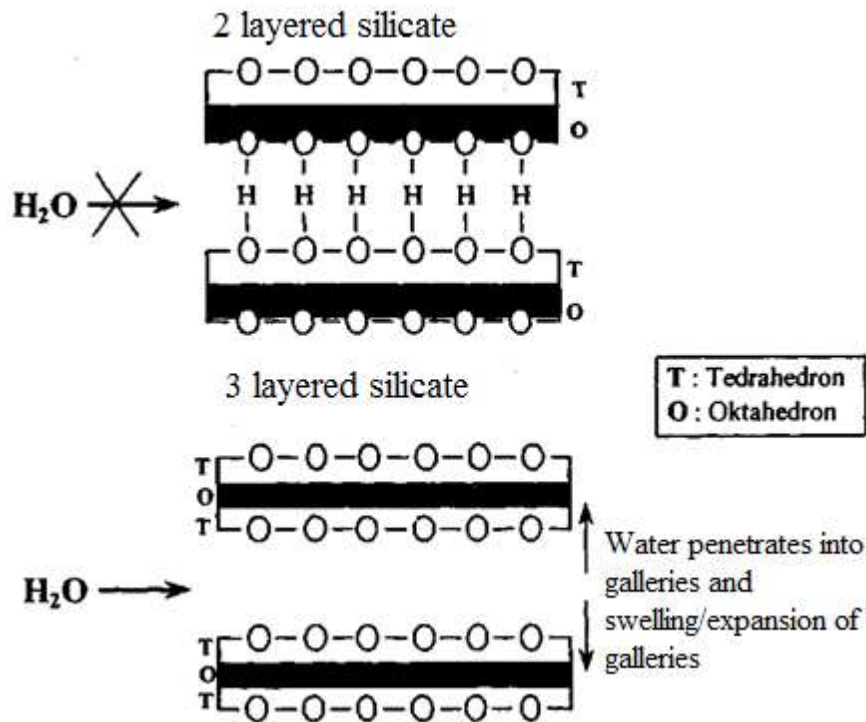


Figure 2. 9. Swelling and cation exchange of clays

Chemical composition and crystal structure of clays are important parameters for their applications. Clays have different chemical compositions: for example, kaolinite has a high content of alumina and low content of silica whereas montmorillonite (MMT) has a low content of alumina and a high content of silica. Different characteristics of three common layered silicates of clay minerals were compared in Table 2.8.

Table 2. 8. Crystal structure and properties of three kinds of clay minerals (Source: Cossio et al, 2012)

Clay	Layer type	Distance between layers (10-1 nm)	Attractive forces between layers	CEC (mmol/100 g clay)
Kaolinite	1:1	7.2	Hydrogen bonds, very strong	3-15
MMT	2:1	9.6-40	Intermolecular force, weak	70-130
Illite	2:1	10	Electrostatic, strong	20-40



Montmorillonite (MMT) is one of the mostly used layered silicate for polymer nanocomposites and a member of smectites or phyllosilicate clay family. Montmorillonite has a 2:1 structure consisting of triple layer sandwich structure that consists of a central octahedral sheet dominated by alumina, bonded to two silica tetrahedral sheets by oxygen ions that belong to both sheets. Additionally, there are hydroxyl groups at the edges of each clay platelet (Figure 2.10) (Utracki, 2004; Cuppoletti, 2011). The general formula and structure of MMT is given (Cuppoletti, 2011):

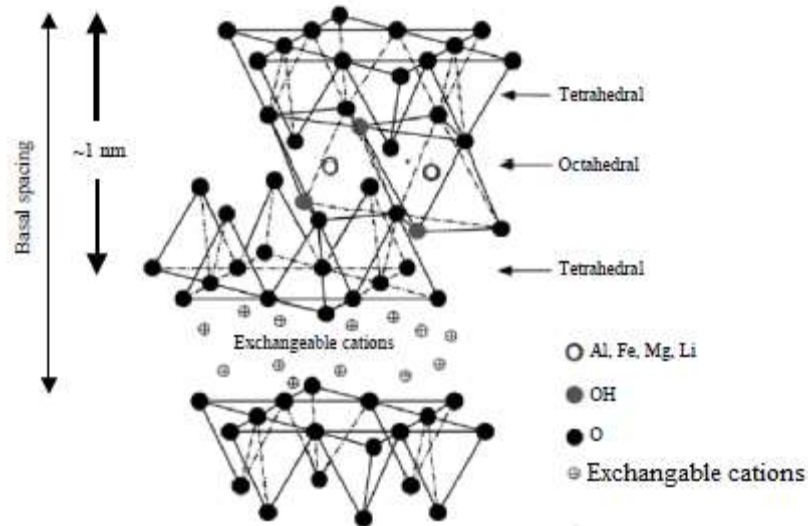
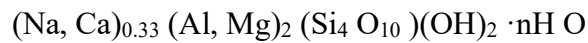


Figure 2. 10. Sandwich structure of 2:1 layered silicate  
(Source: Okamoto, 2009)

Pure silica oxide (quartz) has no charge. In comparison, most of the clay minerals tend to have a negative charge due to the isomorphous substitution in the clay-sheet structure. This isomorphous substitution leads to tendency of clay sheets to positive charges (Uddin, 2008). Isomorphous substitution occurs between some atoms in the crystal structure and other atoms with different valence without any change in the crystal structure. Isomorphous substitution can take place in both octahedral and tetrahedral lattices. For example, a portion of  $\text{Si}^{4+}$  in tetrahedral sheets can be replaced with  $\text{Al}^{3+}$ , and a part of  $\text{Al}^{3+}$  in octahedral lattice can be substituted with  $\text{Mg}^{2+}$ ,  $\text{Fe}^{2+}$  or  $\text{Zn}^{2+}$  or  $\text{Mg}^{2+}$  replaced by Li. For example, an isomorphous substitution between  $\text{Mg}^{2+}$  and  $\text{Al}^{3+}$  in the

octahedral lattice results negative charge which is counterbalanced by cations – mainly sodium and calcium ions, existing hydrated in the interlayer (Cuppoletti, 2011; Ke and Stroeve, 2005). Incorporation of nanoscale filler into host polymers improves polymer nanostructured composites in comparison to traditional fillers. Since the nanocomposite structure depends on the polymer-layered silicate compatibility and on the processing conditions, the enhancement in properties is highly depending on the dispersion of layered silicates in polymer matrix. The dispersion of layered silicates is mainly defined as intercalated or exfoliated structures. Structure of layered silicates in polymer matrix depends on the nature of the polymer (molecular weight, polarity etc.) and layered silicate (organomodification, etc). Besides, preparation method of polymer nanocomposites is also a key parameter that affects dispersion level of layered silicates in polymer matrix.

There are three main types of clay dispersion in polymer matrix. Various polymer/clay structural configurations and dispersion level of layered silicates in polymer matrix have been shown in Figure 2.11. They are classified according to level of dispersion:

**1. Phase separated structure:** The polymer is unable to intercalate within the clay layers. Therefore, clay particles are dispersed as aggregates and found as stacks in the polymer matrix. This composite structure is referred as “phase separated”.

**2. Intercalated structure:** Incorporation of clay in polymer causes to the increasing of the inter layer spacing. Although polymer chains in the clay galleries causes to the decreasing of electrostatic forces between the layers, clay layers are not fully dispersed and dissolved. Thus, clay layers have well-ordered multilayer morphology.

**3. Exfoliated structure:** Exfoliated or delaminated structure is obtained when clay layers are fully separated one another and individual layers are dispersed within the polymer matrix. Due to the well dispersion of individual clay layers, high aspect ratio is obtained and therefore lower clay content is required for exfoliated nanocomposites. This exfoliated structure is important because of surface interactions between polymer and clay leading to significant improvement and enhancement of polymer properties (Utracki, 2004).

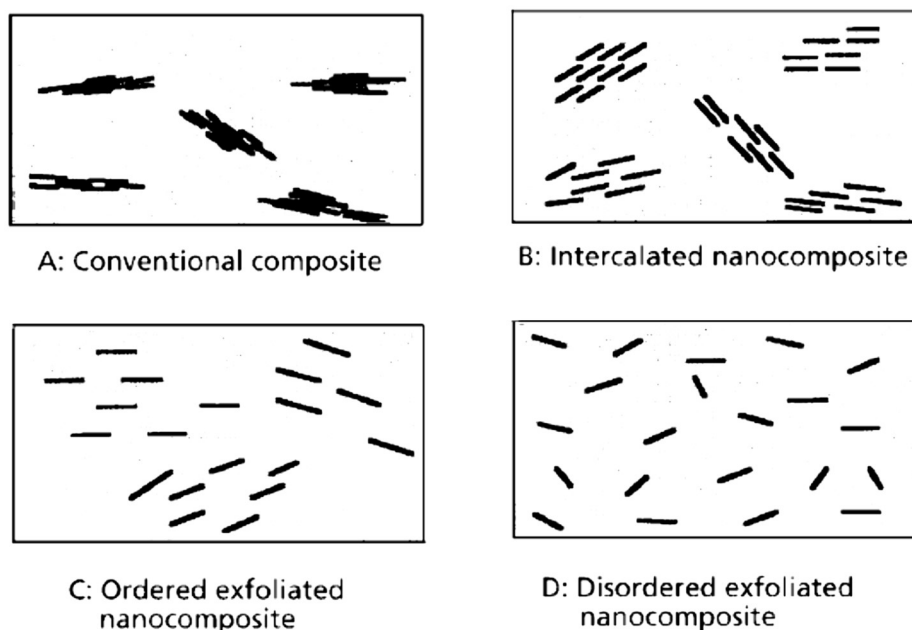


Figure 2. 11. Dispersion of clay platelet in a polymeric matrix  
(Source: Utracki, 2010)

## 2.6.2. Pharmaceutical Applications

Clay minerals are among the most widely used materials in pharmaceutical formulation, because of their properties as excipients and/or their biological activities. These features depend on both their colloidal dimensions and high surface areas, resulting in optimal rheological characteristics and/or sorption capacities. Clay minerals are classified according to their functionality as excipient in solid dosage forms (Table 2.9).

Table 2. 9. Use of clay minerals as excipients in solid dosage forms

Excipient	Dosage form	Function
Kaolin	Tablets and capsules	Diluent and adsorbent
Tale	Tablets, capsules and powders	Coating aid, lubricant, diluent and glidant
Bentonite	Tablets, capsules and granules	Adsorbent, binder and disintegrant
Magnesium Amulinium silicate		
Magnesium Trisilicate	Tablets and capsules	Adsorbent, glidant, binder and disintegrant

Silicate minerals are characterized by a layered structure and exhibit properties such as good water absorption, swelling, adsorbability and cation exchange ability that are considered beneficial from the viewpoint of synthesis of pharmaceutical products, as both inactive and active substances. In this regard, clay minerals have been used as stabilizers or emulsifying agents for the formulation of liquid drugs – in this case it was observed that the bioavailability of drugs was reduced. This led to the suggestion that an interaction between the drug and clay inhibited or delayed release of the drug. Clay minerals are natural cationic exchangers and thus can bind with cationic drugs in solution via electrostatic interaction. Depending on the cation exchange capacity of the clay, the cationicity of the drug and pH of the release medium determine the kinetics of drug release. Apart from electrostatic force, there also exist the possibility of other interactions, including hydrophobic, hydrogen bonding, ligand exchange and water bridging. These properties have encouraged the use of clay minerals for sustained release of drugs and improved drug dissolution.

The main advantages of chitosan–clay nanocomposite carrier are: (a) the intercalation of cationic chitosan in the expandable aluminosilicate structure of clay is expected to neutralize the strong binding of cationic drug by anionic clay; (b) the solubility of chitosan at the low pH of gastric fluid will decrease and premature release of the drug in the gastric environment can be minimized; (c) cationic chitosan provides the possibility of efficiently loading negatively charged drugs compared with clay; and (d) the presence of reactive amine groups on chitosan provides ligand attachment sites for targeted delivery (Aguzzi et al., 2010).

The use of silicate clay minerals in controlled release systems takes attention in recent years and several research studies have been performed. Depan et al., (2009) developed Ibuprofen loaded chitosan-g-lactic acid and MMT hybrids in the form of film and porous scaffold for controlled delivery and tissue engineering applications. MMT incorporation controlled the drug release rate and swelling property decreased by increased MMT content. Chitosan/MMT based hydrogel systems wherein Ofloxacin was a model drug, improved drug loading and release in both SGF and pH 7.4 (Hua et al., 2010). In another study based on chitosan/MMT hydrogel wherein Thyophylline was model drug, swelling degree and release kinetic constant,  $k$  decreased with increased clay content (Cojocariu et al., 2012). Sarmah et al. 2015 prepared gelatin/MMT nanoparticles loaded with Isoniazid. They found that swelling degree and release (%) decreased with increased MMT and

gluteraldehyde content. The mucoadhesivity of the nanoparticles increased with increased MMT content.

Nanoclays could also be directly used in gastroretentive applications. For example, a cationic montmorillonite nanoclay, MMT, exhibits enhanced gel strength, mucoadhesive capability to cross the gastrointestinal (GI) barrier and adsorb bacterial and metabolic toxins such as steroidal metabolites. MMT is a common ingredient as both the excipient and active substance in pharmaceutical products. Interaction between clay minerals and different organic groups is given in Table 2.10. Cationic drugs can be intercalated into MMT by ion exchange (Ha and Xanthos, 2011; Hua, Yang, Wang, et al., 2010).

Table 2. 10. Interactions between clay minerals and organic compounds  
(Source: Suresh et al., 2010)

<b>Mechanism</b>	<b>Examples</b>	<b>Organic functional groups</b>
Hydrophobic interaction (Vander Waals)	Clay with neutral sites (kaolinite, smectites)	Uncharged, non-polar
Hydrogen bonding	Clay with oxygen surfaces	Amines, carbonyl, carboxyl,
Protonation	(kaolinite)	heterocycle N
Ligand exchange	Aluminosilicate edge sites,	Amines, carbonyl,
Cation exchange	Fe & Al oxides, imogolite	carboxylate, heterocycle N
pH dependent charge sites	Aluminosilicate edge sites, Fe & Al oxides, imogolite	Carboxylate, phenolate
Cation bridging	Smectite, vermiculite, illite	Amines, ring NH, heterocycle N
Water bridging	Aluminosilicate edge sites, Fe & Al oxides, imogolite Smectite, vermiculite, illite	Carboxylate for anion exchange, amines, ring NH, heterocycle N for cation exchange Carboxylate, amines, carbonyl, alcoholic-OH

Forano has used antibiotic-clay compounds in the treatment of gastric ulcer caused by *H. pylori* and it was found that addition of clay improved the penetration of the drug through the gastrointestinal barrier compared to pure antibiotic use (Forano, 2004).

## CHAPTER 3

# MICROENCAPSULATION OF ESSENTIAL OILS FOR PHARMACEUTICAL APPLICATION

### 3.1. General Aspects

Microencapsulation is a process that entraps active compounds within a matrix or another substance (wall material) to achieve desirable effects. The material inside the microcapsule is referred to as the core, internal phase, or fill, whereas the wall is named as shell, coating, or membrane. Especially in the food and pharmaceutical industry, encapsulation process can be applied for a variety of reasons. Encapsulation is a useful tool to improve delivery of bioactive molecules (e.g. antioxidants, minerals, vitamins, phytosterols, lutein, fatty acids, lycopene) and living cells (e.g. probiotics) into foods (Nedovic et al., 2011; Sahil et al., 2011). Oils are encapsulated for various reasons, such as for conversion of liquid to solid form to facilitate handling, transportation or incorporation into other components. Oil encapsulation provides taste/smell masking, protection from evaporation or oxidation as well as controlled-release applications. Encapsulation of many different oils including including fish oil, alpha-tocopherol, wheat germ oil, evening primrose oil, lemon oil, and citronella oil for nutrition, therapeutics, flavoring or aroma has been reported up to the present. The choice of encapsulation material and process is governed by three main criteria: the application, economics and safety (Chan, 2011). Additionally there are some design criteria in microencapsulation process (Table 3.1).

**Size:** Size of micro/nanospheres may be critical to the desired function of an assay. Particle size, shape, and surface properties play a crucial role in the cellular absorption and uptake of delivery systems across the mucosal membrane. Nanosized systems may may increase bioefficacy. The nanocarriers with particle size of 50–300 nm, positive zeta potential and hydrophobic surface are more preferable for uptake in comparison to their counterparts.

**Hydrophobicity:** Surface hydrophobicity is important in cell interaction and cell spreadability. In general, polymeric particles and beads are hydrophobic and therefore have high protein binding abilities. However, surfactant such as tween or SLS is required in order to enhance solubility properties of poorly soluble drugs or bioactives.

**Charge:** Surface charge has an effect on the interaction of microspheres with charged drugs, and also on the adhesion of drug delivery systems onto biological surfaces. It allows site specific binding and targeting action site such as mucosal surfaces.

Table 3. 1. Main considerations in microencapsulation parameters  
(Source: Sahil et al., 2011)

Property	Parameter
Size	Diameter Uniformity/distribution
Composition	Density Refractive index Hydrophobicity Nonspecific binding Autofluorescence
Surface chemistry	Reactive groups Functionalization Charge
Special properties	

Microencapsulation is mostly applied when isolating the core material such as vitamins from the deteriorating effects of oxygen, retarding evaporation of a volatile core, improving the handling properties of a sticky material, or isolating a reactive core from chemical attack are required. Even when the aim of a microencapsulation application is the isolation of the core from its surrounding, the wall must be ruptured at the time of use. Many walls are ruptured easily by pressure or shear stress. Also, capsule contents may be released by melting the wall, or dissolving it under particular conditions, as in the case of an enteric drug coating. In other systems, the wall is broken by solvent action, enzyme attack, chemical reaction, hydrolysis, or slow disintegration (Gouin, 2004).

### **3.1.1. Advantages and Limitations of Encapsulation**

The encapsulation of bioactive molecules has some advantages in comparison to conventional methods:

1. Microencapsulation (e.g. microspheres) provides constant and prolonged therapeutic effect.
2. Reduces the dosing frequency and thereby improve the patient compliance.
3. Micro/nanospheres could be easily injected into the body due to the spherical shape and smaller size.
4. Better drug utilization will improve the bioavailability and reduce the incidence or intensity of adverse effects.
5. Microsphere morphology allows a controllable variability in degradation and drug release.
6. Encapsulation technique protect the user/patient from side effects of direct contact of bioactive agent.

There are also some disadvantages. These limitations and disadvantages could be listed as:

1. The modified release from the formulations.
2. The release rate of the controlled release dosage form may vary from a variety of factors like food and the rate of transit though gut.
3. Differences in the release rate from one dose to another.
4. Controlled release formulations generally contain a higher drug load and thus any loss of integrity of the release characteristics of the dosage form may lead to potential toxicity (Sahil et al., 2011).

### **3.2. Production Techniques**

Encapsulated product such as micro/nanospheres, and nanoemulsions are widely used in different applications including food, pharmaceutical, agricultural, biotechnology, biomedical and biosensor industries. To date, various microencapsulation methods were developed listed in Table 3.2. Although there are several techniques for



encapsulation of bioactive agents such as essential oils, these techniques have some advantages and disadvantages when compared each other (Table 3.3).

Table 3. 2. Different techniques for microencapsulation

<b>Chemical processes</b>	<b>Physico-chemical</b>	<b>Physico-mechanical</b>
<ul style="list-style-type: none"> <li>• Suspension, dispersion and emulsion polymerization</li> <li>• Polycondensation</li> </ul>	<ul style="list-style-type: none"> <li>• Coacervation/Phase separation</li> <li>• Layer by layer (LBL) assembly</li> <li>• Solvent evaporation</li> <li>• Ionotropic gelation</li> <li>• Emulsification/Crosslinking</li> </ul>	<ul style="list-style-type: none"> <li>• Spray-drying</li> <li>• Fluidized bed coating</li> <li>• Centrifugal extrusion</li> <li>• Hot melt extrusion</li> <li>• Electrospray</li> <li>• Lyophilization</li> </ul>

Table 3. 3. Comparison of different techniques

<b>Method</b>	<b>Advantages</b>	<b>Disadvantages</b>
Spray drying	Rapid drying Easily scale-up Single-stage and simple method Can be operated continuously Low cost	Temperature sensitive products
Coacervation	Useful for high value active molecules or unstable substances High payloads	Particles are not perfectly spherical High production cost
Emulsification/crosslinking Solvent evaporation	Stability of spheres	Exposure of bioactive to chemicals

### 3.2.1. Spray Drying

Spray-drying is a well-known technique to produce powders, granules or agglomerates from the mixture of drug-excipient solutions and suspensions. The method is based on drying of atomized droplets in a stream of hot air.

In this method, the solution or dispersion containing active ingredient is atomized in a stream of hot air by nozzle using compressed gas to atomize the liquid feed or rotary

atomizer using a wheel rotating at high speed. This heated gas directly comes into contact with feed via gas dispenser. Atomization leads to the formation of small droplets as a result of solvent evaporation as seen in Figure 3.1. Spray drying is very rapid drying method because of very large surface area created by atomization of feed. The main advantages of this method are easily scale-up, low cost and flexible process which makes it an attractive process in food and pharma industry. Also, it is a single-stage including encapsulation and drying process and simple method which can be operated continuously. Although the main advantages of spray-drying, processing variables must be well controlled to avoid difficulties such as low yields, sticking, or high moisture content, which are often encountered with laboratory scale spray dryers. The optimization of spray drying process involves parameters related with spray-dryer and feed formulation (Rokstad et al., 2014). Various process parameters are to be controlled to get the desired size of particles. Particle size depends upon the size of nozzle, spray flow rate, atomization pressure, inlet air temperature and extent of crosslinking (Agnihotri et al., 2004).

Spray drying is a very popular method. Recently, a number of articles have been published related with the preparation of microspheres by spray drying methods. For example, He et al., (1999) prepared crosslinked and uncrosslinked chitosan microspheres by spray drying for the delivery of cimetidine, famotidine, nizatidine and vitamin C. Glutaraldehyde was used in most of the studies as a crosslinker agent. Conti et al. produced cetylpyridinium chloride, an anti-infective agent chitosan microspheres by spray-drying method containing crosslinking agents. Extent of crosslinking was controlled by crosslinking time. Agnihotri et al. (2004) reported that spray drying technique is fast, simple and reliable method to obtain microspheres. Microspheres were prepared by spray drying of aqueous chitosan dispersions containing metoclopramide hydrochloride using different amounts of formaldehyde as a cross-linker. Microspheres released the drug for more than 8 h, independent of the pH of the medium.

The particle size of the microspheres prepared by spray drying method ranged from a few microns to several tens of microns, and had a relatively narrow distribution. The microspheres were positively charged in order to enhance the mucoadhesive properties and make these suitable for delivery of drugs via the nasal or gastrointestinal routes of delivery ( He et al., 1999; Desai et al., 2006).

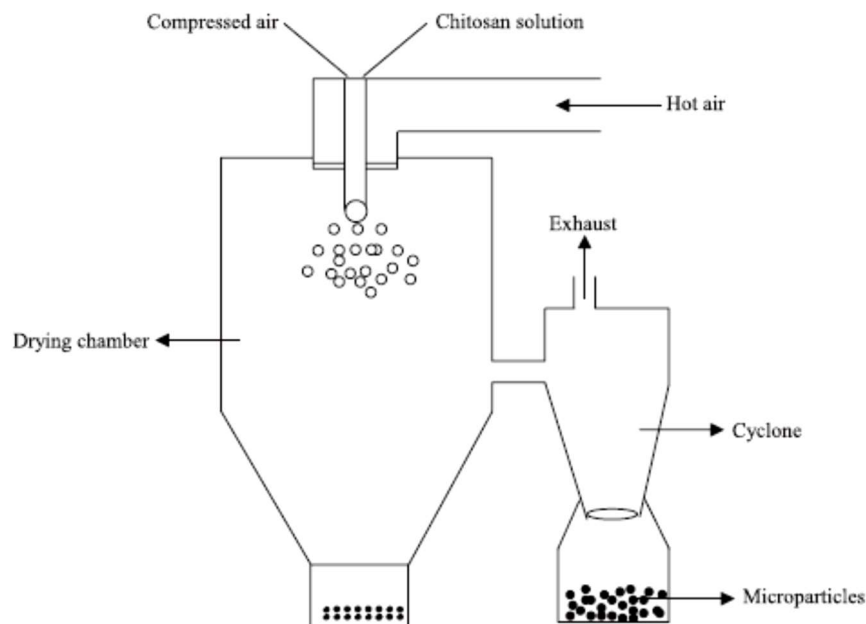


Figure 3. 1. Schematic illustration of microsphere formation by spray drying  
(Source: Agnihotri et al., 2004)

In this study, spray drying was selected for preparation of cinnamon oil loaded chitosan microspheres and nanocomposite microspheres. Because, it is a rapid high-yield technique and applicable at industrial scale and that enables small microspheres to be obtained from polymers.

### 3.2.2. Encapsulation by Supercritical Fluids

In recent years, using of supercritical fluid technology in encapsulation process takes attention due to the fact that satisfy the disadvantages of other methods such as using large quantity of organic solvents, toxic residues, requirement of post-treatment procedures. The properties of supercritical fluids can be thought as intermediate between liquid and gas. These properties can be easily changed depending on temperature and pH. Carbon dioxide has low critical temperature ( $T_c=304$  K) and pressure ( $P_c=7.38$  MPa) which makes it one of the most used supercritical fluid especially for processing of heat-sensitive materials.

### 3.2.3. Ionotropic Gelation

This technique consists of the ionic cross-linking of chitosan with low molecular weight counterions, hydrophobic counterions and high molecular weight ions. The use of complexation between oppositely charged macromolecules to prepare chitosan microspheres has attracted much attention because the process is very simple and mild. In addition, reversible physical cross-linking by electrostatic interaction, instead of chemical cross-linking, has been applied to avoid the possible toxicity of reagents and other undesirable effects. Sodium tripolyphosphate (TPP) is commonly used crosslinker to provoke the ionotropic gelation of chitosan. Tripolyphosphate (TPP) is a polyanion, which can interact with the cationic chitosan by electrostatic forces. In the ionic gelation method, chitosan is dissolved in aqueous acidic solution to obtain the cation of chitosan. This solution is then added dropwise under constant stirring to polyanionic TPP solution. Due to the complexation between oppositely charged species, Chitosan undergoes ionic gelation and precipitates to form spherical particles (Figure 3.2) (Agnihotri et al., 2004; Paños et al., 2008).

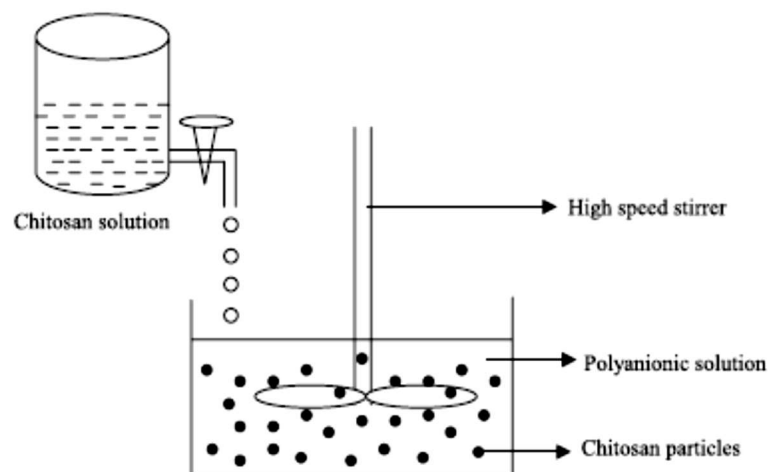


Figure 3. 2. Formation by ionotropic gelation  
(Source: Agnihotri et al., 2004)

### 3.2.4. Emulsification-Solvent Evaporation

The emulsification-solvent evaporation method consists of preparing an emulsion, with different external phase depending on the nature of the polymer and the drug used

for the encapsulation, and evaporating the solvent with the subsequent formation of the microspheres. When the drug for encapsulation is hydrophobic, the method changes and the emulsion to be prepared must have an organic internal phase (Paños et al., 2008).

### **3.2.5. Coacervation**

Coacervation techniques involve the separation of a polymer solution into two coexisting phases: a dense coacervate phase, which is rich in colloids and a diluted equilibrium phase or supernatant, which is poor in colloids. Coacervation in aqueous systems is subdivided into simple and complex coacervation. Simple coacervation is one of the oldest and widely used microencapsulation methods wherein active agent (liquid or solid) is dispersed in a homogeneous aqueous polymer solution. The formation of polymer aggregates (coacervates) is brought about by a change in temperature or pH. Thus, the polymer is deposited on an active agent surface, leading to the formation of microcapsules. Hydrophilic polymers such as gelatin, PVA, methyl cellulose and cellulose acetate are mostly used in this process.

Complex coacervation is similar to simple coacervation where another complimentary polyelectrolyte is used. It is the separation of an aqueous polymeric solution into two miscible liquid phases: a dense coacervate phase and a dilute equilibrium phase. The dense coacervate phase wraps as a uniform layer around suspended core materials. Complex coacervation parameters are the pH, the ionic strength, the temperature, the molecular weight and the concentration. It occurs with the neutralization of two oppositely charged polymers.

## **3.3. Pharmaceutical Applications of Essential Oils**

The controlled release formulations have several advantages in comparison to conventional formulations. The controlled release of EOs offers improved efficacy, reduced cytotoxicity, improved patient compliance and convenience. Particle size, morphology and release rate of bioactive molecules at target site should be taken into consideration when design a micro/nanoparticle system (Pedro et al., 2013).

Natural products and their derivatives represent more than 50% of all the drugs in clinical use in the world. Essential oils are volatile, natural, complex compounds characterized by a strong odour and are formed by aromatic plants as secondary metabolites. Since the middle ages, essential oils have been widely used as therapeutic products for bactericidal, virucidal, fungicidal, antiparasitical, insecticidal, medicinal and cosmetic applications, especially nowadays in pharmaceutical, sanitary, cosmetic, agricultural and food industries. They have antibacterial, antiviral, anti-inflammatory, anticarcinogenic and antioxidant properties. EOs are used in preservation of foods and as antimicrobial, analgesic, sedative, anti-inflammatory, spasmolytic and locally anesthetic treatments due to their antiseptic, medicinal properties and fragrance (Bilia et al., 2014). Because of the extraction method, mostly by distillation from aromatic plants, they contain a variety of volatile molecules such as terpenes and terpenoids, phenol-derived aromatic components and aliphatic components.

Essential oils, as natural sources of phenolic components, are evaluated for their activity as antioxidants or free radical scavengers. The essential oils of basil, cinnamon, clove, nutmeg, oregano and thyme have been proven radical-scavenging and antioxidant properties in the DPPH radical assay at room temperature. Essential oils are a rich source of biologically active compounds. There has been an increased interest in looking at antimicrobial properties of extracts from aromatic plants particularly essential oils. Therefore, it is reasonable to expect a variety of plant compounds in these oils with specific as well as general antimicrobial activity and antibiotic potential.

There are 3000 essential oils are known, of which 300 are commercially important in 300 of which are commercially important especially for the pharmaceutical, agronomic, food, sanitary, cosmetic and perfume industries. Chemically they are derived from terpenes and their oxygenated compounds. Each of these constituents contributes to the beneficial or adverse effects. Essential oils such as aniseed, calamus, camphor, cedarwood, cinnamon, citronella, clove, eucalyptus, geranium, lavender, lemon, lemongrass, lime, mint, nutmeg, orange, palmarosa, rosemary, basil, vetiver and wintergreen have been traditionally used by people for various purposes in different parts of the world. Cinnamon, clove and rosemary oils had shown antibacterial and antifungal activity; cinnamon oil also possesses antidiabetic property (Prabuseenivasan et al., 2006).

It is known that from the literature, cinnamon essential oil has antimicrobial activity. Cinnamon bark, leaves, flowers and fruits can be used to prepare essential oils. The volatile components and chemical composition of cinnamon essential oils depend on

the part of the plant from which they are extracted. For example, in cinnamon leaf essential oil, the main component is eugenol with 80% of the composition whereas in the essential oil extracted from cinnamon fruit and flowers, (*E*)-cinnamyl acetate and caryophyllene are the major components. In cinnamon bark essential oil, cinnamaldehyde is the major component, with a content ranging from 60% to 80% depending on the type of extraction (Ooi et al., 2006; Singh et al., 2007; Nabavi et al., 2015).

### **Antimicrobial activities:**

Several research were conducted in order to investigate antimicrobial effects of different EOs and lemongrass, oregano, peppermint, rosemary, clove, thyme, lemon and cinnamon oil were shown as large spectrum antimicrobial agents. Use of natural medicinal extracts such as essential oils fulfils several pharmaceutical applications and in vivo patient care. It has been shown that essential oils have antibacterial, antifungal, antiviral and antioxidant properties due to their biologically active compounds such as carvacrol, eugenol, and thymol. It has been reported that many EOs, such as thyme oil, lavender, clove, peppermint, cinnamon, tea tree, rosemary, eucalyptus, lemongrass exhibit particular antimicrobial properties activity whereas lemon and rosemary oils also have antioxidant property (Ioannis Liakos et al., 2014; Altioek et al., 2010).

The high hydrophobicity and short carbon chains of EOs components provide interaction with lipid cell membranes. The oil constituents can pass the cell membrane and bind in order to inhibit specific proteins (Pedro et al., 2013). Essential oils destabilize and damage of phospholipid bilayer of cell membranes, enzyme systems and genetic material of bacteria (Abdollahzadeh et al., 2014). It has been reported that they can adhere to or intercale into DNA or RNA. Although the mechanism is not fully understood, the components of EOs effect synergistically and reduce possible resistance. Therefore they are promising bioactive agents to combat against microorganisms in comparison to synthetic antibiotics. Peng and Li (2014) reported that lemon, thyme, cinnamon oil and combinations were incorporated into chitosan film solutions showed antimicrobial activity against *E. coli* and *S. aureus*. They indicated that *S. aureus* was found more sensitive to film solutions than *E. coli*, due to the relatively impermeable outer membrane that surrounds Gram-negative bacteria whereas Altioek et al. (2010) showed that thyme oil incorporated chitosan films was more effective on *E. coli*.

### **Anticancer and antimutagenic activities:**

EOs from aromatic plants possess anticancer properties. Although EOs based therapy cannot be a substitute to the standard chemotherapy and radiotherapy but it could be used in combination with cancer therapy to decrease the side effects of the drugs. Anticancer activity of EOs could be attributed to chemoprevention and cancer suppression. Mechanisms involved in cancer treatment are activation of detoxification enzymes, modulation of DNA repair signaling, antimetastasis, and antiangiogenesis. This makes EOs suitable anticancer agents with no huge effects on the normal cells (Gautam et al., 2014). Recent studies shown that certain essential oils exhibited antimutagenicity toward mutation caused by UV lights. Antimutagenic properties of EOs could be attributed to inhibition of penetration of the mutagens into the cells, inactivation of the mutagens by direct scavenging, antioxidant scavenging of radicals produced by mutagen or activation of cell antioxidant enzymes, inhibition of metabolic conversion by P450 of promutagens into mutagens or activation of enzymatic detoxification of mutagens for instance by plant extracts. Some EOs exhibit strong anti-mutagenic activity which could be related to anticarcinogenic activity. Also recent studies showed that some constituents of EOs efficiently reduce local tumor volume or tumor cell proliferation by apoptotic and/or necrotic effects (Bakkali et al., 2008). For example, Limonene which is the major component in many Citrus essential oils, has chemo-preventive and therapeutic effects against mammary tumors in rats and metastasis of human gastric cancer (Shaaban et al., 2012).

### **Antioxidant and Anti-inflammatory:**

Some essential oils have antioxidant activity by free radical scavenging, inhibition of lipid peroxidation. EOs have also anti-inflammatory activity. The anti-inflammatory activities of EOs could not be attributed not only to their antioxidant activity but also their interactions with signaling cascades including cytokines and regulatory transcription factors. For example, cinnamaldehyde, isolated from an essential oil produced from the leaves of *Cinnamomum osmophloeum*, was reported to inhibit the secretion of IL-1 $\beta$  and TNF- $\alpha$  within LPS or lipoteichoic acid (LTA) stimulated murine J774A.1 macrophages. It was reported that cinnamaldehyde also suppressed the production of these cytokines (Miguel, 2010). As a result, it could be indicated that cinnamaldehyde shows



antiinflammatory activity by decreasing inflammatory enzymes and mediators and by increasing antiinflammatory mediators (Pannee et al., 2014).

### **3.3.1. Encapsulated Essential Oils**

One of the most common way to use EOs is by external application such as mouthwashes, topical applications. Also they are used orally even if it is generally regarded as safe (GRAS) to ingest. They should be diluted with milk, soy milk, or olive oil if they are taken orally. Although topical application is generally safe, the EO can cause some skin reactions and irritation. Besides, EOs can easily decompose due to direct exposure to heat, humidity, light, or oxygen (Bilia et al., 2014). Because of all above these reasons, encapsulation technology is an efficient tool for improving the stability and efficacy of essential oil-based formulations used in pharmaceutical and biomedical applications (Sarmiento et al., 2008). As alternative routes of administration of EOs are oral intake and inhalation, the delivery systems encounter the mucosal lining of the nasal, lung, oral cavity, stomach, and gut. Nanocarriers also provide the desired therapeutic levels in target tissues for the required duration time with lower dose frequency, and might ensure an optimal pharmacokinetic profile to meet specific requirements. Among various absorption mechanisms, two mechanisms have been predominantly used: the paracellular route and transcellular route which is responsible for the transport of lipophilic drugs that show a rate dependency on their lipophilicity. Drug also passes cell membranes by an active transport route via carrier-mediated means or transports through the opening of tight junctions interacting with the tight junction proteins. Mechanism of delivery systems penetration through enteric mucosa is presented in Figure 3.3.

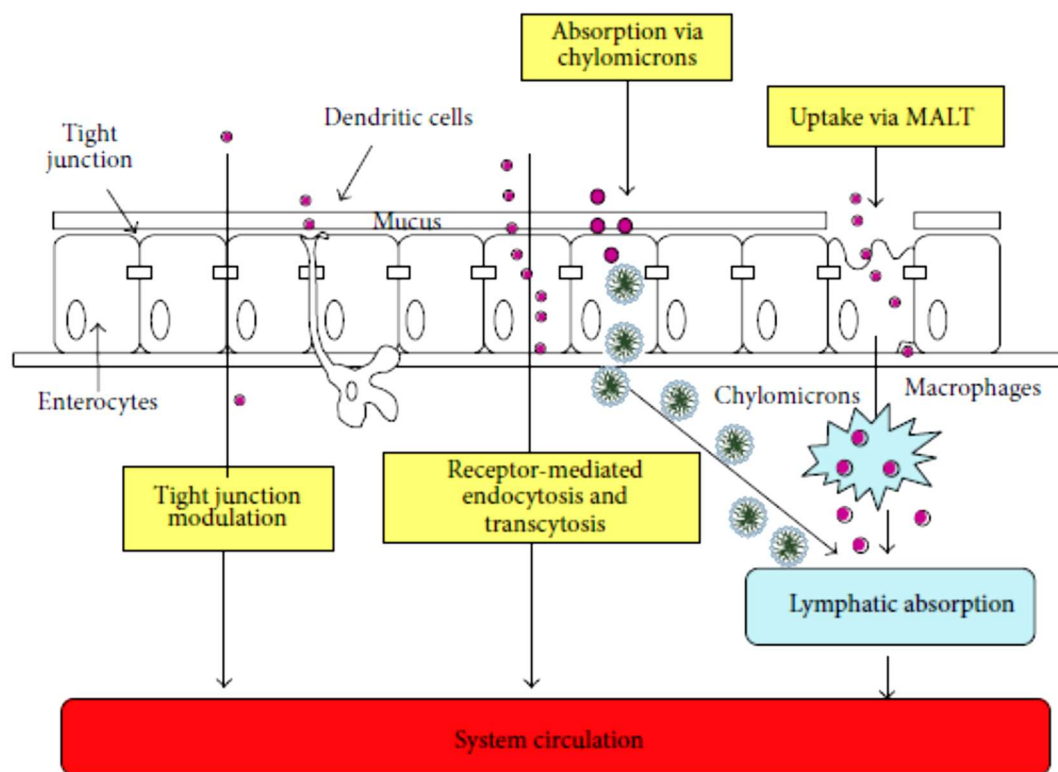


Figure 3. 3. Mechanisms of carriers enhanced absorption by enteric mucosa  
(Source: Bilia et al. 2014)

A number of encapsulated EOs have been available in the literature with different size from micrometric size to nanometrics (Table 3.4). Encapsulation of essential oils is used for the protection of the active compounds against environmental factors (e.g., oxygen, light, moisture, and pH) (Donsi, Annunziata, Sessa, and Ferrari, 2011), reduction in oil volatility and transformation of oil into a powder form, masking the taste and controlling the active compound release. Encapsulation in nanometric particles may serve as an alternative way for increasing the cellular absorption mechanisms and increasing bioefficacy due to the subcellular size (Bilia et al., 2014).

Table 3. 4.Examples of encapsulated EOS for different polymer-active agent systems

<b>Formulation</b>	<b>Active ingredient</b>	<b>Application of formulation</b>	<b>Biological activity</b>	<b>Method</b>	<b>Route</b>
Zeodary oil microspheres	Zeodary oil	Sustained release and bioavailability	Hepato-protection anticancer and anti-bacterial	Emulsion solvent diffusion method	Oral
Chitosan	Oregano oil	Controlled release and stability of EOS	Antimicrobial activity	Oil-in-water emulsion and ionic gelation	-
Polylactic glycolic acid	Eugenol or trans-cinnamaldehyde	Controlled release and antimicrobial activity	Antimicrobial activity	Emulsion evaporation	-
Berberine nano-emulsion	Berberine	Improve residence time and absorption	Anticancer	Phase diagram	Oral
Rutin-alg-chi-micro-capsules	Rutin	Targeting cardiovascular region	Cardiovascular diseases	Complex coacervation method	<i>In vitro</i>
Quercetin microspheres	Quercetin	Decrease the dose size	Anticancer	Solvent evaporation	<i>In vitro</i>
Cynara scolymus microspheres	Cynara scolymus	Controlled release of nutraceuticals	Nutritional supplement	Spray drying	Oral
Zein-sodium caseinate nanoparticles	Thymol	Efficient antimicrobial activity and two-phase release profile	Antimicrobial activity against <i>E. coli</i> and <i>Salmonella</i>	Film casting	

### 3.3.2. Essential Oils for *H. pylori* Eradication Treatment

Especially, antimicrobial substances other than antibiotics would be very useful in the treatment of *H. pylori* infection if they were shown to be effective against both antibiotic-resistant and –susceptible *H. pylori* strains. In fact, a number of drugs and natural substance such as ecabet sodium, tea catechins, garlic extracts and honey have been shown to have an antibacterial effect against *H. pylori in vitro*. Essential oils, which are extracted from plants have also been used for many years to treat a variety of medical ailments, although the mechanism of their action is generally not clarified. The antimicrobial activity of natural compounds has been reported, including a few reports on the effects of essential oils.

The activities of 60 essential oils against *H. pylori* were evaluated and the results showed that 30 oils were able to affect the growth *in vitro*, and 15 showed strong activity. Among the individual constituents of these oils, carvacrol, isoeugenol, nerol, citral and sabinene exhibited the strongest anti-*H. pylori* effects (Bergonzelli et al., 2003). Ohno et al. (2003) have found the bacteriocidal effect of lemongrass and lemon verbena essential oils with a concentration of 0.01% (v/v) on *H. pylori*. Table 3.5. summarizes the effects of essential oils extracted by ethanol or propylene glycol (PG) on *H. pylori* growth. Most essential oils showed inhibitory effect in both solvents and Cinnamon bark oil showed the highest antimicrobial activity among tested essential oils (Ohno et al., 2003). Therefore, cinnamon bark oil was used in this study for antimicrobial activity against *H. pylori*.

Table 3. 5. Effects of essential oils on *H. pylori* growth; GI, partial growth inhibition; ND, not determined (Source: Bergonzelli et al., 2003)

Essential oil	Inhibition zone (cm)	
	PG	EtOH
Cinnamon bark	4.5	6.3
Lemongrass	3.2	2.3
Vervein	2.9	<0.6
White grapefruit	2.9	1.7
Clove leaf	2.5	ND
Savory	2.5	1.3
Manuka	2.3	ND
Pine	2.2	1.4
Oregano	1.9	GI
Red thyme	1.9	ND
Lemongrass	1.6	1.4
Thyme	1.5	1.2
Clove bud	1.3	ND

Regarding to *H.pylori* eradication treatment, Altiok (2011) prepared cinnamon bark oil loaded chitosan microspheres by spray drying and investigated the antimicrobial effect against *H. pylori*. MIC was firstly determined by agar dilution method and found as 8  $\mu\text{g/mL}$ . Cinnamon bark oil released from chitosan microspheres inhibited *H. pylori* growth. However, approximately 80% cinnamon bark oil was released from microspheres in a few minutes (Altiok, 2011). Therefore, novel chitosan based microspheres has been needed to be developed for release of cinnamon bark oil in a controlled manner.

## CHAPTER 4

### MATERIALS AND METHODS

#### 4.1. Materials

High molecular weight (HMW) chitosan was purchased from Sigma-Aldrich (Germany, Cat. No. 419419, deacetylation degree %86) for production of chitosan microspheres. The organic modified montmorillonite (OMMT) (Cloisite 10A, Southern Clay Products Inc.) was used as nanoclay. FDA approved Cinnamon bark oil was purchased from Sigma (Cat. No. W229105, FDA 21 CFR, Germany). Clarithromycin was supplied by Ranbaxy Pharmaceuticals Inc. Glacial acetic acid (Merck Chemicals, Germany) was used as a solvent for preparation of chitosan solution. HPLC grade ethanol (Merck Chemicals, Germany) was used as a solvent to dissolve cinnamon bark oil. <sup>99m</sup>Tc-sodium pertechnetate (140 keV, half-life 6 h) was obtained from Ege University, Department of Nuclear Medicine for radiolabeling study. Rhodamine B was supplied from Sigma (Germany) to label chitosan microspheres for cellular uptake study. Simulated gastric fluid (SGF) was prepared according to USP XXII Pharmacopodia recommendation and adjusted to pH 1.2. SGF was prepared by dissolving NaCl (2 g/L), and 7 mL HCl in distilled water. Pepsin (3.2 g/L) was also added into SGF for biodegradation study. Phosphate buffer solution (PBS) was prepared for pH 4.5. Periodic acid and Schiff (PAS) reagent kit was purchased from Sigma (Germany). Mucin from porcine stomach was provided by Sigma for mucoadhesion assays. Mueller-Hinton Agar (Oxoid, UK) and defibrinated sheep blood (Oxoid, UK) were used in the antimicrobial susceptibility testing. Columbia Blood agar (Oxoid, UK), defibrinated horse blood (Oxoid, UK) and *H. pylori* selective supplement DENT (Oxoid, UK) were used in *H. pylori* culture media. Gas Pak Campy Container System (Becton Dickinson) was used to provide microaerophilic conditions for *H. pylori* culture. Methyl thiazole tetrazolium (MTT) was purchased from Sigma (Germany) and WST-1 was purchased from Biovision (USA) for *in vitro* cell viability and proliferation assays. Dulbecco's Modified Eagle Medium (DMEM), fetal bovine serum (FBS), phosphate-buffered saline (PBS),

Penicillin–streptomycin antibiotic solution were purchased from Gibco (USA). RPMI 1640 (Capricorn, Germany) was used in MKN45 cell culture. DAPI (4', 6-diamidino-2-phenylindole, dihydrochloride) was supplied from Cell Signaling (USA). 37% paraformaldehyde was provided by Merck (Germany) and diluted to 3.7% for fixation of cells.

*Helicobacter pylori* NCTC 11637 standard strain was used for antimicrobial susceptibility testing studies. NIH3T3 fibroblast cell line was used for *in vitro* cytocompatibility evaluation of microspheres. MKN45 adenocarcinoma gastric cell line was supplied from INEB-Instituto de Engenharia Biomedica, Universidade do Porto as a gift, was used for *in vitro* cell proliferation and cellular uptake experiments. This cell line was originally derived from a poorly differentiated adenocarcinoma.

## **4.2. Methods**

### **4.2.1. Determination of Minimum Inhibitory Concentration (MIC) of Cinnamon Bark Oil**

#### **4.2.1.1. *Helicobacter pylori* Culture and Inoculum Preparation**

Columbia Blood agar medium was used for the culture of *H. pylori* and isolated colonies were prepared in Brain Heart Infusion (BHI) Broth (Beckton Dickinson and Company) with 20% glycerol at -80 °C. The culture medium was prepared as:

##### ***H. pylori* Culture Medium Preparation**

Columbia Blood agar (Oxoid) supplemented with 7% defibrinated horse blood (Oxoid) and *H. pylori* selective supplement (DENT) (Oxoid) was prepared for *H. pylori* culture. 19.5 g Columbia Blood agar (Oxoid) was dissolved in 465 mL distilled water and autoclaved at 121°C for 15 min. 35 mL of sterile defibrinated horse blood (Oxoid) and 2 mL of *H. pylori* Selective Supplement (DENT) (Oxoid) were added to the Columbia Blood agar media at 50°C. The culture medium was poured into petri dishes.

### ***H. pylori* Stock Culture Medium with 20% Glycerol**

40 mL of glycerol solution (Baked Analyzed) was added into 60 mL distilled water and also 7.4 g of Brain Heart Infusion Broth (BHI) (Beckton Dickinson and Company) was dissolved in 80 mL distilled water. Then, they were autoclaved at 121°C for 15 min separately. Final concentration of glycerol was adjusted to 20% (v/v). BHI broth and glycerol solution were mixed together and 20 mL of fresh human serum (DEU, Faculty of Medicine, Central Serology Laboratory, confirmed by serologic tests) was added to medium; aliquoted in sterile eppendorf tubes and kept at +4°C until used.

*H. pylori* NCTC 11637 standard strain from stock bacterial culture in brain heart infusion (BHI) broth (Oxoid) containing 20% glycerol (Baked Analyzed) was inoculated onto Columbia Blood agar (Oxoid) supplemented with 7% defibrinated horse blood (Oxoid) and *H. pylori* selective supplement (DENT, Oxoid). *H. pylori* culture was incubated in microaerophilic conditions with Gas Pak Campy Container System (Becton Dickinson and Company) in anaerobic jar (Oxoid) at 37 °C for 72 h. *H. pylori* was identified by colony morphology, motility, Gram staining and oxidase, catalase and urease tests. *H. pylori* colonies were used for antimicrobial susceptibility testing to determine MIC value of cinnamon bark oil and to investigate the effects of released oil from the prepared microspheres on *H. pylori* growth. Cultured and confirmed *H. pylori* colonies were used for antibacterial susceptibility testing to determine MIC values of clarithromycin and cinnamon bark oil, respectively.

#### **4.2.1.2. Standardization of agar dilution method**

Antimicrobial susceptibility testing for clarithromycin was performed by the agar dilution method recommended by Clinical and Laboratory Standards Institute; using Mueller-Hinton agar (MHA) supplemented with 5% defibrinated sheep blood (CLSI, 2007).

#### **Preparation of Clarithromycin Stock Solution:**

Clarithromycin stock solution was prepared by dissolving 25 mg clarithromycin in 25 ml methanol (Merck, Germany). Nine mL of PBS was added into one mL of



clarithromycin solution and the concentration of the stock solution was adjusted to 100 µg/mL (w/v). The solution was filtered through 0.22 µm sterile syringe filter membrane (Minisart, Sartorius Stedim) for sterilization. Two fold serial dilutions were prepared with PBS in the range of 50-1.75 µg/mL. The tested concentrations of clarithromycin were obtained in the range of 1-0.0037 µg/mL when added into 50 mL Mueller-Hinton agar medium supplemented with 5% defibrinated sheep blood (Oxoid).

#### **MIC Determination of Clarithromycin by Agar Dilution Method:**

Antimicrobial susceptibility testing for clarithromycin was performed by the agar dilution method recommended by Clinical and Laboratory Standards Institute (CLSI, 2007). Mueller-Hinton agar (Oxoid) supplemented with 5% defibrinated sheep blood (Oxoid) containing various concentrations of clarithromycin was prepared for the determination of minimum inhibition concentration (MIC) of clarithromycin by agar dilution method.

1.9 g of Mueller-Hinton Agar (Oxoid) was dissolved in 46.5 mL distilled water and autoclaved at 121°C for 15 min. 2.5 mL sterile defibrinated sheep blood (Oxoid) and one mL of each clarithromycin dilutions were added into Mueller-Hinton agar (Oxoid) medium. PBS (Biochrom) was used as negative control and 1 mL of PBS was added into MHA supplemented with 5% sheep blood-medium instead of clarithromycin dilution. Mueller-Hinton Agar (Oxoid) medium was allocated into two sterile petri dishes.

After 72 h incubation The cultured colonies were harvested from Columbia Blood agar supplemented with 7% defibrinated horse blood (Oxoid) and *H. pylori* selective supplement (DENT) (Oxoid) and bacterial inoculum concentration was adjusted to McFarland 2 ( $6 \times 10^8$  CFU/mL) in Brucella Broth (Beckton Dickinson) by Densimat (Biomerieux). Three µL of prepared bacterial suspension was spotted onto Mueller - Hinton agar (Oxoid) supplemented with 5 % defibrinated sheep blood (Oxoid) containing different concentrations of clarithromycin. Inoculated plates were incubated in a microaerophilic conditions with a GasPak Campy Container System (Becton Dickinson) at 37 °C for 72 h. After incubation period, the MIC was defined as the lowest concentration at which no visible growth was observed.

At the same conditions, *H. pylori* was inoculated onto MHA supplemented with 5 % defibrinated sheep blood without clarithromycin as a positive control, also Brucella broth (Beckton Dickinson) without bacteria was used as a negative control. Besides, agar

plates containing methanol or PBS instead of clarithromycin dilution were also tested as controls to show whether methanol or PBS had any adverse (or negative) effect on *H. pylori* growth *in vitro*. All the control plates were incubated at 37 °C for 72 h under the same microaerophilic conditions. Experiments were performed in duplicate for each test run.

#### **MIC Determination of Clarithromycin by E-test:**

The colonies after 72 h incubation were harvested from Columbia Blood agar supplemented with 7% defibrinated horse blood (Oxoid) and *H. pylori* selective supplement (DENT) (Oxoid) plates, then inoculum concentration was adjusted to McFarland 3 ( $9 \times 10^8$  CFU/mL) in Brucella Broth (Beckton Dickinson) with Densimat (Biomérieux). 100  $\mu$ L of prepared bacterial suspension was spread onto Mueller-Hinton agar (Oxoid) supplemented with 5 % defibrinated sheep blood (Oxoid). E-test strip was placed onto plate. Inoculated agar plates were incubated in a microaerophilic conditions with a GasPak Campy Container System (Becton Dickinson Company) at 37 °C for 72 h. After incubation period, the MIC was determined. MIC value of clarithromycin were evaluated for E-test:  $\leq 1$   $\mu$ g/mL as sensitive, and  $> 1$   $\mu$ g/mL as resistant (Agudo et al., 2010; Agudo et al., 2011; Francesco et al., 2009; Karczewska et al., 2011; Oleastro et al., 2003).

#### **4.2.1.3. MIC Determination of Cinnamon Bark Oil by Agar Dilution Method**

Agar dilution method was also used to determine the MIC value of cinnamon bark oil by adapting CLSI protocol using Mueller-Hinton agar (MHA) supplemented with 5% defibrinated sheep blood. Minimum inhibitory concentration (MIC) was defined as the lowest concentration that did not result in any visible growth of the microorganism in comparison with the growth in the control plate (Hammer, 1999).

72 hours cultured colonies were harvested from the plates, resuspended in Brucella Broth and inoculum concentration was adjusted to McFarland 2 ( $6 \times 10^8$

CFU/mL). Agar dilution method was also used to determine the MIC value of cinnamon bark oil by adapting CLSI protocol.

#### **Preparation of Cinnamon bark oil Stock Solution:**

Cinnamon bark oil (Sigma) stock solution was dissolved in 96% ethanol (Merck) and vortexed for 1 min. The stock solution concentration of cinnamon bark oil was adjusted to 100 mg/mL (w/v). The solution was filtered through 0.22  $\mu$ m sterile syringe filter membrane (Minisart, Sartorius Stedim) for sterilization. Two fold serial dilutions were prepared with PBS (Biochrom) and obtained in the range of 50 mg/mL-50 $\mu$ g/mL. The final concentrations of cinnamon bark oil were adjusted to 1-1000  $\mu$ g/mL when added into each 50 mL MHA supplemented with 5% defibrinated sheep blood (Oxoid).

#### **MIC Determination**

MHA supplemented with 5% defibrinated sheep blood containing various concentrations of cinnamon bark oil were prepared to determine minimum inhibition concentration (MIC) value by agar dilution method. Each dilution of cinnamon bark oil was added into MHA medium. PBS was used as control and 1 mL of PBS was added into agar dilution medium instead of clarithromycin or oil dilution.

1.9 g of MHA was dissolved in 46.5 mL distilled water and autoclaved at 121°C for 15 min. 2.5 mL sterile defibrinated sheep blood (Oxoid) and one mL of each cinnamon bark oil dilutions were added into MHA medium. PBS (Biochrom) was used as negative control and 1 mL of PBS was added into MHA instead of cinnamon bark oil dilution. MHA medium was allocated into two 90 mm sterile petri dishes.

After 72 hours incubation, *H. pylori* colonies were harvested from Columbia Blood agar supplemented with 7% defibrinated horse blood (Oxoid) and *H. pylori* selective supplement (DENT) (Oxoid) plates, then inoculum concentration was adjusted to McFarland 2 ( $6 \times 10^8$  CFU/mL) in five mL Brucella Broth (Beckton Dickinson). Turbidity of bacterial suspension was measured by Densimat (Biomérieux). Three  $\mu$ L of prepared bacterial suspension was spotted onto MHA supplemented with 5 % defibrinated sheep blood (Oxoid) and containing cinnamon bark oil at different concentrations. Inoculated plates were incubated in a microaerophilic conditions with a GasPak Campy Container System (Becton Dickinson Company) at 37 °C for 72 h. After

incubation period, the growth of the colonies was evaluated and the MIC value of cinnamon bark oil was determined.

At the same conditions, *H. pylori* was inoculated onto agar plates without cinnamon bark oil as a positive control, Brucella broth (Beckton Dickinson) was also used as negative control. Besides, agar plates containing ethanol or PBS instead of cinnamon bark oil dilution were also tested as controls to show whether ethanol or PBS had any adverse (or negative) effect on *H. pylori* growth *in vitro*. Positive and negative control agar plates were incubated at 37 °C for 72 h under the same microaerophilic conditions. All experiments were performed in duplicate for each test run.

### **Investigation of the Effect of Different Parameters on *H. pylori* Growth in Agar Dilution Methods**

Due to the difficulty in visualization of *H. pylori* growth on MHA plates containing cinnamon bark oil for determination of MIC value, the effects of different agar dilution parameters such as inoculum concentration, inoculum amount on bacterial growth were investigated. In order to evaluate the effects of agar dilution parameters on *H. pylori* growth and obtain visible colonies which should be clearly seen in agar dilution plates, sheep blood concentration (5% and 10%), inoculum concentration (McFarland 2, McFarland 3 and McFarland 4) and amount of inoculum (3 µL and 5 µL) were changed. This study was also important for standardization and validation of CLSI protocol for MIC determination of cinnamon bark oil.

*H. pylori* NCTC 11637 standard strain stored in stock media of brain heart infusion (BHI) broth (Oxoid) containing 20% glycerol (Baked Analyzed) was thawed and inoculated onto Columbia blood agar (Oxoid) supplemented with 7% defibrinated horse blood (Oxoid) and *H. pylori* selective supplement (DENT, Oxoid). *H. pylori* culture was incubated in microaerophilic conditions with a Gas Pak Campy Container System (Becton Dickinson and Company) in anaerobic jar (Oxoid) 37 °C for 48 h and subcultured for 48 h to harvest *H. pylori* colonies on log phase of the bacterial growth. *H. pylori* was identified by colony morphology, motility, Gram staining, oxidase, catalase and urease tests. 48 h subcultured *H. pylori* colonies were used for the effects of different parameters on antimicrobial susceptibility testing to evaluate the visualization of *H. pylori* colonies and determine MIC value of cinnamon bark oil.

MHA supplemented with 5% and 10% defibrinated sheep blood (Oxoid) containing various concentrations of cinnamon bark oil was prepared as previously described. 48 hours subcultured colonies were harvested from the plates and bacterial suspension of *H. pylori* was adjusted to McFarland 2 ( $6 \times 10^8$  CFU/mL), McFarland 3 ( $9 \times 10^8$  CFU/mL) and McFarland 4 ( $12 \times 10^8$  CFU/mL) to observe the difference in inoculum concentrations. Bacterial suspensions were inoculated 3  $\mu$ L and 5  $\mu$ L by spotting and spreading directly onto agar plates (Figure 4.1). All these parameters were applied to each MHA including 5% and 10% (v/v) defibrinated sheep blood plates containing different dilutions of cinnamon bark oil (1-1000  $\mu$ g/mL). Inoculated plates were incubated in a microaerophilic atmosphere with a GasPak Campy Container System (Becton Dickinson and Company) in anaerobic jar (Oxoid) at 37 °C for 48 h. After incubation, the growth of *H. pylori* strains on plates were evaluated to visualize for clear appearance of visible colonies and compared with each tested parameters. Additionally, MIC value of cinnamon bark oil was also determined, evaluated and confirmed according to these parameters.

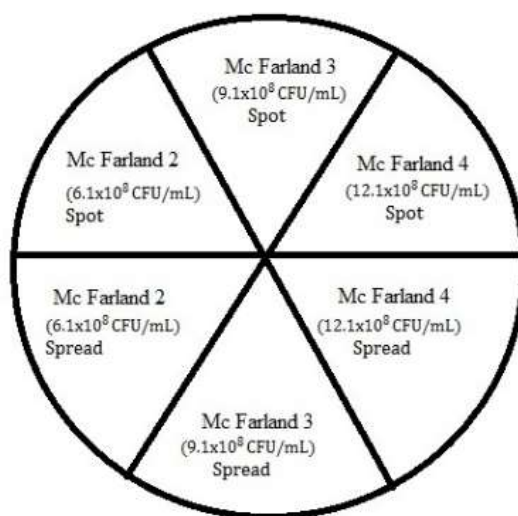


Figure 4. 1. Schematic illustration of agar plates for inoculation of bacterial suspension

#### 4.2.2. Production of Chitosan Microspheres

Cinnamon bark oil loaded and unloaded chitosan microspheres were produced by spray drying process by using Mini Spray Dryer B-290 (Buchi®, Switzerland) with a 0.5 mm standard nozzle and a parallel flow. Principally, the solution was fed to the nozzle with a

peristaltic pump and atomization occurred by the force of the compressed air, disrupting the liquid into small droplets. The droplets, together with hot air, were blown into a chamber where the solvent in the droplets was evaporated and discharged out through an exhaust tube. Drying air and feed solution move in a parallel flow. The dry product was collected in a collection bottle passing through a cyclone.

Organic modified montmorillonite was used in this study to improve stability and release properties of microspheres in gastric conditions. Organic modified montmorillonite, Cloisite 10A (with benzyl(hydrogenated tallow alkyl) dimethyl surface modification), was used in different amounts (1%-3%-5% w/w).

Cinnamon bark oil concentration for encapsulation was determined according to MIC value. Microspheres with different formulations (Table 4.1) were prepared by spray drying method (Figure 4.2). Briefly, 1% chitosan (HMW) (w/v) was dissolved in 2% (v/v) acetic acid solution and left overnight to completely dissolve. Selected amounts of nanoclay (1, 3 and 5% w/w) were dispersed in 2% acetic acid and vigorously stirred for 24 h. Nanoclay dispersion was added into the solution, followed by a continuous stirring at room temperature for 1 h and sonicated for 30 min. After sonication, 1.5% cinnamon oil (v/v) was added dropwise into the chitosan/nanoclay dispersion under magnetic stirring and sonicated for 15 min before the spray drying process. Sonication process was used for intercalation and distribution of nanoclay in chitosan matrix and particle size reduction. Nanoclay incorporated chitosan microspheres were nomenclatured as chitosan nanocomposite microspheres in this thesis. The effect of different spray drying parameters such as inlet temperature, pump rate on microsphere characteristics was investigated. Different temperatures (180 °C, 190 °C and 200 °C) and pump rates (6 mL/min, 7 mL/min and 8 mL/min) were performed initially to determine the optimum conditions of the dryer. Outlet temperatures were varied according to the inlet temperatures. Figure 4.3 shows the spray drying apparatus used in this study. Spray drying runs were performed in duplicate. Optimum spray drying conditions were determined based on the particle size, humidity content of the microspheres, and the process yield. Humidity (%) of the spray dried microspheres was measured by moisture analyzer (Sartorius MA100, Germany). The particle size distribution, shape and surface properties were examined by scanning electron microscope (Quanta 250FEG, FEI Company, Netherlands) in Center for Materials Research in İzmir Institute of Technology, Izmir. Process yield was calculated to determine the recovered microspheres after the manufacturing process as in Eq. 4.1;

$$\text{Yield(\%)} = \frac{\text{Weight of spray dried microspheres}}{\text{Total weight at initial}} \times 100 \quad (4.1)$$

All the rest formulations were produced at the optimum process conditions (6 mL/min feed rate; 190 °C inlet temperature). The formulation codes of the samples prepared by spray drying at the optimum process conditions (6 mL/min feed rate; 190 °C inlet temperature) were listed in Table 4.1. Oil unloaded chitosan microspheres were used as control microspheres and prepared in similar way. Also, oil unloaded chitosan microspheres were prepared as neat chitosan microspheres.

*In vitro* cellular uptake studies were conducted using Rhodamine B labelled spheres. The microspheres were labelled with rhodamine in order to track the internalization of chitosan particles by MKN45 cells. This fluorescent dye attaches to chitosan through primary and secondary amine and hydroxyl functional groups and allows to observe the cellular uptake of particles (Q. Jin, Schexnailder, Gaharwar, and Schmidt, 2009). Rhodamine B was dissolved in DMSO at a concentration of 50 mg/mL. Ten microliters of the rhodamine B solution was added to 100 mL of cinnamon bark oil loaded chitosan/nanoclay dispersion and stirred for 1 h under dark conditions. Rhodamine labelled microspheres were then produced by spray drying at the same process conditions.

Table 4. 1. Formulation codes and content of microspheres produced by spray drying

<b>Sample</b>	<b>Chitosan (% w/v)</b>	<b>OMMT (w/w)</b>	<b>Cinnamon bark oil (v/v)</b>
Chitosan (Chi)	1	-	-
CO (Chi/oil)	1	-	1.5
COM1 (Chi/oil/1MMT)	1	1	1.5
COM3 (Chi/oil/3MMT)	1	3	1.5
COM5 (Chi/oil/5MMT)	1	5	1.5
CM1 (Chi/1MMT)	1	1	-
CM3 (Chi/3MMT)	1	3	-
CM5 (Chi/5MMT)	1	5	-

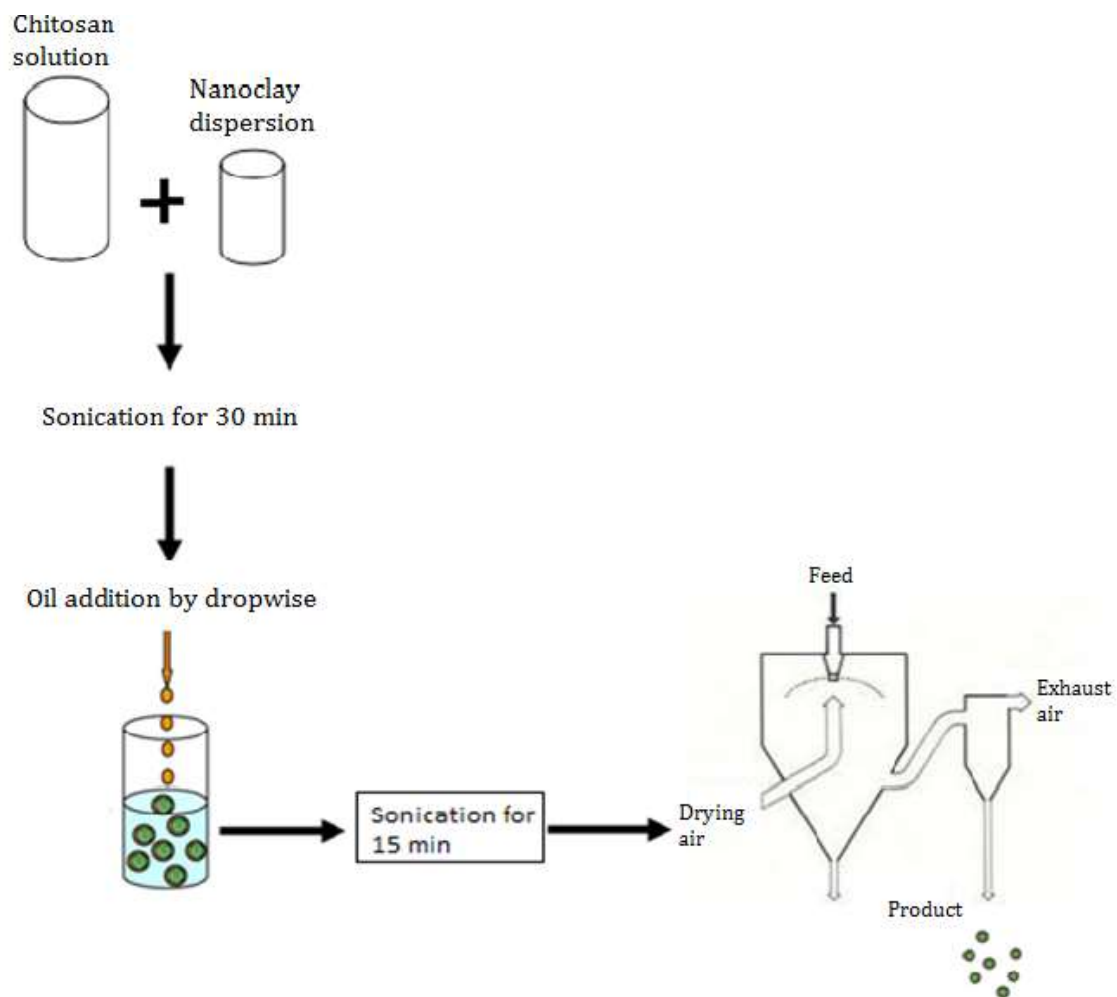


Figure 4. 2. Flow diagram of chitosan microsphere production



Figure 4. 3. Spray drying apparatus used in this study



### **4.2.3. Characterization of Chitosan Microspheres**

#### **4.2.3.1. Morphological Characterization and Particle Size**

The shape, surface morphology, and particle size of the microspheres were examined using Scanning Electron Microscopy (SEM) (Quanta 250FEG, FEI Company, Netherlands) in Center for Materials Research in İzmir Institute of Technology, Izmir, Turkey. Microspheres were mounted onto aluminum specimen stubs using double-sided adhesive tape. The samples were coated with gold under argon atmosphere for 60 sec before examination. The mean particle size and particle size distribution (PSD) of prepared microspheres were calculated by measuring about 200 particles using ImageJ programme. In addition to SEM analysis, Transmission Electron Microscopy (TEM) was also used in order to characterize the particle size and shape of the spheres. Microspheres were dispersed in ethanol and the solution was dropped onto 400-mesh carbon coated copper grids and dried at room temperature. TEM micrographs were taken using FEI Tecnai G<sup>2</sup> Spirit Bio (TWIN) transmission electron microscope (Central Laboratory, Middle East Technical University) under an accelerating voltage of 120 kV.

#### **4.2.3.2. Surface Charge**

The surface charge of microspheres was determined by zeta potential measuring the electrophoretic mobility by forcing an electrolyte through a measuring cell unit containing the microspheres. Surface charges of microspheres is significant factor for adhesion of particles to gastric mucin and cells. Therefore the zeta potential of microspheres was measured in both SGF and pH 4.5 which mimics the stomach in fasted and fed state, respectively. Samples were dispersed in SGF (pH 1.2) and pH 4.5 phosphate buffer, vortexed well and sonicated to prevent agglomeration. Then sample was injected in the Malvern Zetasizer 3000 (Malvern Instruments). The measurements were carried out in the fully automatic mode and each sample was analysed in triplicate.

#### 4.2.3.3. Encapsulation Efficiency and Drug Loading

5 mg of prepared chitosan microspheres were dissolved in 5 mL of SGF and ethanol mixture. Microspheres were disrupted by bead beater for 1 min. The solution was filtered through Millipore filters and the amount of encapsulated essential oil was measured after suitable dilution at 288nm by UV-Vis spectrophotometry (Perkin Elmer). The wavelength was determined as 288 nm where the maximum absorbance occurred. The calibration curve was obtained by different concentrations of cinnamon bark oil in ethanol. The encapsulation efficiency (EE) and drug loading in microspheres were calculated by formula given below:

$$\% EE = \frac{\text{Oil content in prepared ms}}{\text{Amount of oil loaded}} * 100 \quad (4.2)$$

$$\% \text{ Drug Loading} = \frac{\text{Oil content in microspheres}}{\text{Total amount of microspheres}} * 100 \quad (4.3)$$

#### 4.2.3.4. Chemical Characterization

Fourier transform infrared spectroscopy (FT-IR) and Raman spectroscopy were used to examine the chemical groups of each component in microspheres. The interaction between the polymer, nanoclay and cinnamon bark oil was evaluated by Fourier Transform Infrared Spectroscopy (Excalibur Series FTS 3000 MX FTIR) and Raman spectroscopy (Horiba). For FTIR analysis, the samples were prepared by KBr pellet method and scanned in range of 4000-400  $\text{cm}^{-1}$ . Raman spectroscopy measurements were performed using a 600 gr/mm grating at 785 nm excitation with output power. Measurements were recorded at 1  $\text{cm}^{-1}$  resolution in the range of 300-3500  $\text{cm}^{-1}$  wavenumber.

The chemical structures of cinnamon bark oil and oil loaded chitosan nanocomposites were also investigated by Nuclear Magnetic Resonance Spectrometry (Varian 400 MHz) analysis ( $^1\text{H-NMR}$ ). Approximately 10 mg of prepared microspheres were dissolved in 1 mL of deuterium oxide ( $\text{D}_2\text{O}$ ) and methanol solution.

### 4.2.3.5. Nanocomposite Structure

#### X-ray Diffraction (XRD) and TEM

The structural configurations and level of nanoclay dispersion within chitosan matrix were characterized by both XRD and TEM analyses. The XRD diffraction patterns of chitosan microspheres and nanocomposite microspheres were determined in a range of diffraction angle ( $2\theta$ ) of  $5-30^\circ$  using Phillipx X'Pert Pro MRD with Cu K radiation ( $\lambda=0.154$  nm) under a voltage of 40kV and a current of 40mA. The distance between the silicate layers (d spacing) was calculated using Bragg's law (Equation 4.4), where  $\lambda$  is the wavelength of the incident beam,  $\theta$  is the diffraction angle and d is the distance between silicate layers.

$$\lambda = 2d\sin\theta \quad (4.4)$$

TEM micrographs were taken using FEI Tecnai G<sup>2</sup> Spirit Bio (TWIN) transmission electron microscope (Central Laboratory, Middle East Technical University) under an accelerating voltage of 120 kV. Microspheres were diluted in 2% acetic acid and the solution was dropped onto 400-mesh carbon coated copper grids and dried at room temperature.

### 4.2.3.6. Swelling and Biodegradation Study

Swelling degree (% SD) of microspheres was determined to understand water absorption behaviour and elucidate release mechanism. The swelling degree was determined in SGF and pH 4.5 phosphate buffer. 10 mg of microspheres were added into 5 mL of SGF and pH 4.5 phosphate buffer, separately and incubated at  $37^\circ\text{C}$  for 4 h and 24 h. At the equilibrium, the microspheres were carefully taken out from the solution and filtered for the removal of the free water on the surfaces, and then weighed. The percentage of SD of samples was calculated by using the following equation:

$$\% \text{ SD} = \frac{W_t - W_i}{W_i} * 100 \quad (4.5)$$

Rapid degradation of bioactive agents and chitosan microspheres in acidic environment of stomach is one of the major problem for gastrointestinal delivery systems. To overcome this problem, nanoclay was introduced into chitosan microspheres. Therefore, biodegradation of prepared microspheres was evaluated in SGF with pepsin. 10 mg microspheres were suspended in SGF with pepsin at 37 °C in 5 mL of each medium in 15 mL plastic tubes. After incubation, the microspheres were carefully removed from the solution and dried until constant weight. The % degradation of microspheres were calculated as:

$$\% \text{ Degradation} = \frac{W_i - W_d}{W_i} * 100 \quad (4.6)$$

#### **4.2.3.6. Mucoadhesion**

##### **Contact angle measurement**

The hydrophilic nature of a surface is directly correlated with the water contact angle. Contact angle is defined as the angle between the film surface and the tangent line at the point of contact of the water droplet with the surface. Surface wetting theory is one of the mucoadhesion determination method and an intimate contact which is an important factor and prerequisite for bond formation between the bioadhesive polymer and mucus. The affinity to the surface could be found by using the contact angle. The surface hydrophobicity or wettability of cinnamon bark oil loaded chitosan microspheres were evaluated by contact angle measurements carried out using sessile drop method with KSC-Attension Theta Optical Tensiometer. Before measurements, the microsphere samples were pressed as pellet form. The contact angle measurements were carried out by dropping 6 µl of PBS on the surface of the sample. The angle between the baseline of the drop and the tangent at the drop boundary was measured.

### **Adsorption of Mucin on Chitosan Microspheres with Mucus Glycoprotein Assay (*In vitro* Mucoadhesion Test)**

Periodic acid/Schiff (PAS) colorimetric method (He, 1998) was used to determine the free mucin concentration for assessment the amount of mucin adsorbed on the chitosan microspheres. Two reagents were used for analysis of free mucin content: Schiff reagent (Sigma) and periodic acid reagent (Sigma). Standard calibration curve was prepared from 2 mL of mucin standard solutions (0.25, 0.5, 0.75 and 1 mg/2 mL). After adding 0.2 mL of periodic acid reagent, the samples were incubated at 37°C in water bath for 2 h. Then, 0.2 mL of Schiff reagent was added at room temperature. 30 min later, the absorbance of the solution was measured at 555 nm in a UV-Vis spectrophotometer. The mucin content was calculated from the standard calibration curve.

Surface mucin adsorption was determined using the following adsorption experiment: 10 mg of microspheres were suspended in 5 mL of mucin stock solution (0.5 mg/mL), vortexed and shaken at 37 °C for 2 h. After incubation, the suspension was centrifuged at 4000 rpm for 2 min and the supernatant was determined using a Periodic acid/Schiff colorimetry method. The amount of mucin absorbed by the microspheres was calculated as the difference between the total amount of mucin added and the free mucin in supernatant. Experiments were performed in triplicate. % Mucoadhesion level was determined by Equation 4.7:

$$\% \text{ Mucoadhesion} = \frac{\text{Adsorbed mucin}}{\text{Total mucin amount}} * 100 \quad (4.7)$$

#### **4.2.4. *In vitro* Release**

The release of cinnamon bark oil from microspheres in SGF and phosphate buffer solution at pH 4.5 recommended by USP Pharmacopedia was performed at 37°C and 75 rpm. 15 mg microspheres were transferred into each vessel containing 150 mL of release media and incubated at 37.0 ± 0.5°C with rotation speed of 75 rpm (Table 4.2). Sample was taken at predetermined time intervals. 1 mL of sample was taken and replaced with fresh release media for keeping constant volume and then the sample was filtered through 0.45µm syringe filter. Amount of cinnamon bark oil released from chitosan

nanocomposite microspheres to release media was determined using UV-Visible Spectrophotometer at 288 nm wavelength. Cinnamon bark oil concentration in the release media was calculated from the calibration curve. The release data obtained were also fitted into various mathematical models.

Table 4. 2. Release parameters and conditions

Parameter	Value
Rotation speed	75 rpm
Release medium and pH of medium	SGF, pH 4.5
Volume	150 mL
Temperature	37 °C
Time intervals	0., 15., 30., 60., 90., ...1440. min.
Sample volume	1 mL
Wavelength	288 nm
Filter membranes	0.45 $\mu$

#### 4.2.5. Determination of the Antibacterial Effect of Released Cinnamon Bark oil on *H. pylori*

The antimicrobial activity of cinnamon bark oil released from chitosan microspheres against *H. pylori* was evaluated by the incorporation of microspheres into Brucella Broth (Beckton Dickinson) supplemented with 5% fetal bovine serum (FBS) (Biochrom).

1.8 g of Brucella Broth (Beckton Dickinson, BD) was dissolved in 95 ml of distilled water and autoclaved at 121°C for 15 min. FBS (Biochrom AG) was sterilized by 0.22  $\mu$ m syringe filter (Sartorius Stedim) and 5 mL of FBS was added to each broth when the Brucella Broth was cooled to 50°C.

*H. pylori* NCTC 11637 standard strain was cultured on Columbia Blood agar (Oxoid) supplemented with 7% defibrinated horse blood (Oxoid) and *H. pylori* Selective Supplement (DENT) (Oxoid) in microaerophilic conditions with a Gas Pak Campy Container System (Becton Dickinson and Company) in anaerobic jar (Oxoid) at 37 °C for

72 h. Colonies were resuspended in 40 mL Brucella Broth (Beckton Dickinson) containing 5% FBS (Biochrom) adjusted to McFarland 2 ( $6 \times 10^8$  CFU/mL).

*H. pylori* was inoculated into Brucella Broth containing sterilized cinnamon bark oil loaded chitosan nanocomposite microspheres in order to examine the effect of released oil from microspheres on *H. pylori* growth.

*H. pylori* was inoculated and incubated with sterilized cinnamon bark oil loaded microspheres containing different amount of nanoclay (MMT) to observe the effect of nanoclay amount on oil release as a function of time. Nanoclay was incorporated into chitosan microspheres for controlled release, extension of the release and residence time and stability to provide sustainable effect in stomach. The microsphere formulations with constant chitosan and cinnamon bark oil amount were previously prepared with different nanoclay amounts (1%-3%-5% w/w) (section 4.2.2). The experiment was performed as followed: 0.03 g of cinnamon bark oil (1.5% v/v) loaded chitosan microspheres and cinnamon bark oil (1.5% v/v) loaded chitosan nanocomposites were sterilized by UV light for 1 h and added into 40 mL Brucella Broth with bacterial suspension in erlenmeyer flask and incubated at 37°C in a microaerophilic environment for 24 h under magnetic stirring. Chitosan microspheres contains therapeutically effective and active amount of cinnamon bark oil at least equal to MIC value (approximately 11.2 µg/mL cinnamon bark oil after complete release in the Brucella Broth medium) against *H. pylori*. The viable bacterial counts of *H. pylori* were determined using a surface spread-plate method. 100 µL of sample was taken from the bacterial suspension with microspheres at 0 h, 8<sup>th</sup> h and 24<sup>th</sup> h of incubation and serial dilutions ( $10^{-1}$ ,  $10^{-2}$ ,  $10^{-3}$ ,  $10^{-4}$ ,  $10^{-5}$ ,  $10^{-6}$ ,  $10^{-7}$ ,  $10^{-8}$  and  $10^{-9}$ ) were prepared in each sterile eppendorf tubes with 900 µl of Brucella Broth (Beckton Dickinson) containing 5% FBS (Biochrom) for predetermined time intervals. 100 µl of diluted samples from  $10^{-5}$ ,  $10^{-6}$ ,  $10^{-7}$ ,  $10^{-8}$  and  $10^{-9}$  dilutions were separately inoculated and spread onto Columbia Blood agar (Oxoid) supplemented with 7% defibrinated horse blood (Oxoid) and *H. pylori* Selective Supplement (DENT) (Oxoid) and incubated in an anaerobic jar (Oxoid) containing GasPak Campy Container System (Becton Dickinson) at 37 °C in a microaerophilic environment for 72 h. The effect of cinnamon bark oil loaded chitosan and chitosan nanocomposite microspheres on viable cell count were calculated by counting the number of colonies on the agar plates. After the incubation period, the number of visible *H. pylori* colonies were counted and the results after multiplication with dilution factor, were expressed as colony forming unit (CFU). Experiments were carried out in duplicate.

#### **4.2.6. *In vitro* Cell Viability and Proliferation of Chitosan Microspheres and Cinnamon Bark Oil**

##### **Cell Culture**

NIH3T3 mouse fibroblast cell line was cultured in DMEM medium supplemented with 10% (v/v) fetal bovine serum (FBS) and 1% antibiotic (100 units/mL penicillin and 100 µg/mL streptomycin). The cells were maintained fibroblast morphology as confluent monolayer in a cell culture flask at 37 °C in a humidified atmosphere containing 5% CO<sub>2</sub>. Morphology and viability of cells were observed regularly.

*In vitro* cytotoxic and cell proliferation effect of microspheres were evaluated on MKN45 gastric carcinoma cell line. MKN45 cells were used to mimic the *in vitro* gastric mucosa. MKN45 cell line was gift from Instituto de Engenharia Biomédica (INEB) and cells were grown in RPMI1640 (Lonza) supplemented with 10% (v/v) fetal bovine serum (FBS), 1% antibiotic (100 units/mL penicillin and 100 µg/mL streptomycin). The cells were maintained epithelial like morphology in humidified atmosphere containing 5% CO<sub>2</sub> incubator at 37°C. Cells were observed under light microscope (Olympus CKX31) and inverted phase contrast microscope (Olympus CKX41).

##### ***In vitro* Cell Viability and Proliferation**

The cell viability and cytocompatibility of chitosan microspheres on NIH3T3 fibroblast cells were investigated. The cytotoxicity was quantified by using MTT assay following indirect cytotoxicity ISO standard (10993-5). According to ISO 10993-5 standart, microspheres were incubated in DMEM for 24 h for extraction procedure. Cinnamon bark oil loaded chitosan and chitosan nanocomposite microspheres were dispersed in DMEM supplemented with 10% FBS and incubated at 37 °C for extraction procedure. Briefly, fibroblast cells were seeded in 96 well-plate at the density of  $1 \times 10^4$  cell/well and incubated at 37 °C for 24 h. The medium containing 100 µL of each extract was added to the pre-seeded cells and incubated for 24 h, 48 h and 72 h. Cell viability was determined by using the yellow methyl thiazole tetrazolium (MTT) assay. Number of surviving cells was determined by MTT dye reduction. This assay is based on the reduction of the yellow tetrazolium salt, MTT, to form insoluble blue formazan product



by mitochondrial enzymes. At the end of each time point, cell culture medium was removed, cells were washed with PBS and 100  $\mu$ L MTT solution (0.5 mg/mL) was added into each well. Plates were incubated at 37  $^{\circ}$ C for 4 h in dark. After 4 h of incubation, samples were centrifuged (1800 rpm, 10 min) to carefully remove non-metabolized MTT. Then, MTT solution was removed and 100  $\mu$ L DMSO was added to dissolve formazan product. Absorbance was determined by using microplate reader (Varioscan Spectrophotometers, Thermo) at 570 nm and cell viability was calculated according to Equation 4.8.

Similarly, indirect cytotoxicity assay was performed in order to investigate the cytotoxic effect of microspheres on MKN45 cell viability. Briefly, cells were seeded in 96 well-plate at the density of  $1 \times 10^4$  cell/well and incubated at 37  $^{\circ}$ C for 24 h. Then the medium containing 100  $\mu$ L of each extract was added to the seeded cells and incubated for 24 h, 48 h and 72 h. Cell viability was determined by using the WST-1 assay. At the end of the incubation time, medium was removed and medium containing 10% WST-1 (Biochemica) was added. Plates were incubated at 37  $^{\circ}$ C for 3 h in darkness. Absorbance was determined by using microplate reader (Varioscan Spectrophotometers, Thermo) at 490 nm and the cell viability was calculated.

*In vitro* cell proliferation and interaction of microspheres with MKN45 gastric epithelial cells were investigated by using WST-1 assay, too. The cells were seeded on 96 well plate at a concentration of  $1 \times 10^4$  cell/well ( $10^5$  cells/mL) and cultured for 24 h at 37  $^{\circ}$ C. The tested microspheres were dispersed in RPMI 1640 culture medium at a concentration of 1 mg/mL. Then, the medium was removed and medium containing microspheres was added. Cells were treated with prepared microspheres for 24 h, 48 h and 72 h. After incubation period, WST-1 was added in order to quantify the MKN45 cell proliferation and read by using microplate reader (Varioscan Spectrophotometers, Thermo) at 490 nm.

$$\% \text{ Cell Viability} = \frac{\text{Absorbance of treated cells}}{\text{Absorbance of control cells}} * 100 \quad (4.8)$$

The effect of cinnamon bark oil on NIH3T3 and MKN45 cell viability was performed by MTT and WST-1 assays on MKN45 gastric epithelial cells. Cinnamon bark oil concentrations were selected in accordance with minimum inhibition concentration study (4-500  $\mu$ g/mL). Stock solution was prepared in ethanol and diluted in cell culture

medium to final concentration. The same procedure mentioned above was used in the rest of the study.

#### **4.2.7. *In Vitro* Cellular Uptake**

*In vitro* cellular uptake of chitosan nanocomposites was determined by using fluorescence microscope (Zeiss, Axio). MNK45 cells were seeded on 6 well plate at a concentration of  $5 \times 10^5$  cells/mL and incubated at 37 °C for 24 h. The cells were exposed to 1mg/mL rhodamine labelled fluorescent microspheres for 2 h and 4 h. Untreated cells were used as control. After incubation period, the cells were fixed with 3.7% paraformaldehyde solution and washed with PBS. To track the internalization, the fixed cells were stained with DAPI at a concentration of 0.5 µg/mL which binds specifically to DNA at the end of 2 h and 4 h treatment. The stained cells were examined and visualized by fluorescent microscopy with excitation of 353 nm and emission of 465 nm for DAPI and 558 nm excitation and 575 nm emission for rhodamine.

#### **4.2.8. *In Vitro* Cell Binding Studies**

##### **4.2.8.1. Radiolabelling of Chitosan Microspheres**

The radiolabeling procedure for oil loaded microspheres was performed by small modification as described before (Gundogdu et al., 2015; Özgenç et al., 2015; Ekinci et al., 2015). Cinnamon bark oil loaded chitosan microspheres were radiolabeled with  $^{99m}\text{Tc}$ . Reduction of  $^{99m}\text{Tc}$  is required for converting  $^{99m}\text{Tc}$  from the  $+7$  state to a desired lower oxidation state, which can complexes with the ligand to form the radiopharmaceuticals. Different types of reduction agents are used for this reason. In this study, stannous chloride was used as reducing agent. To radiolabel chitosan nanoparticles, three micrograms of chitosan microspheres (COM-COM1-COM3-COM5) were suspended in 700 µL SF solution. 3 mg of  $\text{SnCl}_2$  was dissolved in 200 µL SF and this solution was added into microsphere solution under atmosphere of bubbling nitrogen. Radiolabeling was performed with 0.1 mL of  $^{99m}\text{Tc}$  (1 mCi) and incubated for 30 min at room

temperature. The radiolabeled formulations were separated by centrifugation at 5000 rpm for 5 min. At the end of the centrifugation, the supernatant was taken to another eppendorf. The labeling efficiency microspheres (ms) was measured by using a gamma dose calibrator (Bioscan Atomlab 400) and calculated using following equation:

$$\text{Labeling Efficiency (\%)} = \frac{\text{Radioactivity of ms}}{\text{Radioactivity of (ms+Supernatant)}} * 100 \quad (4.9)$$

#### 4.2.8.2. Radiochemical Purity

Radiochemical purity of labeled formulations was determined by Thin Layer Chromatography (TLC). Silica gel sheets were used as stationary phase. Free  $^{99m}\text{Tc}$  was determined by using acetone as the mobile phase. 5  $\mu\text{L}$  of samples were spotted on the chromatographic sheets, in acetone. The chromatography sheets were dried and scanned by using a Radio-TLC scanner. The percentage of radiochemical purity (RP %) of  $^{99m}\text{Tc}$ -chitosan microspheres was calculated from the following equation:

$$\text{Radiochemical purity (\%)} = 100 - (\text{Free } ^{99m}\text{TcO}_4^{-2}\%) \quad (4.10)$$

#### 4.2.8.3. *In vitro* Cell Incorporation Studies

Cell binding studies of  $^{99m}\text{Tc}$  labeled oil loaded chitosan microspheres were performed using MKN45 cells in order to investigate the incorporation of gastric epithelial cell lines. MKN45 cells was harvested and cells were seeded on 6 well plate at a concentration of  $5 \times 10^5$  cells/mL and incubated at 37 °C for 24 h. 1 mCi  $^{99m}\text{Tc}$  labeled formulations were suspended with 1.8 mL cell culture medium and added into each well after medium was removed. Cells were treated with radiolabeled samples for 2 h and 4 h at 37°C. After incubation period, the samples were taken from cell medium and adherent cells were collected into another eppendorf. The amount of radioactivities in the cell medium and cells were counted by a gamma dose calibrator (Bioscan Atomlab 400). The cellular uptake was calculated as the percentage of the activity counted in the cells relative

to the total activity counted. The percentage radioactivity of cells was calculated by following equation:

$$\text{Cell Binding (\%)} = \frac{\text{Radioactivity of Cells}}{\text{Total Radioactivity}} * 100 \quad (4.11)$$

#### **4.9. Statistical Analysis**

The significance of the differences between obtained data was evaluated by One-way and two-way analysis of variance (ANOVA). Experimental results were expressed as mean  $\pm$  standart error.

## CHAPTER 5

### RESULTS AND DISCUSSIONS

#### 5.1. Determination of Minimum Inhibitory Concentration (MIC) of Cinnamon Bark Oil

##### 5.1.1. Minimum Inhibitory Concentration (MIC) of Clarithromycin

Agar dilution method has been approved by CLSI as a gold standard method for antimicrobial susceptibility testing. MIC value of clarithromycin for *H. pylori* strain NCTC 11637 was found as 0.125 µg/mL by agar dilution method and also confirmed by E-test method. Agar dilution and E-test results showed strong agreement. This result was compared with several studies related to MIC value of clarithromycin on *H. pylori* strain NCTC 11638 and NCTC 11637 and similar results were found as 0.125 µg/ml; 0.12 µg/mL, respectively (Vega et al., 2009; Ustun et al., 2006). Consequently, agar dilution method was optimized and validated for antimicrobial susceptibility testing of cinnamon bark oil for *H. pylori* according to CLSI agar dilution method for clarithromycin.

##### 5.1.2. Minimum Inhibitory Concentration (MIC) of Cinnamon Bark Oil

MIC value of cinnamon bark oil was found as 8 µg/mL by agar dilution method. Additionally, the effects of different parameters such as inoculum amount and concentration, culture media, inoculation type on antimicrobial activity of cinnamon bark oil against *H. pylori* were investigated in order to standardize the CLSI protocol for antimicrobial susceptibility testing of essential oil.

No significant difference was observed on colony growth by different McFarland scales and inoculum amounts. During MIC determination experiments, spreading of

bacterial suspension directly onto agar plates was preferred for better visualization of colony growth than spot inoculation due to the transparent and fragile colonies of *H. pylori*. When the effect of the inoculum parameters such as inoculum concentration, inoculum amount and type of inoculum were investigated, the results showed that the inoculum parameters had effect on the bacterial intensity on agar plates but had no effect on the minimum inhibition concentration. Weak growth of *H. pylori* was observed at McFarland 2 and therefore the colonies could not be seen clearly. Our findings showed that McFarland 3 or 4 should be used to evaluate and to obtain the best growth of *H. pylori* for the antimicrobial activity of the cinnamon bark oil as an essential oil; and also spreading plate methodology could be considered instead of spot inoculation for precise decision of inhibition concentration. Antimicrobial efficacy of cinnamon bark oil was clearly observed in McFarland 4 and McFarland 3 in comparison to McFarland 2. 5  $\mu\text{L}$  of inoculum amount was selected as better than three  $\mu\text{L}$  of inoculum amount for determination of MIC. As a result, the CLSI agar dilution method for antimicrobial susceptibility testing could be used to determine the MIC values of essential oils as well as broth microdilution method (Lambert et al., 2001).

These results indicate that the cinnamon bark oil has antimicrobial activity against *H. pylori*, thus the natural antimicrobial activity of cinnamon bark oil could be an alternative approach for preventing *H. pylori* growth *in vitro*. Ooi et al. (2006) determined the antimicrobial activity of cinnamon bark oil against different microorganisms and they showed that cinnamon bark oil and cinnamaldehyde seems to be good broad spectrum antimicrobial agents. Bassolé and Juliani (2012) reported that essential oils containing aldehydes or phenols, such as cinnamaldehyde, citral, carvacrol, eugenol or thymol as main constituents have the highest antibacterial activity, followed by essential oils containing terpene alcohols. The chemical components of *Cinnamomum* oil differs according to the bark, the branches and the leaves and among bark of different ages of trees. Additionally, the components of *Cinnamomum cassia* oil is also affected by growing and harvested seasons for branches and leaves and different extracted parts (bark or xylem) for branches (Geng et al., 2011). Cinnamon bark oil used in this study is obtained from genus *Cinnamomum* and the major volatile compounds present in the cinnamon bark oil are cinnamaldehyde (65–80%), eugenol, and trans-cinnamic acid (5–10%) (Ooi et al., 2006). Altiok (2011) previously determined the major components of standardized cinnamon bark oil (Sigma) which we used this study and Cinnamaldehyde (%72) was found as the main component of cinnamon bark oil (Altiok, 2011). This

component might be responsible for antimicrobial activity (Ali et al., 2005). The *in vitro* effects of eugenol and cinnamaldehyde against indigenous and standard *H. pylori* strains, their MIC values and time course lethal effects at various pH were also evaluated by Ali et al. (2005). The authors used commercial preparations of eugenol and cinnamaldehyde in order to determine the MIC value by agar dilution method. Their results showed that eugenol and cinnamaldehyde completely inhibited all the strains (both sensitive and resistant) at a concentration of 2 µg/mL. They also found that eugenol and cinnamaldehyde inhibited *H. pylori* ATCC 26695 strain at 2 µg/mL concentration within 9 and 12 hours of incubation by time course viability studies. Cinnamaldehyde shows antimicrobial activity due to its lipophilicity of terpenoids and phenyl propanoids which can penetrate the cell membrane and damage the bacterial enzyme system (Babu et al., 2011).

Bergonzelli et al. (2003) determined the MBC (minimum bactericidal concentration) of cinnamon bark oil against *H. pylori* as 40 µg/mL. However, the climate, soil type and age of plant affect the antimicrobial properties as well as harvested period due to the quality, amount and composition of essential oil (Bergonzelli et al., 2003). Lu et al. (2011) investigated the antibacterial effect of cinnamon oil alone and in combination with thyme and clove oil by agar dilution method. They resulted that combination of cinnamon and thyme oil showed an additive effect against both Gram-negative and Gram-positive bacteria whereas combination of cinnamon and clove oil displayed an additive effect only against *B. subtilis*, *B. cereus*, *S. aureus*. In practice, using antioxidants is essential to heal peptic ulcer and/or to prevent the oxidative stress. Furthermore, they indicated that these compounds are nontoxic at specified doses being consumed and they have antioxidant property as well as antimicrobial property. Ohno et al. (2003) investigated the antimicrobial effect of different essential oils (cypress, juniper, tea tree, lemon verbena, basil, peppermint, marjoram sweet, eucalyptus, ravensara, lavender, lemon, lemongrass, rosemary) against *H. pylori*. Thirteen essential oils used in this study completely inhibited the growth of *H. pylori in vitro* at a concentration of 0.1% (v/v) whereas *Cymbopogon citratus* (lemongrass) and *Lippia citriodora* (lemon verbena) have bactericidal activity against *H. pylori* at 0.01% concentration.

Based on this result, cinnamon bark oil was encapsulated within chitosan microspheres including MIC value of 8 µg/mL against *H. pylori*.

## 5.2. Effects of Spray Drying Parameters on Microsphere Characteristic

Spray drying is one of the most common process to encapsulate bioactive compounds. The solution was fed to the nozzle with a peristaltic pump and atomization occurred by the force of the compressed air, disrupting the liquid into small droplets during the process. The droplets were blown into a chamber where the solvent in the droplets was evaporated with the help of hot air and discharged out through an exhaust tube. The solvent evaporation rate depends on the feed rate, temperature of air, flow rate of air, size of droplets and total solid concentration (Desai and Park 2006). Properties (surface morphology, particle size, process yield, encapsulation efficiency) of microspheres are influenced by manufacturing parameters such as inlet temperature, and pump rate. Several studies were conducted to examine the effects of different parameters on particle characterization. Therefore, we investigated the effects of inlet temperature and feed rate on the characteristics of spray-dried chitosan microspheres. The experiments were performed with different inlet temperatures (180 °C, 190 °C, 200 °C) and pump rates (6 mL/min, 7 mL/min, 8 mL/min) and effects of these parameters on % humidity, particle size and % yield were evaluated. The effect of inlet temperature and pump rate on the properties of prepared chitosan nanocomposite microspheres were presented in Table 5.1.

Table 5. 1. Effects of spray drying parameters on product humidity, yield and size of microsphere

Parameters		Responses		
T (°C)	Pump (mL/s)	% Humidity	Size (µm)	Yield (%)
180	6	6.4	0.900	14
180	7	16.5	1.1	14
180	8	20	1.3	26
<b>190</b>	<b>6</b>	<b>7.6</b>	<b>0.97</b>	<b>50</b>
190	7	8.6	1.4	37.5
190	8	8.8	1	50
200	6	8	1.2	50
200	7	8.8	1.10	36
200	8	8.9	0.92	53



An increase in the feed rate increases the amount of solvent to be evaporated and material to be dried. It also increases the bulk density of the product, particle size and humidity of the final product. As depicted in the Table 5.1, increased pump (feed) rate resulted in higher moisture content, especially at lower inlet temperature ( $p < 0.1$ ). Higher feed rates lead to decrease in the outlet temperature. Outlet temperature also changed depending on inlet temperature. For instance, at 180 °C of the inlet temperature, outlet temperature decreased to 60-64 °C. In this condition, sticky and wet particles were obtained as a result of incompleting atomization.

Inlet temperature is another important parameter. Low temperature leads to condensation inside the chamber and the dry particles stick to the walls of chamber and therefore cannot be collected properly. Thus process yield was low. The % yield of the chitosan microspheres decreased slightly with an increase in the liquid flow rate and decrease in the inlet temperature. For example, % yield decreased to 14% at 180 °C of inlet temperature when compared to 190 °C and 200 °C. The reason could be due to the fact that at higher feed rate, complete drying of the spray-dried chitosan microspheres was not achieved (Desai and Park, 2005). The stickiness is related to moisture content and humidity of the product. The inlet air temperature was found to be the most effective parameter on moisture content. Feed rate alone was not an effective parameter, but the interaction with inlet temperature indicated significance.

Size of the chitosan microspheres prepared under the condition of a faster pump rate was found to be larger, due to the fact that large droplets were formed during the spray-drying process. However, the size of the prepared microspheres was not affected much by the change of process parameters studied in this study. The size of the microspheres obtained at various temperatures and pump rates were in the range of 0.9-1.4  $\mu\text{m}$  (Table 5.1).

The optimum inlet temperature and pump rate for the preparation of cinnamon bark oil loaded chitosan microspheres were determined as **190 °C and 6 mL/s** based on the results obtained for lowest humidity and high yield. When the inlet temperature was lower than this temperature or the pump rate was higher than 7 mL/s, the solvent in the droplets could not be fully evaporated.

Altuok (2011), investigated the effects of spray drying parameters on cinnamon bark oil loaded chitosan microspheres and it was found that the inlet temperature was the most effective parameter on water activity and also the interactions with inlet temperature

and concentration indicated significance. The results of this study are in good agreement with our findings.

Drying temperature has also an important role in the microsphere morphology. Microspheres showed that rough surface morphology and dimples on the surface were observed at higher temperatures (Figure 5.1). At higher temperatures, deformation occurs on surface morphology leading to cap-shaped particle formation. In comparison, microspheres had spherical and smoother morphology at lower temperatures. This phenomenon can be explained by the different drying rate at different temperature conditions. Selomulya et al. (2011) explained this situation that high inlet temperature leads to higher drying rate and thus shorter drying time which causes a dry crust and roughness on the surface. Raval et al. prepared chitosan microspheres by spray drying at 140 °C inlet temperatures and 6 mL/min whereas outlet temperature was 90 °C. Similar surface morphology was observed in these spray drying conditions (Raval et al., 2010). Maas et al. (2011) produced mannitol microspheres by spray drying temperatures at different temperatures. They showed that mannitol particles had different surface roughness depending on outlet temperatures and observed some dimples on microparticles (Maas et al., 2011). In the case of exceeding the critical internal pressure that the crust can resist, particles are tendency to collapse and dimple. Shorter drying time results in quicker heat and mass transfer.

Nowadays, new approaches such as microfluidics based systems and nanospray dryers have been developed to obtain particles with more uniform, controllable size and morphology. Particle size and morphology are crucial properties in pharmaceutical applications because these properties have effect on product degradation, drug release, swelling ability, cellular uptake as well as bioavailability (Selomulya, Liu, Wu, and Chen, 2011).

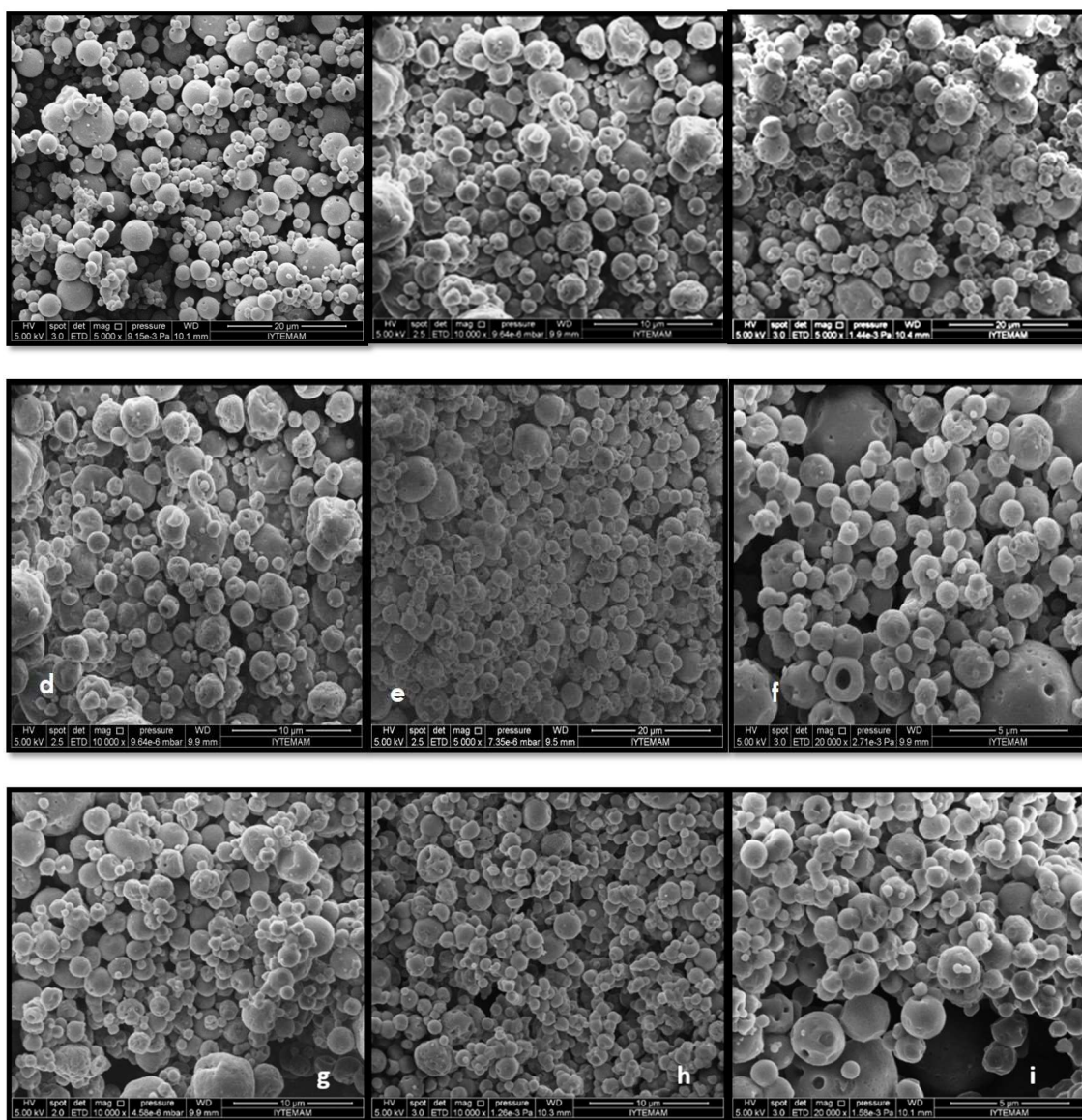


Figure 5. 1. Morphological characterization of chitosan nanocomposite microspheres; a. 6 mL/s, b. 7 mL/s, c. 8 mL/s at 180 °C; d. 6 mL/s, e. 7 mL/s, f. 8 mL/s at 190 °C; g. 6 mL/s, h. 7 mL/s, i. 8 mL/s at 200 °C.

### 5.3. Characterization of Chitosan Microspheres

#### 5.3.1. Particle Size and Morphology

The shape, surface morphology, and particle size of chitosan microspheres were examined using SEM and TEM analyses. Figures 5.2 and 5.3 illustrate the SEM images of unloaded and oil loaded chitosan nanocomposite microspheres. The mean particle size

was calculated by measuring about 200 particles using ImageJ programme and particle size distribution (PSD) of each formulation was represented in Figure 5.2. The particle size of all formulations ranged from 1  $\mu$  to 5  $\mu$  and mean particle size of prepared microspheres was observed between 1-3  $\mu$ . Also sonication step during the production provides not only intercalation of nanoclay but also homogeneous particle size distribution as well as decreasing particle size.

Due to spray drying technique some wrinkles were observed on microspheres as shown in Figure 5.2. In another study, Harris et al. (2010) prepared crosslinked chitosan microspheres by spray drying. The crosslinked microspheres showed smooth surface with some indentation on the surface as a result of rapid particle shrinking during spray drying process (Harris et al., 2010). As seen in Figure 5.2, neat chitosan microspheres had smooth surface. Also chitosan nanocomposite microspheres had spherical shape and smoother surface except CM1 formulation (Figure 5.3). However, with oil incorporation, some dimples were observed on chitosan microspheres. As depicted in Figures 5.2 & 5.3, oil loaded chitosan microspheres (CO) have spherical shape and smoother surface morphology than oil loaded chitosan nanocomposites (COM1-COM3-COM5). In the study of Raval et al. (2010), chitosan microspheres containing amoxicillin were prepared by spray drying method following chemical crosslinking. They also produced fine spherical chitosan microspheres with a small particle (2-4  $\mu$ m) size for controlled release of amoxicillin. It was also explained that chitosan microspheres produced by spray drying process have higher sphericity and specific surface area which are significant properties for drug delivery applications. Our results in terms of size and sphericity are found be consistent with the findings of Raval et al. (2010). The size of the nano/microparticles plays a key role in their adhesion to and interaction with the biological cells, internalization and cellular uptake mechanism. However, too small nanoparticles may result in lower encapsulation efficiency and rapid drug release and therefore would not be preferred for targeted delivery applications (Kulkarni and Feng, 2013). Thus, the suitable size is desired for controlled delivery systems.

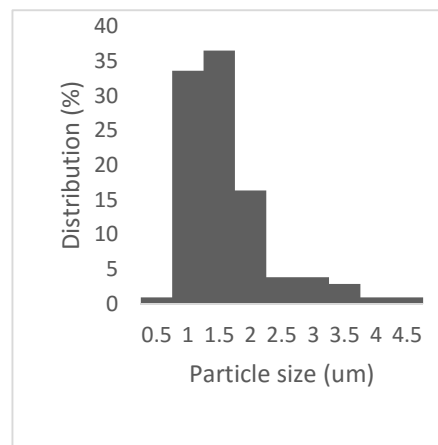
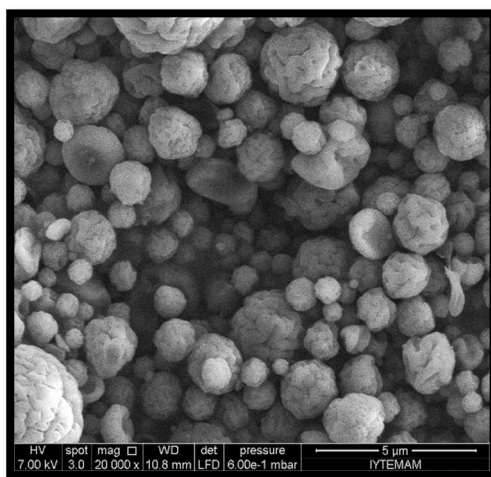
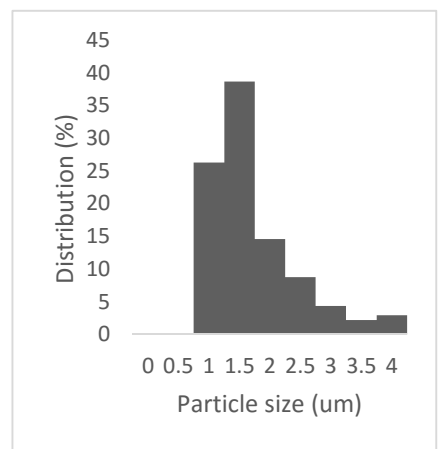
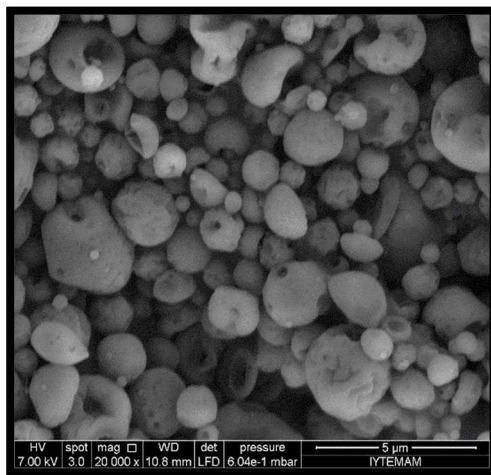
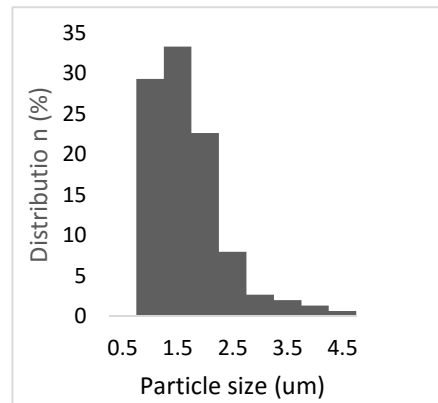
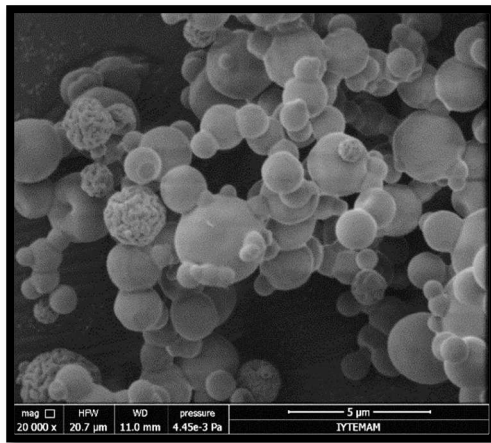


Figure 5. 2. SEM images of the chitosan microspheres a. Chitosan b. CO c. COM1 d. COM3 e. COM5 microspheres

(cont. on next page)



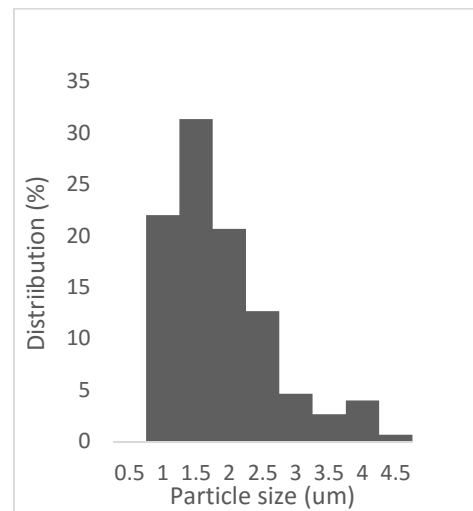
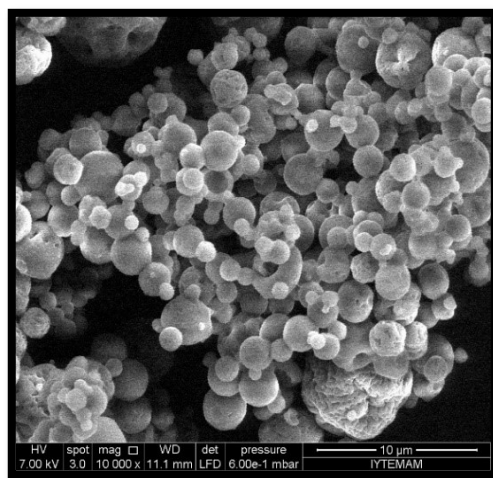
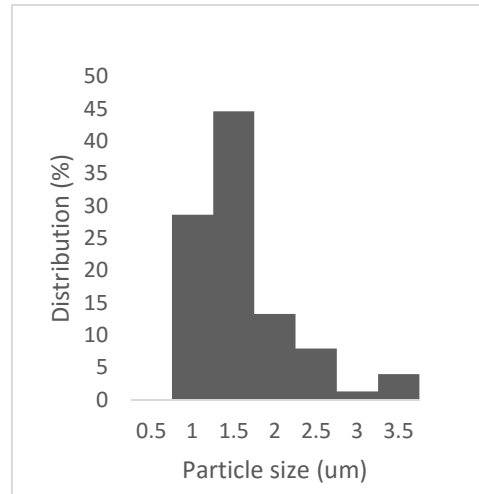
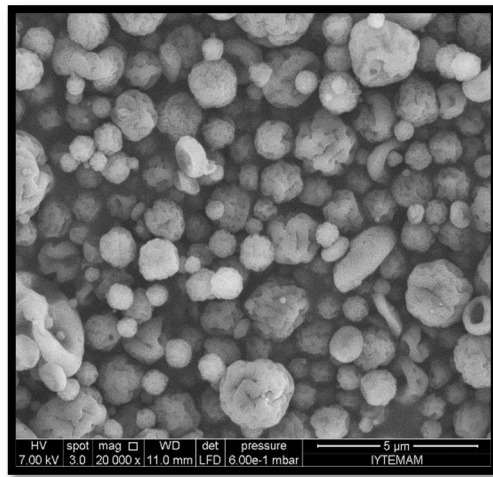


Figure 5.2 (cont.)

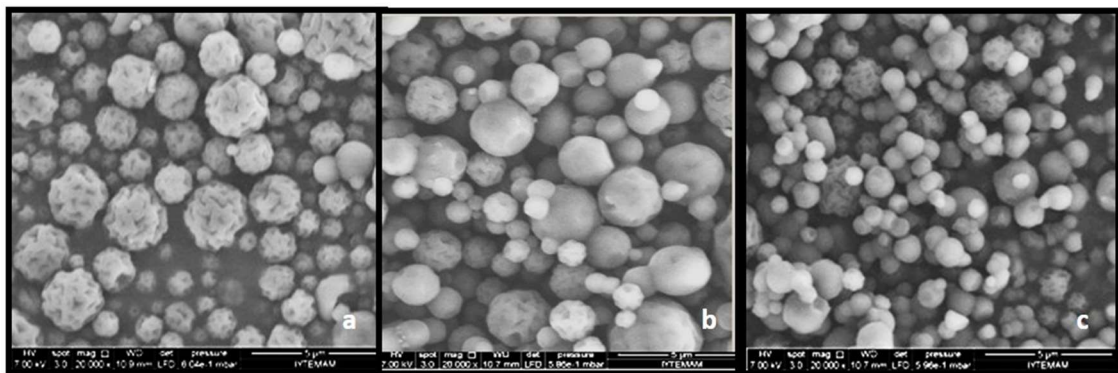


Figure 5. 3. SEM images of a. CM1 b. CM3 c. CM5 microspheres

Additionally, the shape and morphology of chitosan microspheres were also examined by TEM analysis. As shown in Figure 5.4, the prepared microspheres have

spherical shape in the range of 1-3  $\mu\text{m}$ . Similar observations were obtained by Desai and Park (2006) with TPP crosslinked chitosan microspheres.

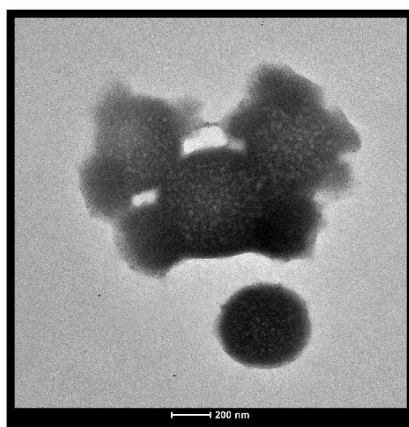


Figure 5.4. TEM images of oil loaded COM5 microspheres

### 5.3.2. Encapsulation Efficiency (EE)

Encapsulation efficiency and drug loading capacity of cinnamon bark oil were determined by Equations 4.2 and 4.3 as explained in the previous section. The amount of encapsulated cinnamon bark oil in chitosan microspheres was calculated based on calibration curve as depicted in Figure 5.5. The results showed that cinnamon bark oil was successfully loaded into chitosan microspheres. The percentage EE of the prepared microspheres was found to be in the range between 40 and 72% as shown in Table 5.3. The %EE was found to be proportional to drug loading (%). Drug loading capacity of cinnamon bark oil loaded microspheres was determined between 24-43%. Encapsulation efficiency and drug loading (%) were significantly different from each other ( $p < 0.05$ ). Although nanoclay ratio did not change encapsulation efficiency significantly, except %1 MMT incorporated microspheres with 40% of EE, the encapsulation degree of cinnamon bark oil was determined between the range of 60-72%. 5% (w/w) MMT intercalation increased encapsulation efficiency up to 72%. This result could be attributed to high adsorption capacity of MMT with large specific area (Hua et al., 2010).

Encapsulation efficiency is related with the surface oil content. Generally, the higher the surface oil means that the lower encapsulation efficiency. In this case, initial burst release occurs due to high amount of oil on the surface in drug release profile.

5% MMT incorporation increased EE in comparison to other formulations (Table 5.3). The reason could be explained by the interaction between chitosan and MMT which forms a suitable network to load the active agent. In a similar study, Hu et al. studied controlled release of ofloxacin as a model drug from chitosan/MMT hydrogel. They found that EE increased with increased amount of MMT and nanoclay incorporation improved entrapment of drug significantly (Hua, Yang, Wang, et al., 2010).

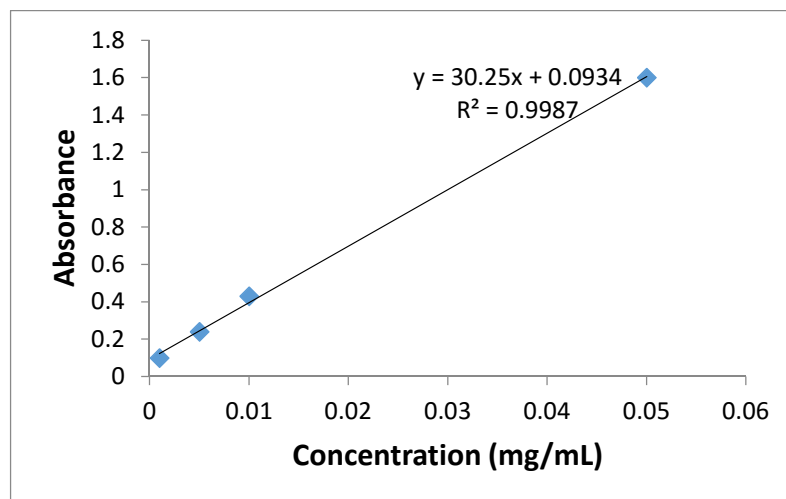


Figure 5. 5. Calibration curve of cinnamon bark oil

Table 5. 2. Encapsulation efficiency of microspheres

Formulation	EE (%)	Drug Loading (%)
CO	60±4.8	36±2.9
COM1	40±1.3	24±0.8
COM3	60±2.5	36±1.5
COM5	72±2.2	43±1.3

### 5.3.3. Surface Charge

Zeta potential is an important property in order to characterize micro/nanoparticles because the stability, adhesion to biological surfaces, and rheological properties of colloids depend on their surface charge. Zeta potential has an effect on the interaction of microspheres with charged drugs, and also on the adhesion of drug delivery systems onto biological surfaces. Therefore, the zeta potential values of the prepared microspheres were determined to investigate the electrostatic interactions in this study.



To examine interaction between chitosan and nanoclay platelets, firstly, the surface charge property of montmorillonite clay was determined. Montmorillonite, a member of the smectite group, is a 2:1 clay, meaning that it has two tetrahedral sheets of silica sandwiching a central octahedral sheet of alumina. Three morphological planes of the montmorillonite having different chemical composition: gibbsite layer, siloxane layer and an edge surface which is a complex oxide of the two constituents  $\text{Al}(\text{OH})_3$  and  $\text{SiO}_2$  are presented in Figure 5.6. Polar sites, mainly consisting of octahedral  $\text{Al}-\text{OH}$  and tetrahedral  $\text{Si}-\text{OH}$  groups, are situated at the broken edges and exposed hydroxyl-terminated planes of clay lamellae. Surface ligands at the gibbsite plane and edge surface: i)  $=\text{MOH}$  groups are involved in proton (acid-base) equilibria; different surface species belong to this ligand type such as  $\text{Al}-\text{OH}-\text{Al}$  groups at the gibbsite surface,  $=\text{AlOH}$  and/or  $=\text{SiOH}$  groups at the edge surface and  $\text{Si}-\text{O}-\text{Si}$  groups at the siloxane layer; ii)  $\text{XO}^-$  groups on the surface of the siloxane layer are induced by isomorphous substitution of  $\text{Si}$  by  $\text{Al}$  ( $\text{Al}-\text{O}-\text{SW}$ ; these groups react by ion exchange (Stumm, 1992; Tombácz and Szekeres, 2006).

Montmorillonite particles carry two kinds of electrical charges: a pH dependent charge due to proton adsorption/desorption reactions on surface hydroxyl groups located at the edges and a structural negative charge resulting from isomorphous substitutions at the faces of platelets (Forano, 2004). The amphoteric sites are conditionally charged, and can be positive or negative charges, depending on the pH. Proton adsorption at high pH takes place mainly on variable charge sites and become positively charged at pH values lower than the point of zero charge (PZC). This surface charge heterogeneity of clay minerals presented originally by Van Olphen (1963) (Forano 2004; Tombácz and Szekeres 2006).

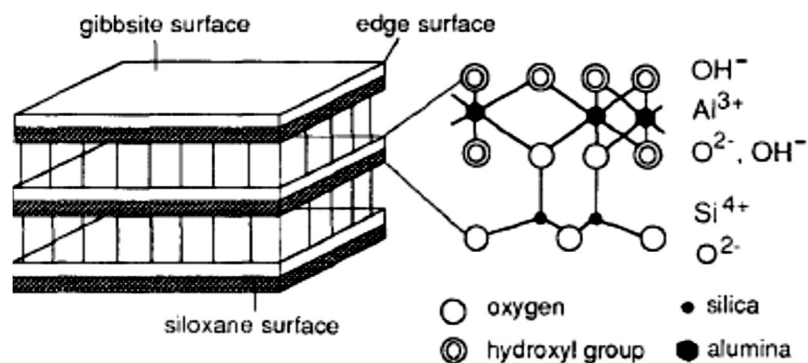


Figure 5. 6. Schematic representation of layered silicate structure (Stumm, 1992)

The Na-montmorillonite (natural nanoclay) has negatively surface charge and shows a negative zeta potential in the whole pH range (3.0-10.0) (Jin and Zhong 2012; Avena et al. 1990). However, montmorillonite can be modified with organic groups. Surface potential of montmorillonite can vary at different pH values due to different reactive site on surface and different bond of surface hydroxyl groups with differing reactivity to acid and base. In order to determine the point of zero charge (PZC), zeta potential of the montmorillonite used in this study (Cloisite 10A) was measured at different pHs and illustrated in Figure 5.7. PZC of Cloisite 10A was approximately found as pH 6.5. Zeta potential of MMT has positive zeta potential below pH 6.5 as depicted in Figure 5.7 and above this pH, MMT became negatively charged. In general, the surface silicate layers of MMT possess negative charge, whereas the edges of layers have positive charge.

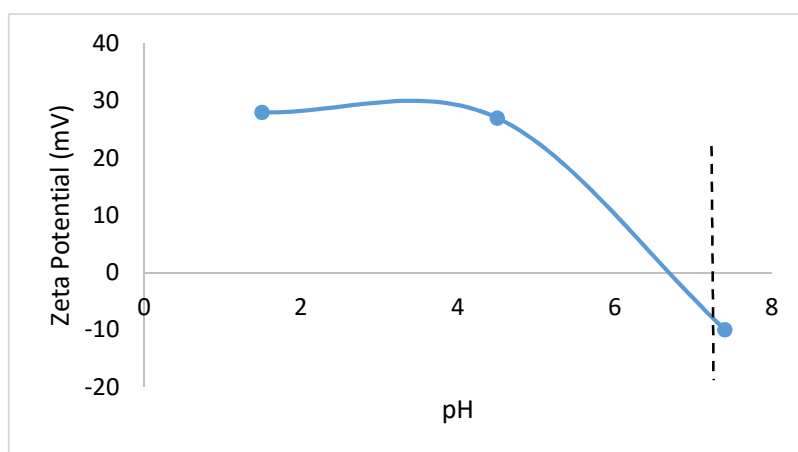


Figure 5. 7. The effect of pH on surface charge of montmorillonite (Cloisite 10A)

Secondly, zeta potential of neat chitosan microspheres was measured and it was found that neat chitosan microspheres have positive zeta potential due to protonation of primary amine groups of chitosan, as expected. Zeta potential of prepared microspheres were determined in SGF and pH 4.5 simulating the fasted and fed state of gastric conditions. Figures 5.3 and 5.4 show the zeta potential values of prepared microspheres at pH 1.2 (SGF) and pH 4.5. It is clear that cinnamon bark oil incorporation leads to a decrease in the surface charge in comparison to neat chitosan due to interaction between cinnamon bark oil and chitosan in both mediums ( $P < 0.05$  and  $F_{\text{calculated}} > F_{\text{critical}}$ ) (Tables 5.3 and 5.4). The electrostatic interaction between the negatively charged surface of MMT and the positively charged amino groups of chitosan may affect the zeta potential.

However, MMT (Cloisite 10 A) has positive surface charge below pH 6.5 and therefore, zeta potential values of oil loaded chitosan nanocomposite microspheres did not change significantly when compared oil loaded chitosan microspheres. Consequently, zeta potential of chitosan microspheres decreased with clay and oil addition.

Additionally, pH of the medium affected the zeta potential of chitosan and chitosan nanocomposite microspheres because of the different ionization levels of chitosan and nanoclay at different pHs (Khunawattanakul, Puttipipatkachorn, Rades, and Pongjanyakul, 2008). Our findings showed that zeta potential of chitosan microspheres were lower in pH 4.5 than in SGF (Tables 5.3 and 5.4). The results demonstrated that all the microspheres showed positive charge in all cases and both pH medium. Since particle size and surface charge of micro/nano particles affect the biodistribution and pharmacokinetic properties of particles in the body, several studies were conducted in order to investigate the effect of surface charge on protein adsorption and cellular uptake. Surface charge of particles affects the attachment of particles to cell membrane, which is the first step of cellular uptake. Generally, particles with positive charge could be more easily uptaken by the cells depending on cell type. It could be concluded that chitosan and oil loaded chitosan composite spheres have mucoadhesive and absorption enhancement properties and can be considered as potential drug release vehicles for gastrointestinal system (Honary and Zahir, 2013).

Table 5. 3. Surface charge of chitosan and oil loaded chitosan nanocomposite microspheres in SGF (n=6)

<b>Formulation</b>	<b>Zeta Potential (mV)</b>
MMT	20.7±1.0
Chitosan	30.1±1.3
CO	21.2±1.0
COM1	20.9±0.7
COM3	24.5±1.0
COM5	22.8±2.0

Table 5. 4. Surface charge of chitosan and oil loaded chitosan nanocomposite microspheres at pH 4.5 phosphate buffer (n=6)

<b>Formulation</b>	<b>Zeta Potential (mV)</b>
Chitosan	19.5±1.3
CO	14.0±0.3
COM1	16.5±0.4
COM3	14.8±0.7
COM5	15.0±0.7

Lin et al. (2013) determined zeta potential values of genipin crosslinked fucosa chitosan/heparin nanoparticles at pH 1.2, pH 4.5 and pH 6.0-7.0 in order to simulate the gastric conditions and *H. pylori* survival condition. Zeta potential value of chitosan nanoparticles was found +30.1 at pH 1.2 whereas -3.1 at pH 7.0 since  $\text{NH}_3^+$  groups were deprotonated of chitosan resulted in collapsing of nanoparticles (Lin et al., 2013).

### 5.3.4. Nanocomposite Structure

The level of nanoclay dispersion within chitosan matrix has been determined by both XRD and TEM analyses, which are the most commonly used methods to study the structure of nanocomposites. Depending on the dispersion level of the clay platelets, nanocomposites are classified into 3 main groups: flocculated, intercalated and exfoliated/delaminated (Wang et al. 2005). Due to the polycationic structure of chitosan in acidic media, MMT could easily penetrate and intercalate into polymer matrix with the help of cation exchange property of MMT.

### XRD

The nanocomposite structure of chitosan nanocomposite microspheres was investigated by XRD analysis. Figures 5.8-5.10 illustrate XRD patterns of neat chitosan, oil loaded chitosan and chitosan nanocomposite microspheres, respectively. The characteristic peak observed at around  $2\theta=22^\circ$  belongs to diffraction of neat chitosan (Figure 5.8). The characteristic diffraction peak of chitosan microspheres prepared by spray drying was also reported as approximately  $22^\circ$  (Desai et al., 2005). The powder

chitosan (unprocessed chitosan) exhibits characteristic peak at around  $2\theta=25^\circ$  (Hosseini et al., 2013). As compared with neat chitosan microspheres, the characteristic peak of oil loaded chitosan microspheres was observed approximately at  $2\theta=20^\circ$  in diffraction spectrum. This finding indicated that oil incorporation resulted a change in the chitosan structure. When oil was incorporated into chitosan microspheres, this characteristic peak of chitosan was broadened and shifted lower angle which indicated amorphous structure of the chitosan (Figure 5.9). Crystallinity of polymer is another important factor in controlled release applications. In general, high crystalline polymers are less penetrable since ordered crystalline structure prevents penetration of small molecules. Alexis 2005 reported that crystallinity dominates the degradation rate and affects drug release rate. The XRD results of neat and oil loaded chitosan microspheres showed amorphous structure morphology after spray drying process. In a similar study, prepared antibiotic loaded chitosan microspheres showed amorphous loose-structure by spray dryer processing (Mi et al. 1998). Faster solvent removal process by spray drying resulted in amorphous microsphere structure since it does not allow enough time to crystallize the drug and polymer (Freiberg and Zhu, 2004).

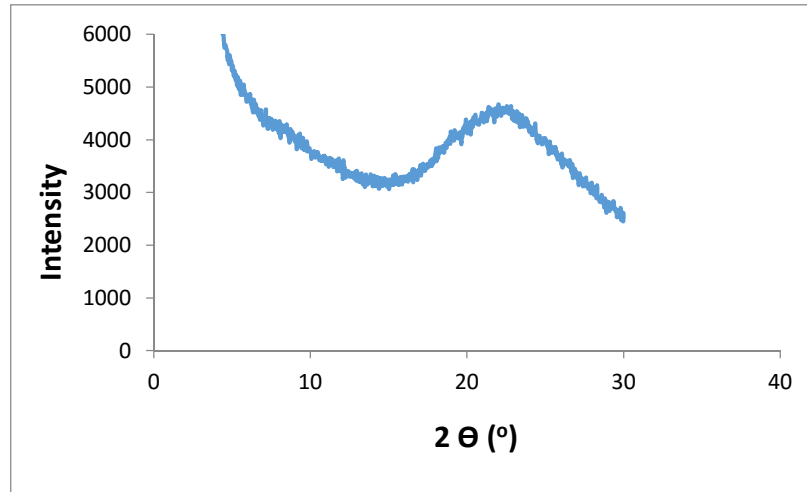


Figure 5. 8. XRD patterns of neat chitosan microspheres

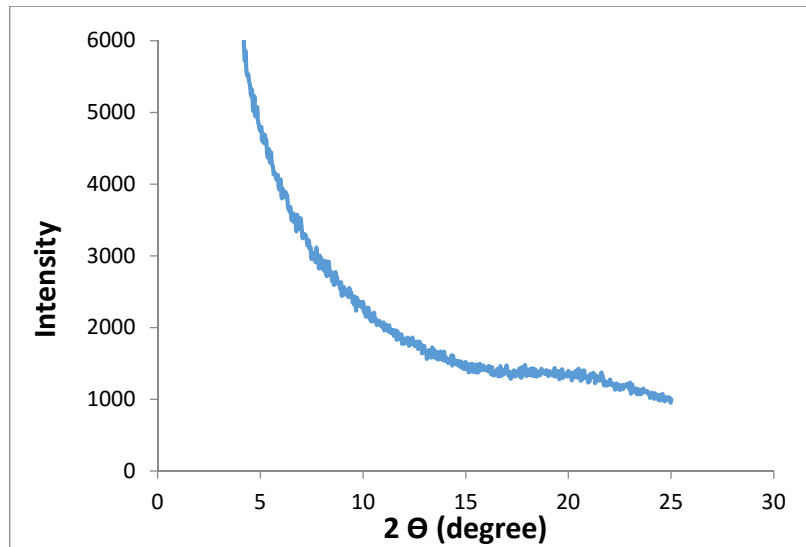


Figure 5. 9. XRD pattern of oil loaded chitosan (CO) microsphere

Figure 5.10 shows the XRD patterns of MMT and oil loaded chitosan nanocomposite microspheres. The intercalation of silicate layers was confirmed by the decrease in  $2\theta$  values with increased intercalation level. The characteristic diffraction spectrum of the nanoclay (Cloisite 10A) was observed approximately at  $2\theta=4.7$  corresponding to basal spacing ( $d$ ) of 1.92 nm (Figure 5.10). The characteristic reflection peak of MMT was broadened and shifted to  $2\theta=3.6$  and  $2\theta=3.2$  for COM1 and COM3 formulations, respectively. According to Bragg's law, the peak shifting of basal reflection of MMT from higher angles to lower diffraction angle indicates the increase in  $d$  spacing and intercalation of MMT whereas disappearance of MMT peak is attributed to complete exfoliation of nanoclay platelets in the polymer matrix. In the complete exfoliated state of nanocomposites, single layered silicate platelets are dispersed in the polymer matrix at several directions and far from each other beyond the detection limit of XRD. Therefore basal spacing increased to 2.45 nm and 2.8 nm when 1% and 3% nanoclay were incorporated into chitosan matrix as a result of intercalation process (Datta 2013; Wang et al. 2005). The reflection peak disappeared in the XRD spectrum for chitosan/nanoclay microspheres when the 5% MMT was incorporated into chitosan indicating formation of exfoliated structure (Abdollahi, Rezaei, and Farzi, 2012). Wang et al. (2008) prepared chitosan (N-2-hydroxyl-propyl-3-trimethylammonium chitosan chloride; HTCC)/MMT nanocomposites with different amount of MMT. Their XRD data showed that MMT peak shifted from  $7.2^\circ$  to  $4.5^\circ$  and interlayer distances increased which

shows that possible bilayers of HTCC sheets intercalated into the interlayer of MMT and resulted an intercalated nanostructure.

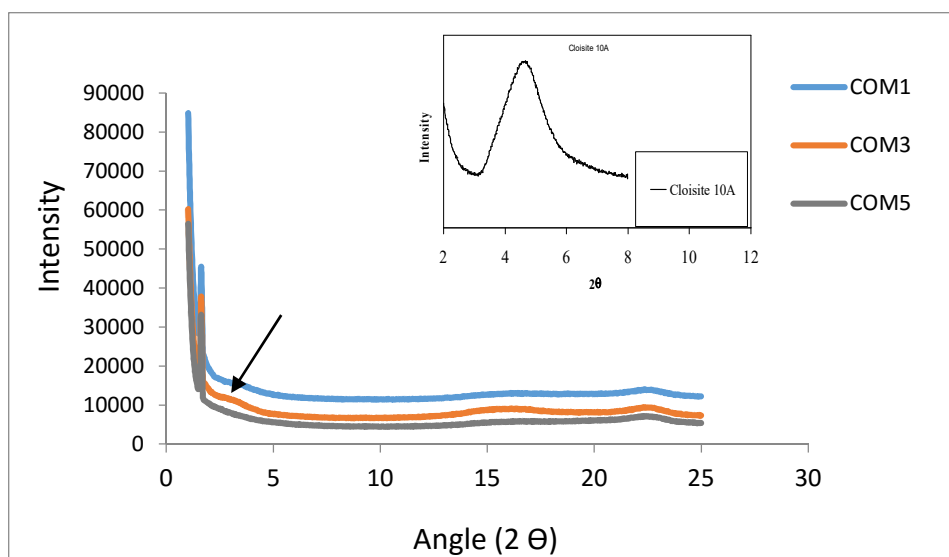


Figure 5. 10. XRD patterns of cinnamon oil loaded chitosan/MMT nanocomposite microspheres (COM1, COM3, COM5)

## TEM

The nanoclay dispersion in chitosan matrix has also been evaluated by TEM analysis. The TEM micrograph of chitosan nanocomposite microspheres (COM5; 5% w/w on the chitosan basis) indicated the exfoliation (stretched and separated lines) of MMT platelets, which were uniformly and well dispersed into chitosan matrix (Figure 5.11). No agglomeration and/or flocculation were observed providing the formation of exfoliated surface morphology. By this way, XRD results were confirmed by the TEM results. Wang et al., 2005 incorporated different amount of MMT (2.5 wt%, 5wt%, 10 wt%) into chitosan matrix. They showed that increasing clay content (5% and 10% w/w) leads to flocculation and resulting intercalated morphology in the chitosan matrix. They confirmed this result with XRD data. The main mechanism might be explained that amino and hydroxyl functional groups of chitosan strongly interact with silicate hydroxylated edge groups of MMT via hydrogen bonds. The possible interaction of nanoclay (Cloisite 10A) and chitosan nanocomposites were proposed by Pandey & Mishra, 2011 and shown in Figure 5.12.

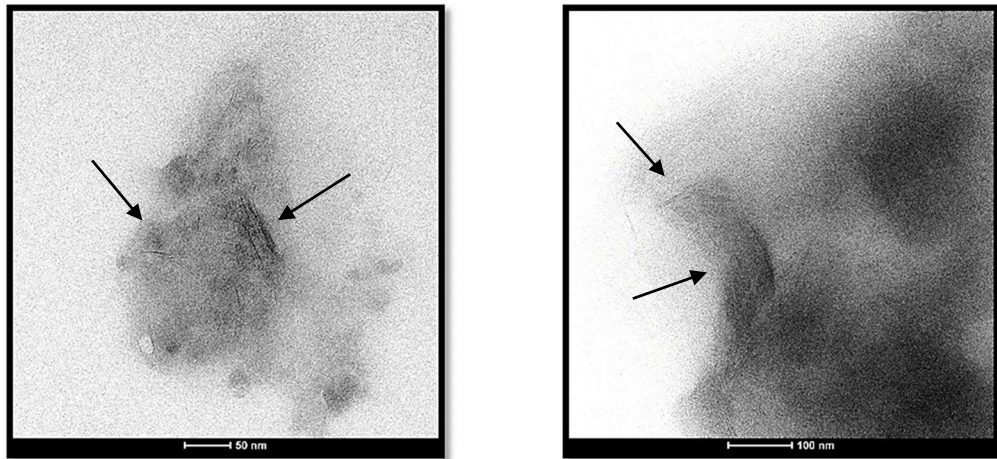


Figure 5. 11. TEM images of oil loaded chitosan/5%MMT microspheres with different magnifications (COM5)

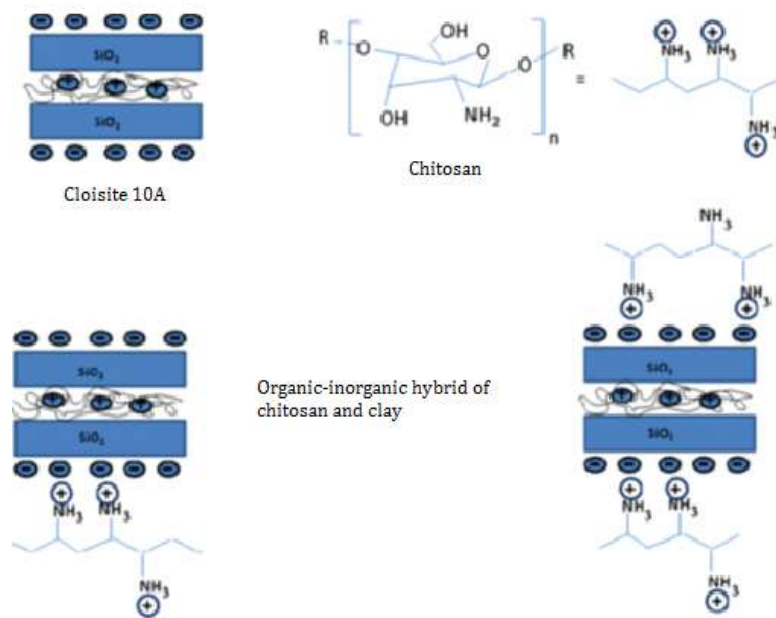


Figure 5. 12. Organic-inorganic interaction of chitosan/MMT nanocomposite (Source: Pandey and Mishra, 2011)

The exfoliated structure of nanoclay platelets in the nanocomposite structure is a crucial parameter in drug delivery systems. This structure provides tortuosity pathway in the polymer structure and reduces porosity which could hinder the diffusion and release of cinnamon bark oil in a controlled manner (Suresh et al., 2010).



### 5.3.5. Chemical Characterization

FTIR, Raman and NMR techniques were used to investigate chemical interactions between the chitosan, cinnamon oil and montmorillonite. Figure 5.13 represents the FT-IR spectra of chitosan, MMT and oil loaded chitosan microspheres. The characteristic bands were tabulated in Table 5.5. From the chitosan spectrum, it can be found that the distinctive absorption bands appeared at  $1654\text{ cm}^{-1}$  (amide I),  $1560\text{ cm}^{-1}$  ( $-\text{NH}_2$  bending of amine II) and  $1380\text{ cm}^{-1}$  (amide III). The absorption bands at  $1380\text{ cm}^{-1}$  belong to the amide III band consisting of components from C-N stretching and N-H in plane bending from amide linkages. The peak of Al-Al-OH stretching vibrations at  $3629\text{ cm}^{-1}$  found in the FT-IR spectrum is typical for MMT with high amount of Al in the octahedral sheet and disappeared in the spectrum of chitosan nanocomposite microspheres. The sharp peak at  $1050\text{ cm}^{-1}$  belongs to Si-O stretching of MMT which was also confirmed by Paluszkiwicz et al. 2011. However, this characteristic peak was shifted to lower frequency in oil loaded chitosan nanocomposites indicating that MMT existing in the nanocomposite structure. This results confirmed the interaction between functional groups of chitosan and MMT (Abdollahi et al., 2012).

The characteristic band corresponding to cinnamon oil was observed between  $1640\text{ cm}^{-1}$  and  $1680\text{ cm}^{-1}$  to C=C and  $1682\text{ cm}^{-1}$  belongs to aldehyde as seen in Figure 5.14. This peak was disappeared in chitosan formulations due to the interaction between amino group of chitosan and aldehyde group of cinnamon bark oil. The aldehyde group of cinnamon bark oil and amino group of chitosan form covalent imine bonds via Schiff reaction (Berger et al., 2004). The peak which was observed at  $1633\text{-}1635\text{ cm}^{-1}$  refers to imine formation. This peak corresponds to the amino group of chitosan reacting with cinnamaldehyde group form a Schiff base which was also depicted by Eldin et al. (2015). Phenyl group had a shoulder appeared at  $3080\text{ cm}^{-1}$  which also confirms imine reaction. Eldin et al. (2015) prepared a cinnamyl chitosan Schiff base cinnamaldehyde which is the main component of cinnamon oil under acidic conditions to form cinnamyl chitosan Schiff base. The new characteristic band observed at  $1634$  was attributed to C=N vibration and indicated that Schiff base (Eldin et al., 2015).

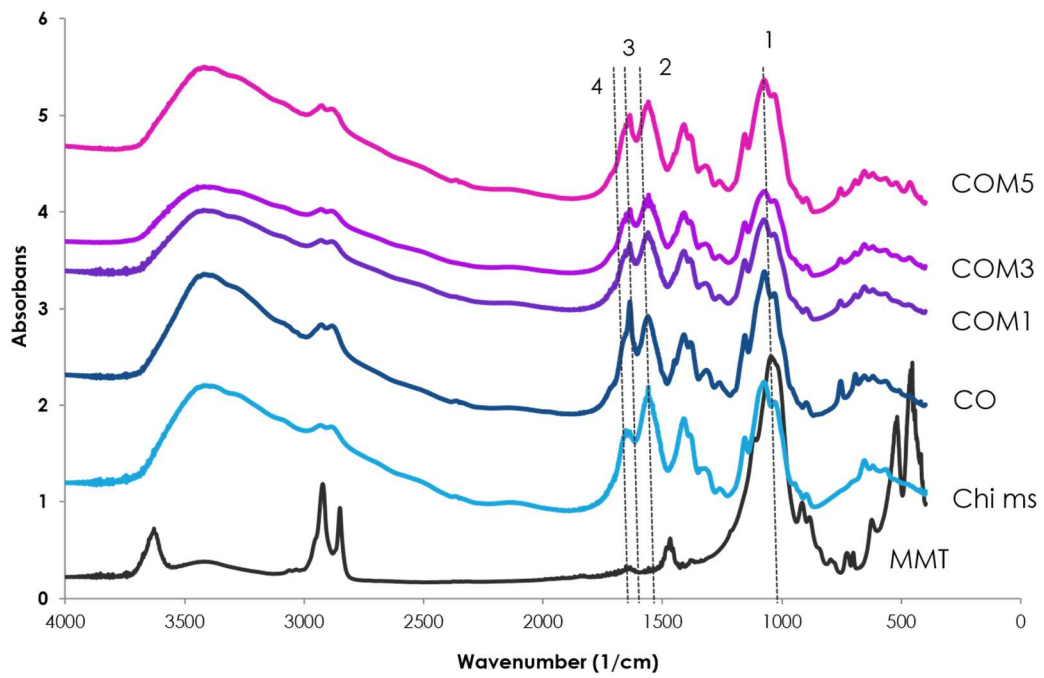


Figure 5. 13. FTIR spectra of chitosan nanocomposite microspheres. Vertical line 1 characteristic band of MMT (Si-O stretching), 2 belongs to  $-\text{NH}_2$  bending of chitosan (amine II), 3 refers to imine formation and 4 refers to characteristic band of chitosan amide I.

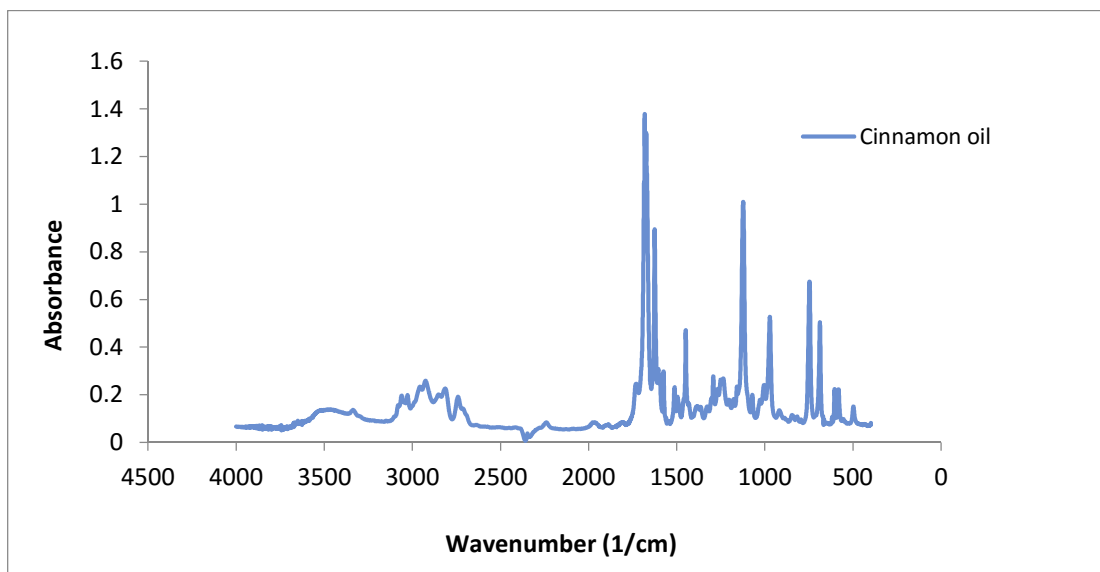


Figure 5. 14. FTIR spectra of cinnamon bark oil

Table 5. 5. FTIR data of chitosan nanocomposite microspheres

Wavenumber (cm <sup>-1</sup> )	Band	Formulation
916	AlAlOH	MMT Chitosan/clay formulations
1050	Si-O stretching	MMT Chitosan/Clay
1682	Aldehyde	Cinnamon oil
1654	C=O (stretch)	Chitosan (amide I)
1560	N-H bending	Chitosan (amine)
1380	C-N stretching	Chitosan (amide III)
1633-1635	C=N vibrations (imine formation)	Chitosan/oil Chitosan/oil/clay
3629	O-H for Al-OH	MMT

Figures 5.15-5.17 illustrate the <sup>1</sup>H-NMR spectra of chitosan microspheres, cinnamon bark oil, and oil loaded both chitosan and chitosan-clay microspheres, respectively. As seen in Figure 5.15, in the range of 9.5-10 ppm, the characteristic signal of aldehyde groups of cinnamon bark oil was observed. This peak was also seen in the NMR spectra of oil loaded microspheres that demonstrates successful oil loading into both chitosan and chitosan nanocomposite microspheres (Figures 5.15 and 5.16). Figures 5.16 and Figure 5.17 refer to a potential Schiff base resulting imine formation between chitosan and cinnamon bark oil. These results were also confirmed by FTIR data.

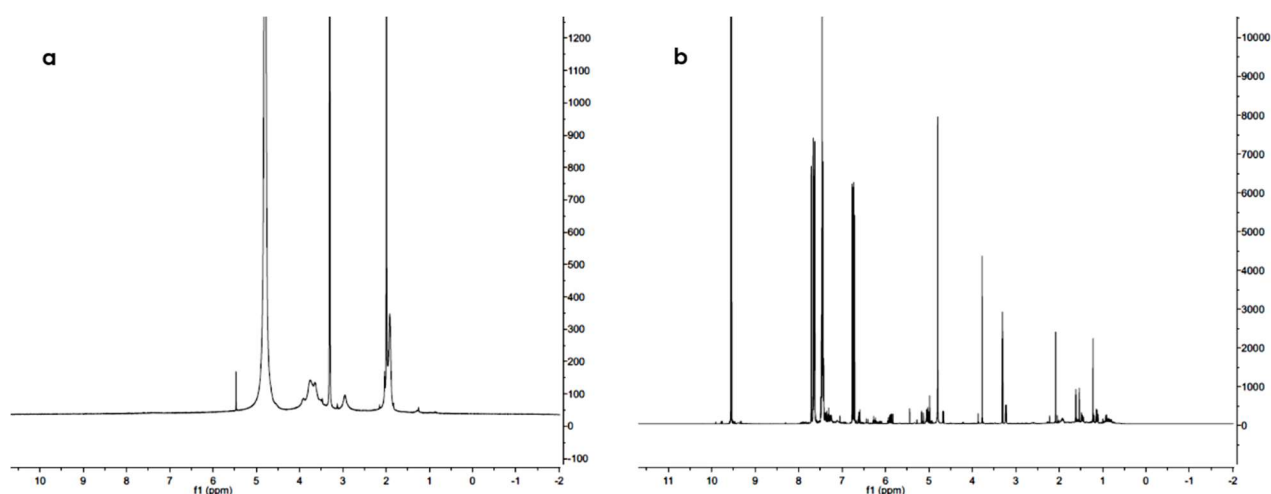


Figure 5. 15. <sup>1</sup>H-NMR spectra: a. control chitosan microspheres, b. cinnamon bark oil

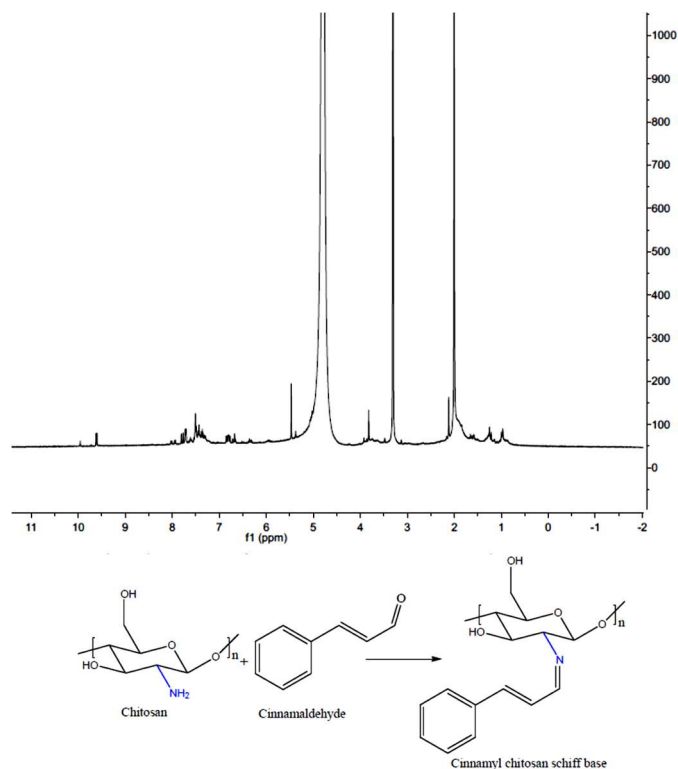


Figure 5. 16. <sup>1</sup>H-NMR spectra of oil loaded chitosan microspheres (CO) and schiff base reaction between chitosan and cinnamaldehyde

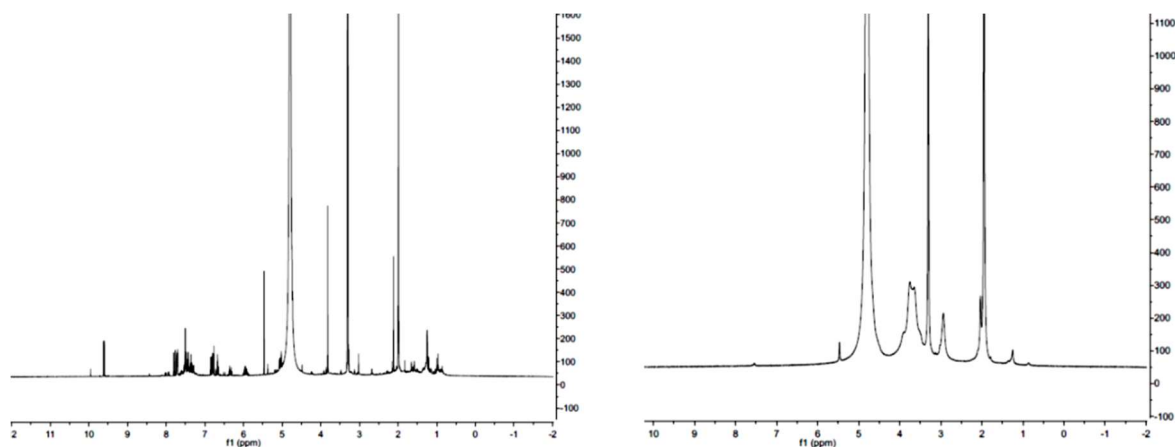


Figure 5. 17. <sup>1</sup>H-NMR spectra: a. chitosan/oil/3MMT (COM3) microspheres, b. chitosan/3MMT microspheres

Raman spectroscopy was also performed to verify the interactions among the MMT, chitosan and oil loaded chitosan nanocomposites. When analysing the spectra of neat chitosan microspheres, several well-defined peaks were found. The characteristic

peak of amide I band was observed at  $1640\text{ cm}^{-1}$ . Amide III band of chitosan was detected at  $1380\text{ cm}^{-1}$ . The peak observed at  $1120\text{ cm}^{-1}$  can be attributed to C-O-C vibrations of polymer backbones (Figure 5.18) (Escamilla-Garcia et al., 2013).

The characteristic peak of nanoclay was observed at  $616\text{ cm}^{-1}$  which belongs to Si-O vibrations (Figure 5.19). This peak shifted to  $622\text{ cm}^{-1}$  in COM5 formulation as seen Figure 5.20 with high nanoclay loading. The intensity of the  $1590\text{-}1630\text{ cm}^{-1}$  decreased in the formulation of chitosan/MMT (CM3) microspheres as seen in Figure 5.20.

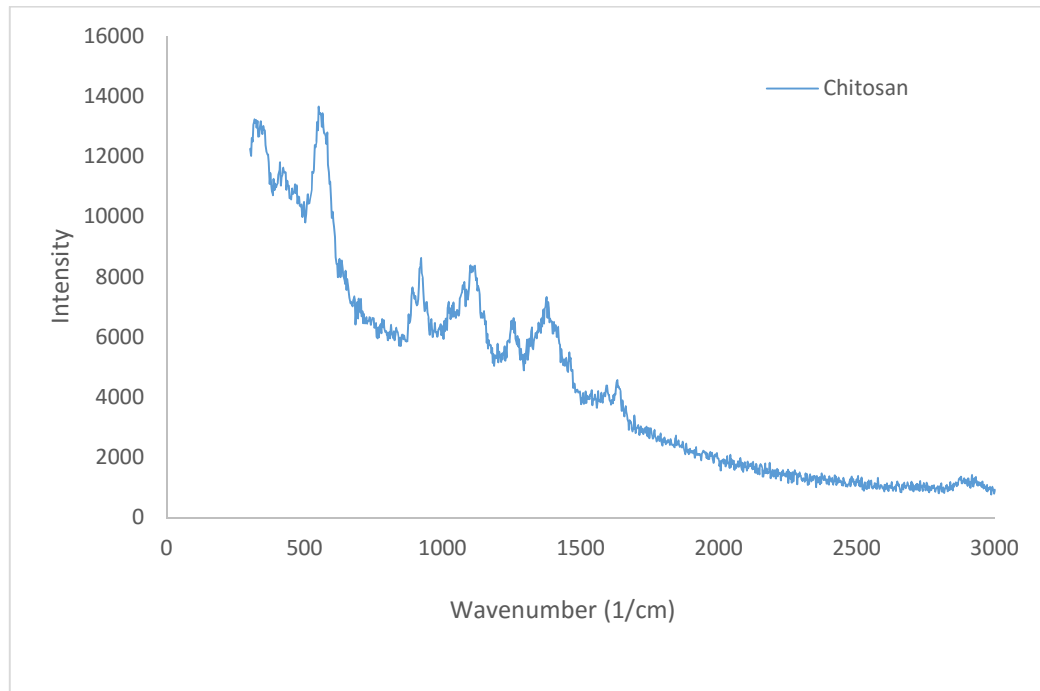


Figure 5. 18. Raman spectra of chitosan microspheres

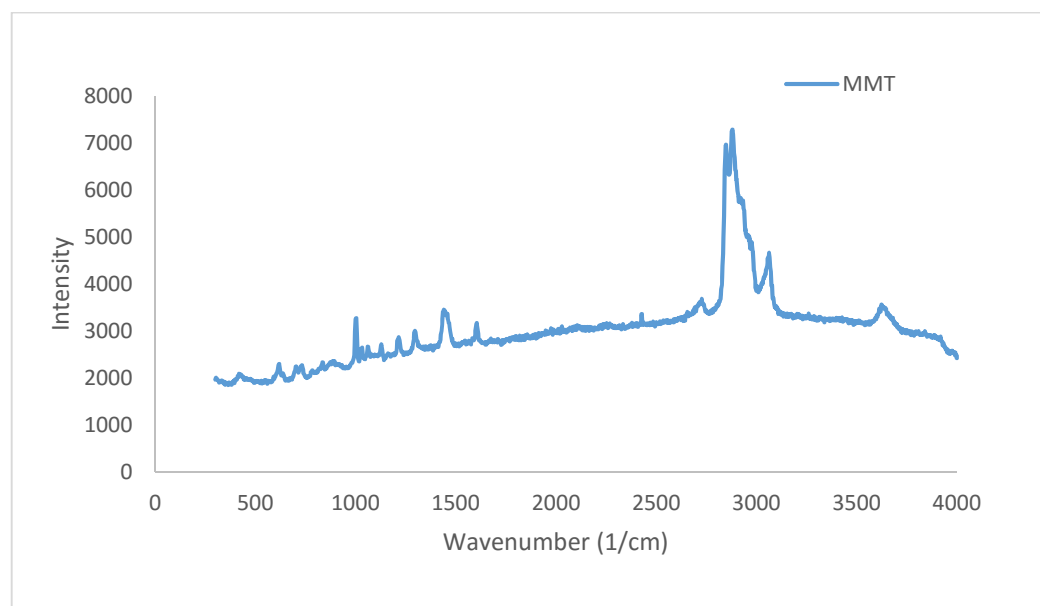


Figure 5. 19. Raman spectra of nanoclay (MMT)

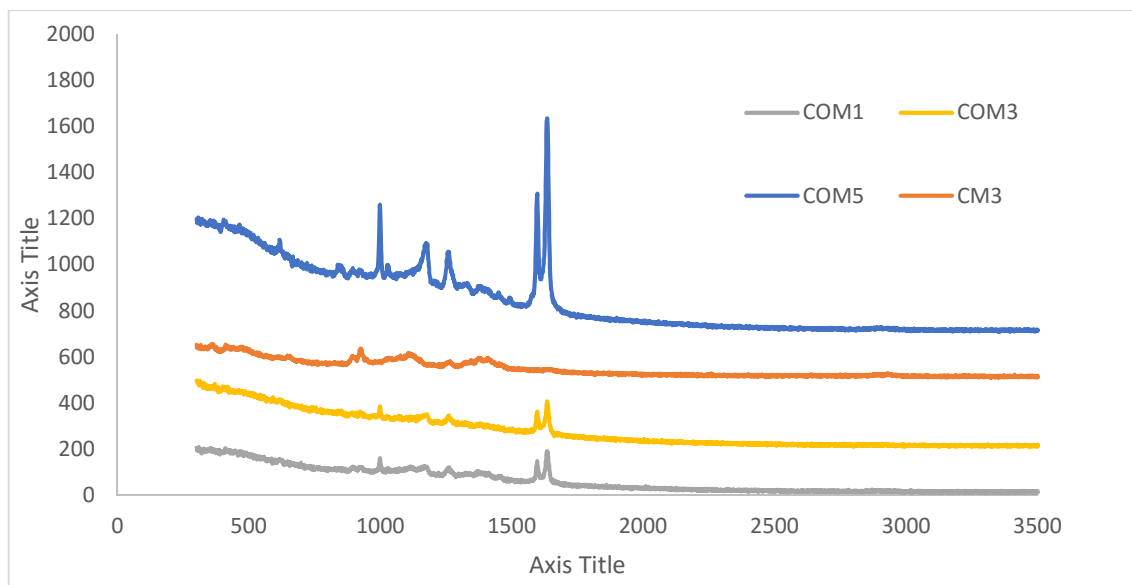


Figure 5. 20. Effects of oil and clay loading on Raman spectra of chitosan microspheres

The characteristic band corresponding to cinnamon oil was observed at  $1627\text{ cm}^{-1}$   $\text{C}=\text{C}$  stretching and  $1676\text{ cm}^{-1}$  belongs to aldehyde as depicted in Figure 5.21. Figure 5.20 shows possible interaction between chitosan, clay and cinnamon bark oil. The characteristic aldehyde groups of cinnamon oil was disappeared in cinnamon bark oil loaded chitosan microspheres and another characteristic peak of chitosan,  $1248\text{ cm}^{-1}$  shifted to  $1259\text{ cm}^{-1}$  in oil loaded chitosan nanocomposite microspheres. The reason could be an interaction with amine groups of chitosan and imine formation between aldehyde groups of cinnamon bark oil. The strong interaction between chitosan and cinnamon bark oil was confirmed by FTIR data and also zeta potential values of chitosan microspheres decreased with oil incorporation. The characteristic peak of cinnamon bark oil and clay was observed at  $1000\text{ cm}^{-1}$ . It is known that several bands for substituted benzenes are observed in the range between  $1600$  and  $1000\text{ cm}^{-1}$  including in-plane C–H bending vibrations that interact with various ring C = C vibrations (Jentzsch and Ciobotă, 2014). The peak intensity at around  $1000\text{ cm}^{-1}$  and  $\sim 1600\text{ cm}^{-1}$  increased for 5% MMT incorporated microspheres due to the higher MMT loading. However this peak was disappeared in the formulation of chitosan/MMT (CM3). It could be resulted that this disapparent peak is mainly related to cinnamon bark oil.

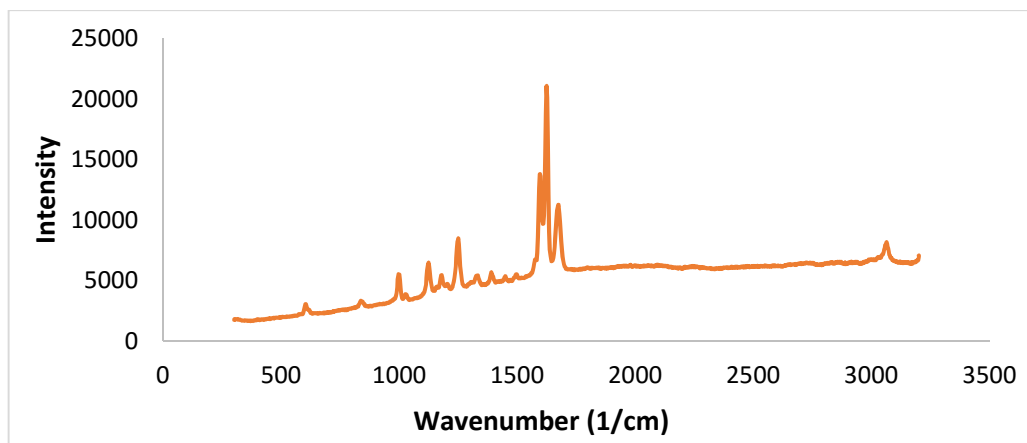


Figure 5. 21. Raman spectra of cinnamon bark oil

### 5.3.6. *In Vitro* Mucoadhesion

#### Contact Angle

Contact angle is one of the wetting properties of biomaterials. A hydrophilic surface exhibits a high wettability and a low water contact angle. In generally, the lower the contact angle indicates greater the affinity as indicated Figure 5.22. The results related to contact angle determination were depicted in Figure 5.23 and 5.24. Contact angle of control chitosan microspheres were found be  $83^\circ$  which is smaller than cinnamon bark oil loaded chitosan microspheres ( $100^\circ$ ). The contact angle values of cinnamon bark oil loaded chitosan microspheres were greater than  $90^\circ$  which indicates slight hydrophobicity of the oil loaded microspheres. Contact angle values significantly differed with oil incorporation ( $p < 0.05$ ,  $F > F_{crit}$ ). Cinnamon bark oil incorporation leads to an increase in contact angle due to hydrophobic nature. On the other hand, there was no significant differences between contact angles of CO, COM1, COM3 and COM5 formulations. Contact angle of microspheres did not significantly change with an increase in nanoclay amount. Chitosan microspheres started to swell immediately after the dropping of the water droplet during the experiment which could effect the contact angle value determination. This situation could be explained by the high swelling ability of chitosan.

The contact angle between polymer and cells or mucus layer should be equal or close to zero to provide sufficient spreadability. Cell adhesion to a surface is critical because adhesion precedes cell spreading, migration and differentiation in tissue

engineering and biomedical applications. It is known that chitosan can induce structural reorganization of the proteins associated to the intercellular junctions and thus promote the absorption of hydrophilic molecules (Flávia Chiva Carvalho, Marcos Luciano Bruschi, Raul Cesar Evangelista, 2011).

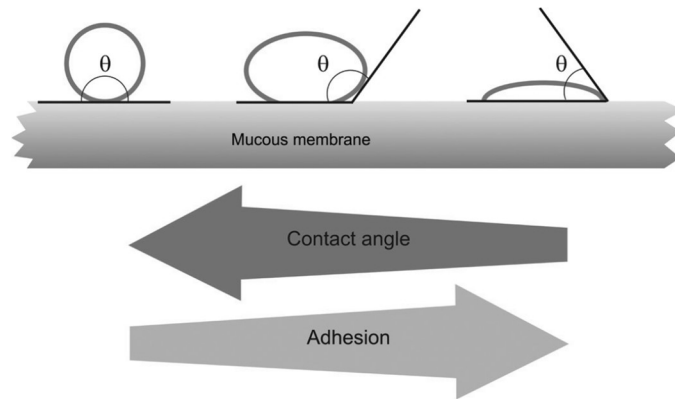


Figure 5. 22. Schematic diagram showing influence of contact angle between device and mucous membrane on bioadhesion (Source: Carvalho et al., 2011)

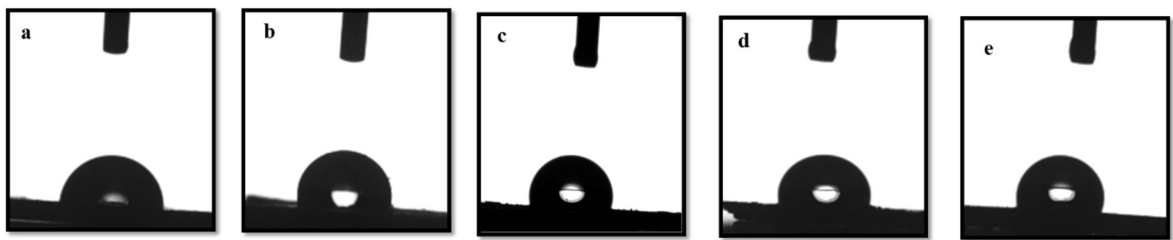


Figure 5.23. Contact angle images of chitosan microspheres a. Neat chitosan; b. C0; c. COM1; d. COM3; e. COM5 nanocomposites

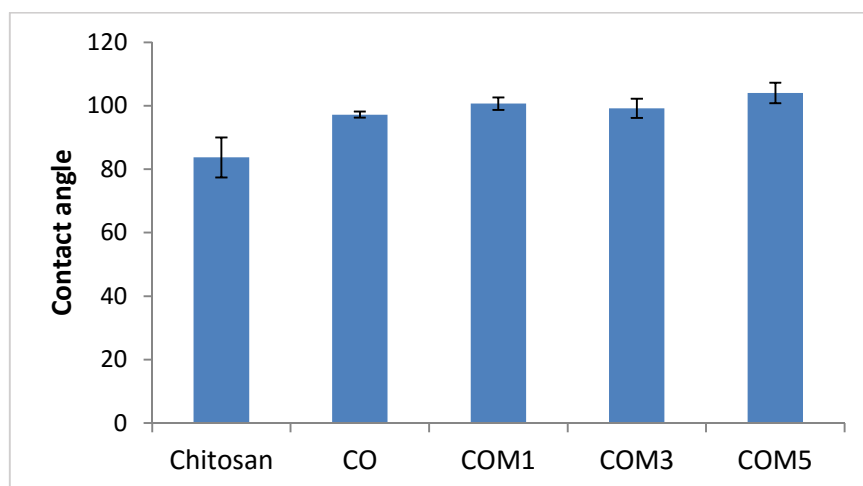


Figure 5. 24. Contact angle values of chitosan microspheres (n=5)



### ***In vitro* Mucoadhesion Assay**

Since mucoadhesive drug delivery systems can prolong the gastric residence time, drug absorption at targeted site is improved as a result of mucoadhesiveness and controlled release. In this study, the mucoadhesive behavior of the prepared chitosan microspheres was determined by Periodic acid/Schiff mucus glycoprotein assay. It is known that chitosan possesses mucoadhesive properties, due to the presence of many amino groups in the polymer chains that form hydrogen bonds with glycoproteins in the mucus and also ionic interactions between positively charged amino groups and negatively charged sialic acid residues of mucin. Clay mineral was also able to interact with the mucin (Salcedo et al., 2012). The percentage mucoadhesion results were presented in Figure 5.25. The results of *in vitro* mucoadhesion showed that all prepared microspheres had satisfactory mucoadhesive property ranging from 55-70% and could adhere to gastric mucosa (Figure 5.25). These results suggested that there is a strong attraction between mucin and chitosan microspheres. It is also clear that the mucoadhesion properties of the prepared microspheres significantly improved with MMT addition when compared to oil loaded chitosan microspheres ( $p < 0.05$ ,  $F > F_{crit}$ ). This could be due to the addition of having cation exchange property of montmorillonite. Percentage mucoadhesion of oil loaded chitosan microspheres was lower compared with control chitosan and chitosan/MMT microspheres. It could be due to the fact that mobility of the polymer chains was reduced by the interaction of oil and reducing contact/interpenetration with the mucin. Patil et al. reported that high flexibility of polymer backbone structure and polar functional groups are required for good mucoadhesion (Patil, Babbar, Mathur, Mishra, and Sawant, 2010). These findings are compatible with zeta potential values which are responsible for interaction with mucin molecules due to positive surface charge. Bioadhesion results of the chitosan –clay nanocomposites in the literature showed similar findings (Pongjanyakul and Suksri, 2009; Salcedo et al., 2012).

It is expected that an ideal mucoadhesive drug delivery system should form a strong non-covalent bond with the mucin-epithelial cell surfaces. Mucoadhesive systems are particularly important in *H. pylori* treatment. All the mucoadhesive results suggested that prepared microspheres can interact with mucin of the stomach and adhere to the mucosal surfaces. This property also allows the adhesion of prepared microspheres to gastric epithelial cells. Therefore, the developed system provides prolonged residence

time and high oil concentration at the gastric mucosa for more effective *H. pylori* eradication and clearance.

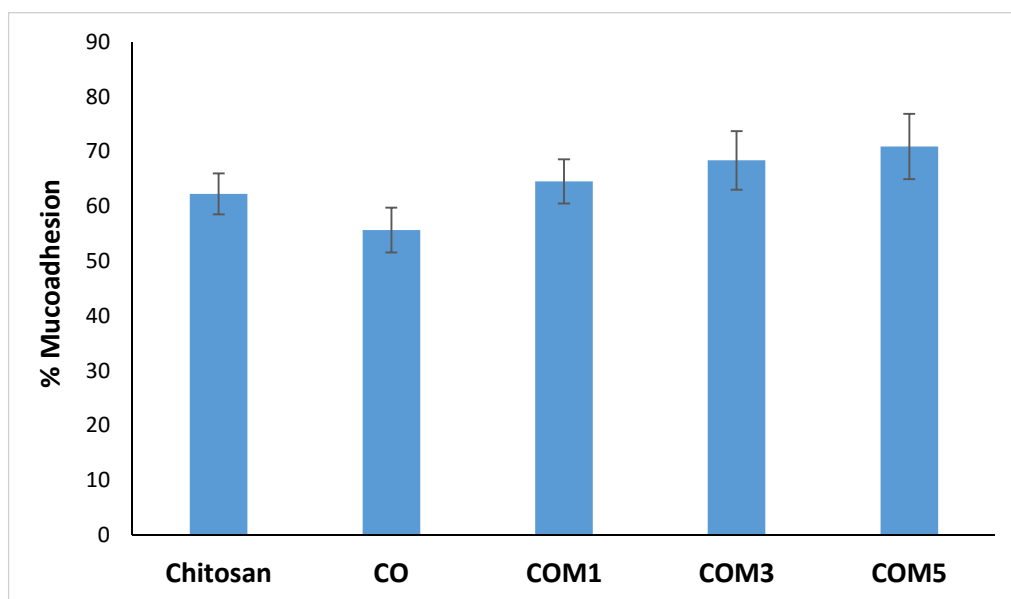


Figure 5.25. Mucoadhesion (%) of oil loaded and unloaded chitosan microspheres (n=4)

### 5.3.7. Swelling Degree

Since chitosan has high solubility and swelling properties in acidic medium, chitosan is unable to provide controlled release in gastric acid conditions. To overcome stability, swelling and burst release problems, layered silicate (nanoclay) was introduced into chitosan matrix in this study. Swelling experiments were performed in SGF and pH 4.5 mediums at physiological temperature of 37 °C. Swelling degree of neat chitosan microspheres could not be determined in SGF because chitosan was completely dissolved in acidic medium. As it can be seen in Figure 5.26, oil loaded control chitosan microspheres absorbed large amounts of water (about 1500%) in the equilibrium state. Addition of nanoclay slightly increased the swelling degree of oil loaded chitosan nanocomposite microspheres in SGF (Figure 5.26). However, swelling degree of oil unloaded microspheres decreased with clay content. With the addition of nanoclay (organic modified Cloisite 10A) consisting of some hydrophobic groups such as  $-CH_2-$  and  $-CH_3$ , the interaction was gradually decreased. Swelling degree of chitosan microspheres decreased from 1523% to 840% with incorporation of nanoclay. MMT

provides physical barrier and the addition of nanoclay to chitosan builds a strong cross-linking structure because of the interaction of negatively charged clay and positively charged  $\text{NH}^{3+}$  groups of chitosan. Therefore, this interaction influences the swelling behavior of the nanocomposite and consequently influences diffusion of the drug through the bulk entity (Q. Yuan et al., 2010). In the case of oil loaded nanocomposite microspheres, swelling properties are affected due to the more dominant interaction that forms imine bond between chitosan and oil. However, there was not a significant difference between oil loaded chitosan nanocomposites with an increase in clay content at pH 1.2 (SGF). It can be concluded that oil loaded and unloaded microspheres showed different swelling characteristic. On the other hand, swelling studies not only describe the amount of water contained within microspheres at equilibrium but also give insight into the network structure of gel and the transport mechanism of water uptake process. So, it is related with the structure of the microspheres. SEM results showed that the oil unloaded chitosan nanocomposite microspheres have smoother surface in comparison the oil loaded microspheres. In oil loaded microspheres, some cracks and wrinkles were observed and this result leads to water transport into microspheres. Cojocariu et al. 2012 investigated the effect of different amount of nanoclay (montmorillonite) on swelling and release properties of chitosan hydrogels. Swelling degree of chitosan hydrogels decreased when MMT was intercalated into chitosan matrix at concentration of 5%, 7% and 9%). Our swelling degree data for oil unloaded nanocomposite spheres agree with their findings. They explained this decrease by hydrophobic character of organic modified nanoclay (MMT) (Cojocariu et al., 2012).

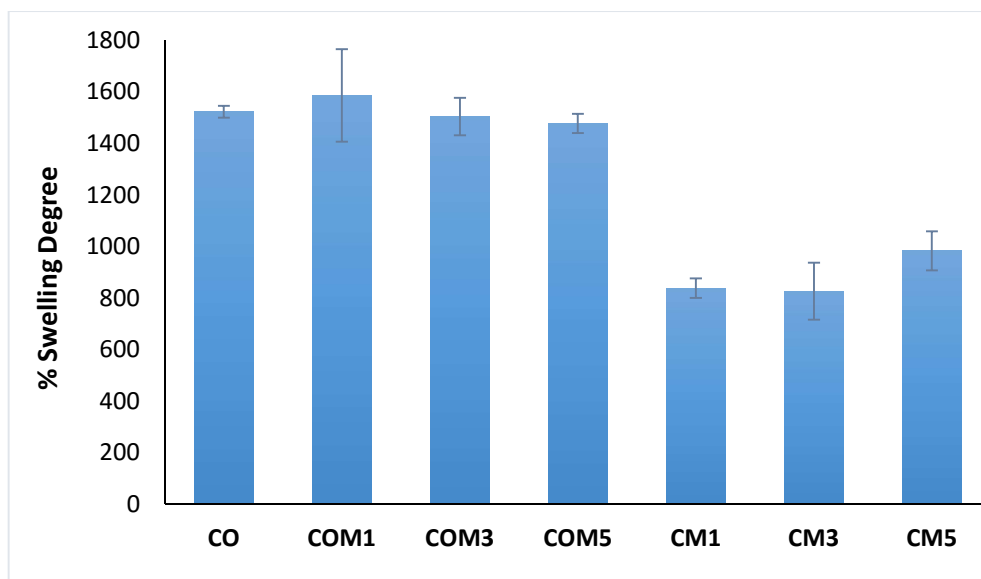


Figure 5. 26. Swelling degree of microspheres in SGF (n=3)

Swelling properties of prepared microspheres were also studied in pH 4.5 to mimic the gastric conditions. The swelling of cinnamon bark oil loaded chitosan microspheres in pH 4.5 were lower than in SGF media (Figure 5.27). Swelling degree decreased approximately 50% percentage in oil loaded chitosan (CO) microspheres in pH 4.5 in comparison to SGF medium. When oil was loaded into chitosan microspheres, swelling degree decreased from 1650% to 708% as a result of oil-chitosan interaction. It was reported that a decrease in pH environment has been led to increase of swelling degree (Chellat et al., 2000). However, when clay was introduced into microspheres, swelling increased and showed an increase trend with clay loading.

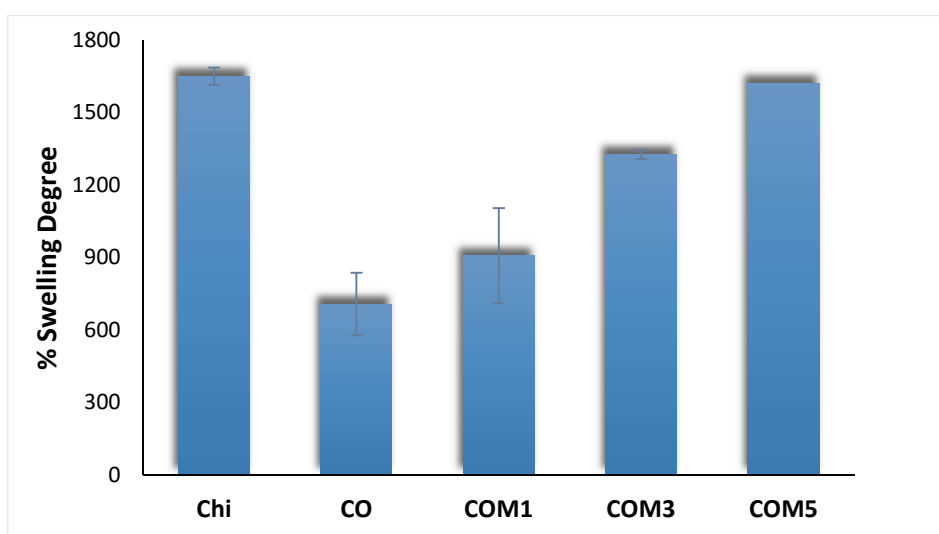


Figure 5. 27. Swelling degree of microspheres in pH 4.5 (n=3)

### 5.3.8. Biodegradation Study

“Biodegradable” is used for materials, where degradation is mediated by a biological system. Stability of microspheres in gastric conditions is important for controlled release of bioactive agent in gastrointestinal system. Biodegradation also affects drug release mechanism in stomach. In this study, biodegradation of chitosan microspheres was investigated in SGF with pepsin at pH 1.2. All experiments were performed at physiological body temperature 37 °C. Figure 5.28 presents biodegradation of the prepared microspheres as a function time upto 7 days. At the end of 4 h incubation period, chitosan nanocomposite microspheres degraded in the range of 18.8-37% which is much slower compared to 62.4% for pure chitosan microspheres and reach equilibrium

during 24 h incubation. The highest clay loaded nanocomposite microspheres (COM5) had the slowest degradation percentage. This could be attributed to the water barrier effect due to the tortuosity caused by nanoclay addition. At the end of the 7 days, biodegradation% of chitosan microspheres (unloaded microspheres) increased sharply from 63 to 93. When oil was incorporated into microspheres, biodegradation % decreased at all incubation times. 45% of the original weight of oil loaded chitosan microspheres was remained after 7 days due to interaction between cinnamon bark oil and chitosan. However, control microspheres remained only 7% of the original weight. As in the case of 5 % clay addition (COM5), approximately 60% of the initial amount remained after the incubation period. Biodegradation results showed control chitosan had faster degradation rate than the chitosan nanocomposite microspheres. In this study, incorporation of nanoclay acts as crosslinker and improves stability of the microspheres in SGF. Some researchers indicated that crosslinker (TPP) in chitosan matrix delays the degradation of cross-linked microspheres in SGF. In general, it was found that incorporation of montmorillonite into polymer matrix decreased percentage of biodegradation (Zhuang et al., 2007). The decrease in biodegradation is attributed to the slower diffusion and permeabilities of solvent molecules in chitosan/nanoclay nanocomposites that could be explained by the good dispersion of clay platelet with large aspect ratios in the polymer matrix. This forces solvent molecules to follow a tortuous path through the polymer matrix surrounding the clay particles by increasing the effective path length for diffusion (Oguzlu and Tihminlioglu, 2010), and therefore MMT incorporated chitosan microspheres were more resistant to degradation.

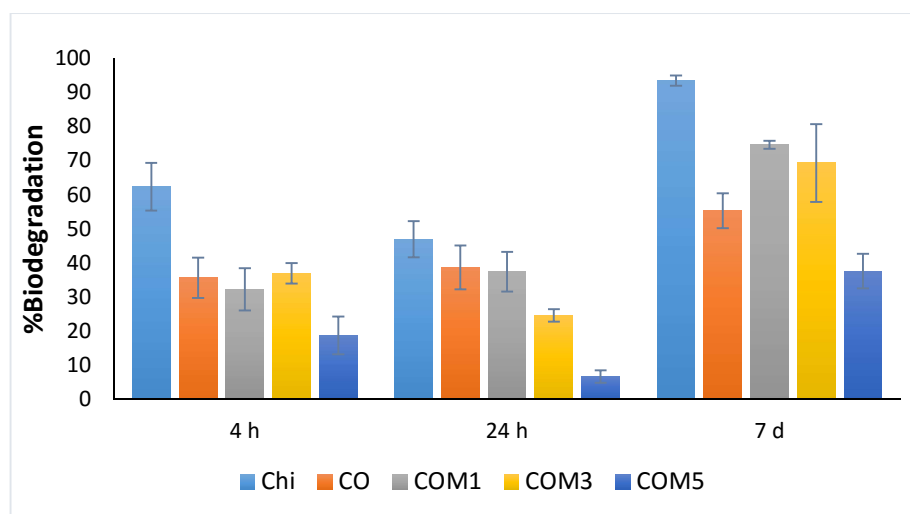


Figure 5. 28. Biodegradation results of oil loaded and unloaded chitosan microspheres in SGF at 37 °C(n=3)

## 5.4. *In Vitro* Release Study

*In vitro* release study was carried out in SGF and phosphate buffer medium pH 4.5 at 37°C, 75 rpm. The amount of cinnamon bark oil release into release medium was determined by UV-Vis spectrophotometer as explained in experimental section. The concentration of released drug was calculated based on calibration curve for cinnamon bark oil at 288 nm (Figure 5.5). Cumulative percentage of released cinnamon bark oil was obtained by dividing the cumulative amount of oil released at each sampling time point ( $M_t$ ) to the initial weight of the oil-loaded in the sample ( $M_0$ ).

Cumulative release % of cinnamon bark oil from both chitosan and chitosan nanocomposite microspheres was determined in SGF and pH4.5 and represented in Figures 5.29 & 5.30. To obtain controlled release profile, nanoclay was introduced into formulation in different concentrations. During the experiments, it was observed that the prepared microspheres swelled quickly and dissolved in release medium. As seen from the figures, the two step process was determined as initial burst release and slower release reaching plateau in both SGF and buffer (pH 4.5). Initial burst release was observed and approximately 60% of cinnamon bark oil released in SGF from control chitosan microspheres (CO) in 2 hours whereas it was retarded up to 34% in chitosan nanocomposite microspheres. Initial burst release of drugs from microparticles is generally explained in two ways. First, burst release occurs mainly due to dissolution and diffusion of oil located close to and/or at the surface of microspheres. Second, morphology of the microparticles causes initial burst. The drugs release from the polymeric matrices through the pores and cracks that form during the microparticle production process (Yeo and Park, 2004). During the release process, 85% of cinnamon oil was released and reached maximum value in 5 hours from neat chitosan microspheres without MMT. In contrast, cumulative release of cinnamon bark oil was about in the range of 43-55% in 7 hours with a controlled manner from chitosan nanocomposite microspheres in SGF medium (Figure 5.29). Based on these results, nanoclay addition not only improved EE of oil, but also brought about a marked reduction in drug release and provided a controlled release.

Drug release profiles of chitosan microspheres in pH 4.5 release medium were represented in Figures 5.29. In comparison, in pH 4.5 total amount of cinnamon bark oil completely was released from control microspheres in 3 hours while approximately 50%

of oil released from chitosan nanocomposite microspheres in 6 hours as seen in Figure 5.30. The percent of drug released in SGF was found to be slightly slower compared to that of at pH 4.5. This result could be explained by the pH sensitivity of the chitosan and chitosan nanocomposites microspheres. Cinnamon bark oil released from chitosan nanocomposite microspheres in a more controlled manner than chitosan microspheres. The release profile was improved with incorporation of nanoclay, as expected. Nanoclay acts as crosslinker and release of cinnamon bark oil was retarded due to the electrostatic interactions of between the positively charged  $\text{NH}_3$  groups of chitosan and anionic groups of nanoclay (MMT). Because of their organized structure of MMT, they can accommodate the various substances in gallery space to form nanohybrids. The interaction between silicate layers and bioactive molecules can be Coulombic interactions, Vander Waals force, and H-bonding. The presence of MMT resulted in less swelling ability as found in section 5.3.7 and acted as physical crosslinking points that were similar mechanism to the crosslinking agent, therefore the release of drug decreases. The electrostatic interaction with delaminated (exfoliated) montmorillonite (MMT) positively charged  $-\text{NH}_3^+$  group of chitosan which leads to a strong crosslinking structure in the nanocomposite. This situation strongly effects the macroscopic property of the nanocomposite and the drug diffusion through the bulk entity (Liu, Liu, Chen, and Liu, 2008). Additionally, MMT could provide a tortuous pathway to diffuse molecules out and release of bioactive agent with the help of exfoliated structure. Silicate layered nanoclay particles result in reduction of solute diffusivity by increasing the distance of diffusion path and reducing cross-area (Cerisuelo et al., 2015). Nanoclay platelets well dispersed with large aspect ratios in chitosan matrix and showed exfoliation which confirmed by XRD and TEM results. Tortuosity increases in the path length of diffusion in comparison to the shortest “straight-through” pathway. Tortuosity tends to reduce the amount of drug release in a given interval of time (Singhvi and Singh, 2011).

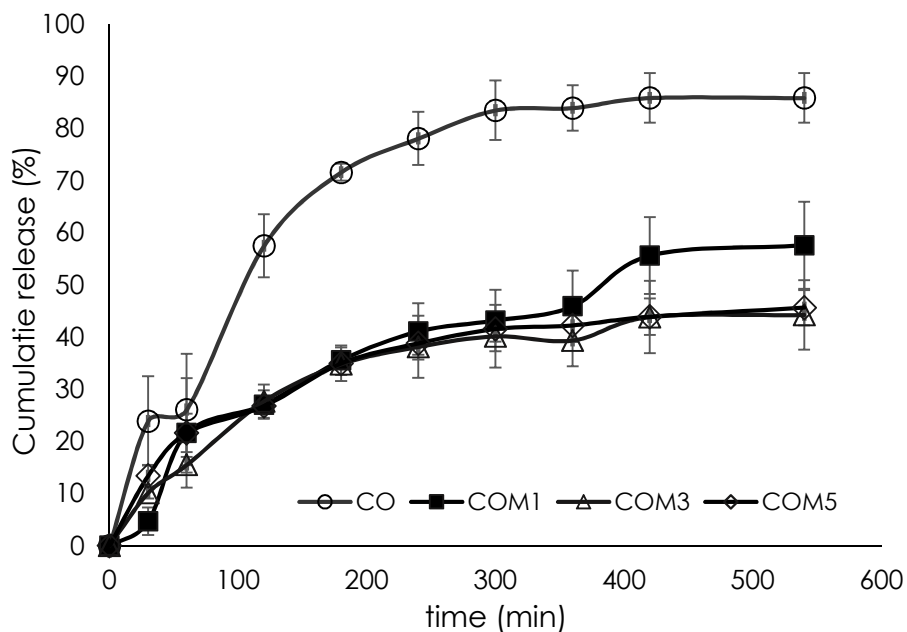


Figure 5. 29. *In vitro* release profile of cinnamon bark oil loaded chitosan microspheres in SGF

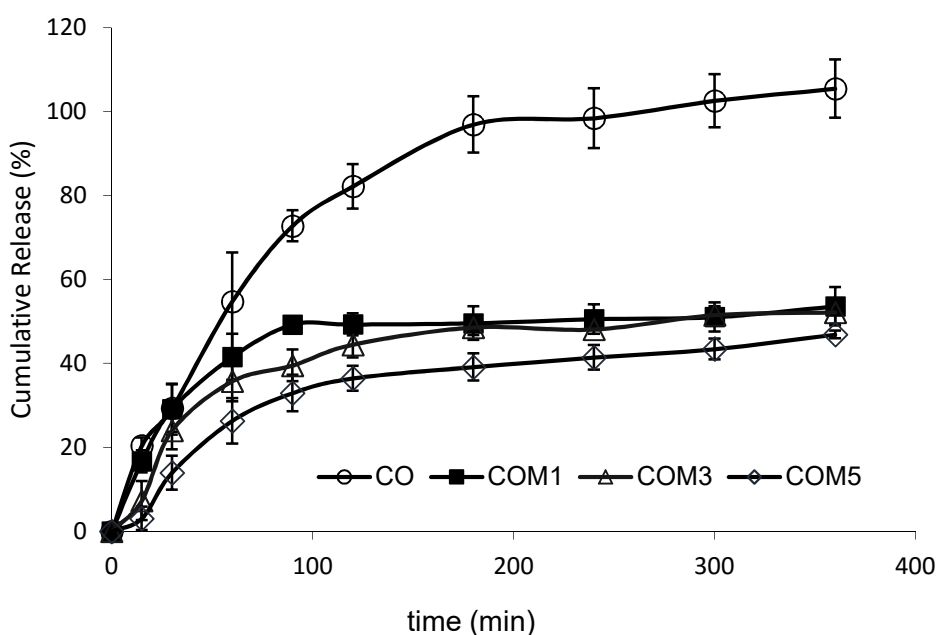


Figure 5. 30. *In vitro* release profile of cinnamon bark oil loaded chitosan microspheres in pH 4.5

Generally, drug release from microspheres occurs by several mechanisms including bioerosion, disintegration, diffusion and swelling. Due to hydrophobic nature of cinnamon bark oil, the drug release could be associated with swelling and/or matrix erosion from chitosan microspheres. In order to investigate the release kinetics and



mechanism of drug release from the spray dried chitosan microspheres, several following models were applied to experimental drug release data: Zero order, First order, Higuchi, Koersmeyer-Peppas and Hixson-Crowell kinetic models (Equations 2.6, 2.8, 2.9, 2.10 and 2.11). In all equations,  $k$  is the release coefficient whereas in Koersmeyer-Peppas model,  $k$  is a constant related to structural and geometric characteristics of the device and  $n$  is the diffusion or release exponent, which can indicate drug release mechanism. The mathematical release kinetics of the chitosan microspheres were demonstrated in Figures 5.31-5.33 and kinetic coefficients with the correlation coefficients  $R^2$  were tabulated in Table 5.6. The  $R^2$  value was used to determine the best model fitted the release, and  $n$  gave insights into release mechanism. The results of kinetic data showed that both Higuchi and Peppas models were found to be best fitted in all dissolution profiles having a higher correlation coefficients with the range of  $R^2$  0.92-0.97.

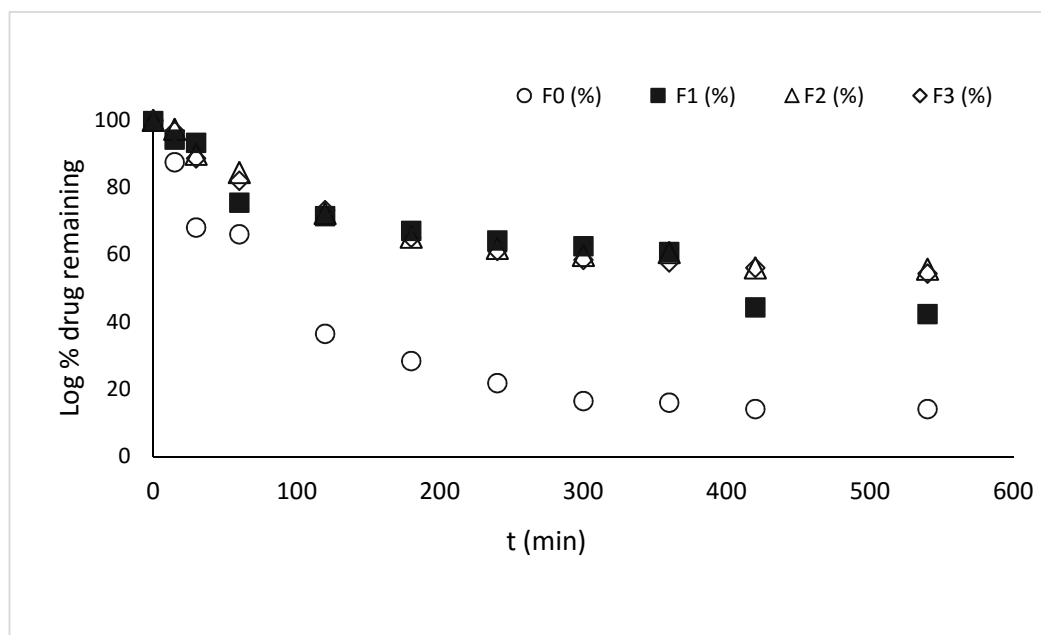


Figure 5. 31. First-order release kinetic model of cinnamon bark oil loaded chitosan microspheres

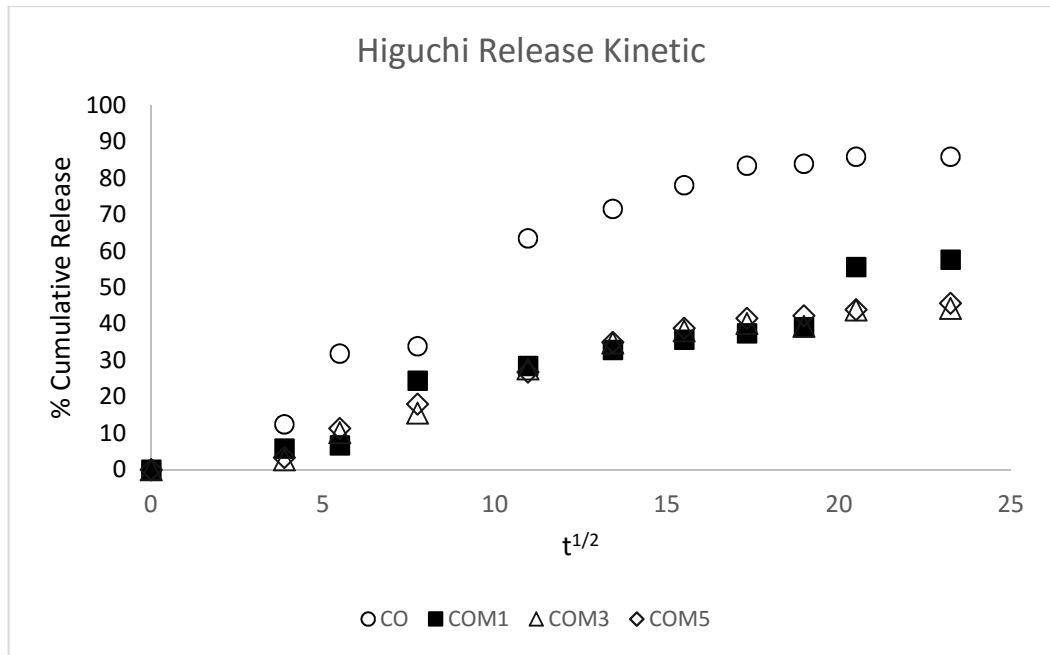


Figure 5. 32. Higuchi release kinetic model for chitosan microspheres

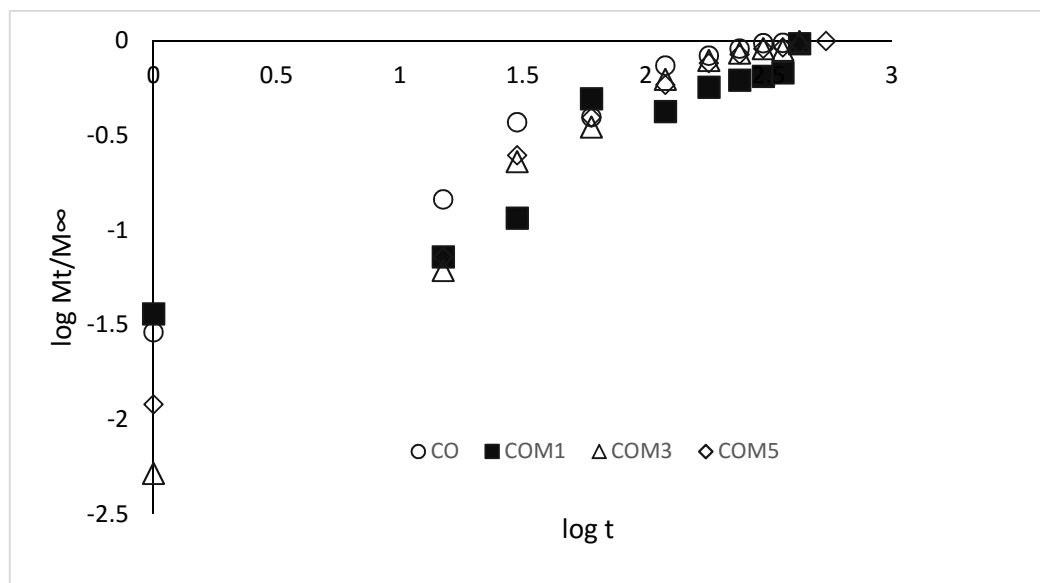


Figure 5. 33. Korsmeyer-Peppas release kinetic model for chitosan microspheres

The exponent  $n$ , in Kosmeyer- Peppas shows the mechanism of release.  $n$  values were found between 0.57 and 0.85 which refers drug release was governed by anomalous diffusion or non-Fickian diffusion. However, best fit results of Higushi model suggests that drug release was predominant by diffusion mechanism. The constant  $k$ , in this model decreased approximately 50% with nanoclay addition. The nanoclay addition improved drug release behaviour.

The release mechanism in anomalous case could be considered as a combination of Case-I & Case-II transport (Yilmaz et al. 1984). This means that cinnamon bark oil release from the prepared microspheres in this study was probably governed by a combination of both diffusion and relaxation controlled rate release (Table 5.6). In this case, the diffusion and relaxation rates are comparable ( $R_{\text{diffusion}} \approx R_{\text{relaxation}}$ ). As Peppas (1995) reported before, the swelling behaviour of swellable polymer is dependent on the contribution of diffusion and polymer relaxation (Magdalena, 2012). Relaxation behaviour of chitosan is influenced by the ionization of functional group depending on pH. Therefore, swelling mechanism could be more relaxation controlled due to protonation of chitosan amine groups in the gastric environment. Permeability is a function of diffusivity and solubility. In filled polymers, permeability is generally expressed as a function of tortuosity and volume fraction of clay (Nielsen, 1967; Waché et al., 2015). Since diffusion of encapsulated molecules from polymeric matrix includes jumps between cavities in the free volume of polymer, in layered silicate nanocomposites, the volume occupied by nanoclay galleries and thus free volume decreases. As a result of this situation, in many layered silicate incorporated polymer drug carrier systems, the drug is released in controlled manner and release is delayed.

Table 5. 6. Release kinetic coefficients for chitosan microspheres

Sample Code	First-order		Korsmeyer-Peppas		Higuchi		Hixson-Crowell	
	k	R <sup>2</sup>	n	R <sup>2</sup>	k	R <sup>2</sup>	k	R <sup>2</sup>
CO (Chitosan/oil)	0.35	0.75	0.58	0.94	4.101	0.92	0.01	0.91
COM1 (Chitosan/oil/1M MT)	0.23	0.88	0.57	0.97	2.490	0.95	0.01	0.72
COM3 (Chitosan/oil/3M MT)	0.19	0.80	0.73	0.95	2.222	0.95	0.01	0.85
COM5 (Chitosan/oil/5M MT)	0.2	0.81	0.85	0.96	2.187	0.96	0.01	0.84

In the study of Hua et al. (2010), the addition of MMT provided slower and continuous release as well as enhancement of encapsulation efficiency of ofloxacin drug at pH 1.2 and pH 7.4.

In another study of Datta (2013) , it was also found that nanoclay incorporation improved release profile of propranolol hydrochloride in both pH 7.4 and pH 1.2. However, released drug at pH 7.4 was found to be higher than pH 1.2 over the period of 8 h due to the stability of nanoclay in acidic media. Thus nanoclay could prevent drug release in SGF. These results demonstrated that our data were found to be consistent with the literature studies.

Furthermore, the release data was analyzed by using the Kopcha's empirical equation (Eq. 2.12) in order to quantify the diffusion (A) and erosion (B) contributions. The values of diffusion and erosion terms; A, B and the ratio of A/B, obtained using Eq. 2.12 were represented in Table 5.7. According to the results, in all formulations diffusion coefficient, A was greater than erosion coefficient, B ( $A/B > 1$ ) so release mechanism of the microspheres prepared in this study was dominantly controlled by diffusion.

Table 5. 7. Diffusion and erosion coefficient values of chitosan microspheres using Kopcha equation

Sample code	Kopcha Parameters		
	A	B	A/B
CO	4	0.033	121
COM1	2.9	0.025	116
COM3	1.5	0.07	21.6
COM5	1.98	0.044	45

Since the release mechanism is mainly contributed by diffusion mechanism, the diffusion coefficient of cinnamon oil was ( $D$ ) also calculated by fitting the theoretical data to experimental data using short term solution of Crank equation (Eq. 2.3 and Eq. 2.4) and results were tabulated in Table 5.8. Additionally, fitted data was represented in the Figures (5.34-5.37). It can be seen that good agreement was obtained between theoretical and experimental data. Diffusion coefficient of cinnamon oil from chitosan nanocomposites decreased one order of magnitude compared to neat chitosan microspheres.

Table 5. 8. Diffusion coefficients by using Crank equation

Sample code	D (m <sup>2</sup> /s)
CO	2.3E-18
COM1	9.0E-19
COM3	4.4E-19
COM5	9.5E-19

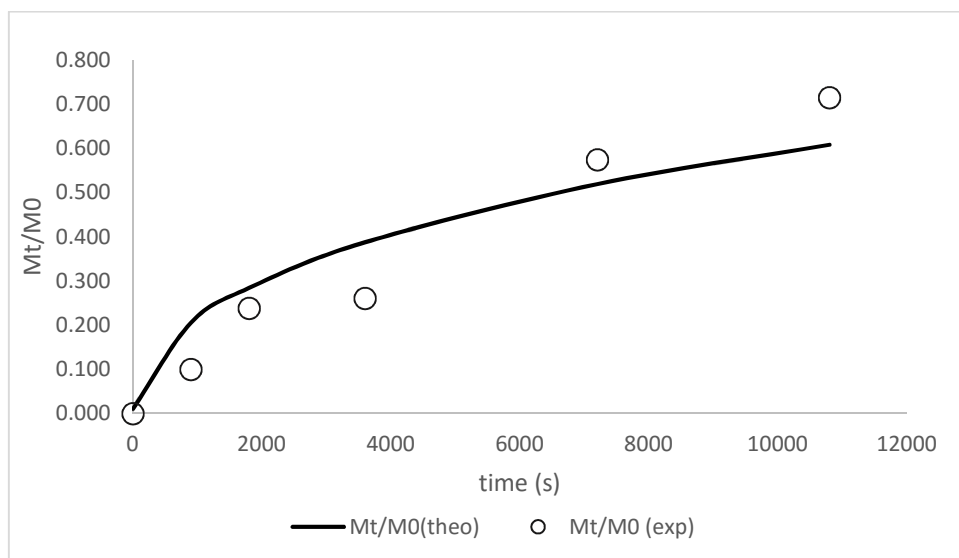


Figure 5. 34. Fit of model to experimental data, cinnamon bark oil release from CO microspheres

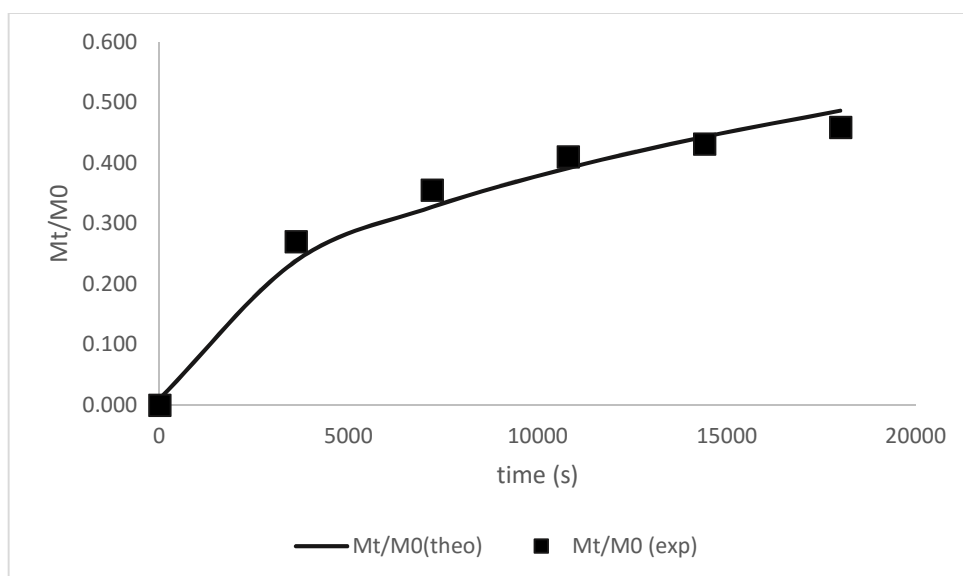


Figure 5. 35. Fit of model to experimental data, cinnamon bark oil release from COM1 microspheres

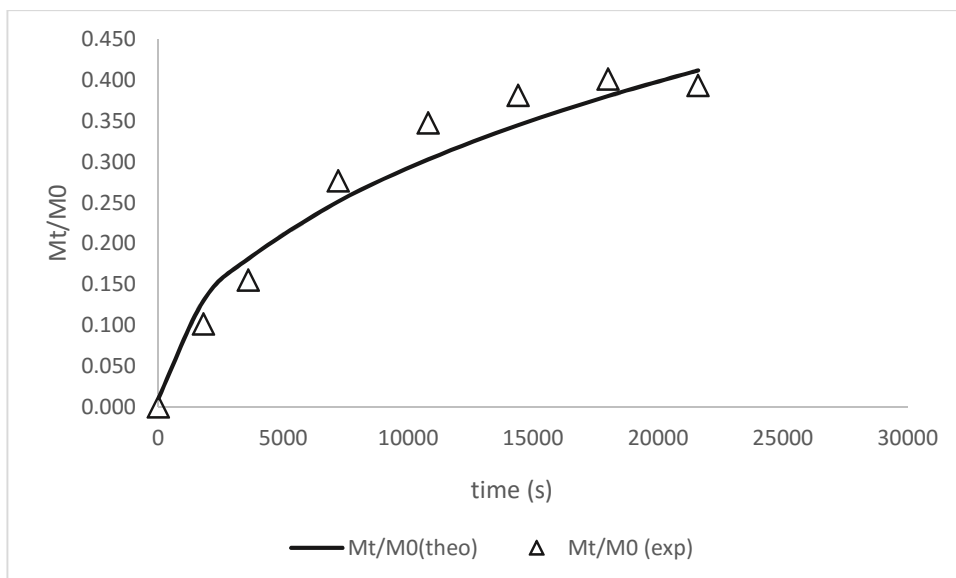


Figure 5. 36. Fit of model to experimental data, cinnamon bark oil release from COM3 microspheres

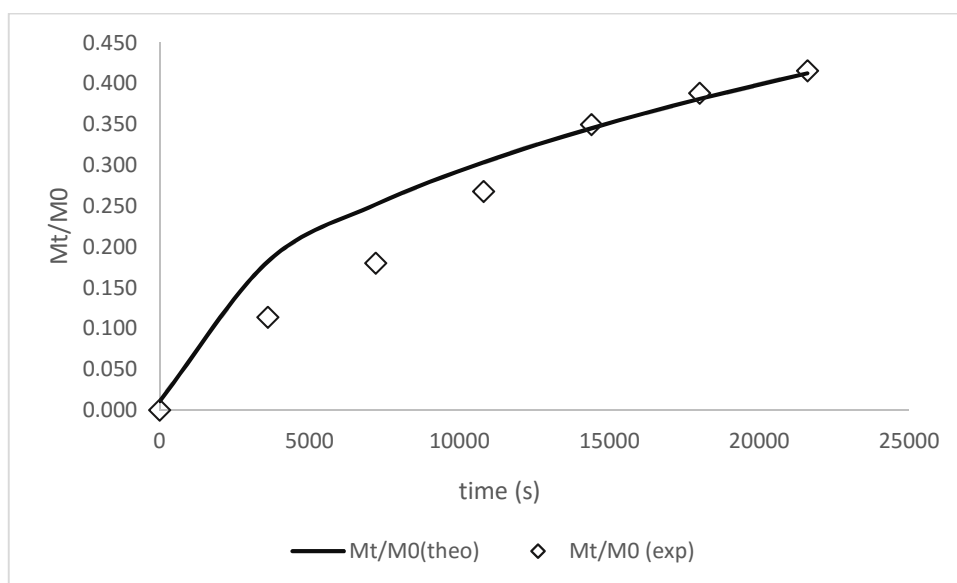


Figure 5. 37. Fit of model to experimental data, cinnamon bark oil release from COM5 microspheres

### 5.5. The Effects of Released Cinnamon Bark oil on *H.pylori*

The antimicrobial effect of released cinnamon bark oil from chitosan microspheres was assessed by *in vitro* *H. pylori* culture using surface spread plate method. Nanoclay was used in chitosan microsphere formulations (COM1-COM3-COM5) to

provide controlled release of cinnamon bark oil. Therefore *H. pylori* was incubated with cinnamon bark oil loaded chitosan nanocomposites containing various amount of nanoclay (MMT) in order to investigate the effect of released oil from microspheres on *H. pylori* growth. Samples taken at 0 h, 8 h, 24 h of incubation period were spread onto Columbia Blood agar supplemented with 7% horse blood and *H. pylori* Selective Supplement (DENT) and incubated in anaerobic jar (Oxoid) containing GasPak Campy Container System (Becton Dickinson and Company) at 37°C in a microaerophilic environment for 72 hours. The effects of cinnamon bark oil which was released from chitosan microspheres were assessed by viable colony counts in antimicrobial activity test (Table 5.9). Before the inhibition tests, it was proved that *H. pylori* can grow in liquid growth medium (Brucella Broth supplemented with 5% FBS) for 72 hours.

Table 5.9 shows that the prepared chitosan microspheres could contact with *H. pylori*, thus releasing cinnamon bark oil from microspheres to inhibit the *H. pylori* growth. *In vitro* released results showed that maximum amount of cinnamon bark oil released from microspheres at the end of the 8 h and there was not any growth in the 8 h and 24 h samples taken from the cinnamon bark oil loaded microspheres suspended growth medium. The results showed that cinnamon bark oil released from the all microsphere formulations inhibited the growth of *H. pylori*. Therefore, it was concluded that cinnamon bark oil loaded into chitosan microspheres had bioactivity against *H. pylori*.

Although antimicrobial effect of montmorillonite nanoclay against certain microorganisms have been reported before (Maryan et al., 2013; Negi et al., 2011; Yushan et al., 2009), we only examine the antimicrobial effect of final product of nanocomposite microsphere formulations against *H. pylori*. It was reported that montmorillonite is more effective against Gram-negative strains than Gram-positive (Negi et al., 2011).



Table 5. 9. Viable colony counts of *H.pylori* (CFU) treated with different cinnamon bark oil chitosan microspheres and chitosan nanocomposite microspheres

Formulation	Colony forming unit, CFU x10 <sup>9</sup>		
	t=0 h	t=8 h	t=24 h
CO (Chitosan/oil)	10	0	0
COM1 (Chitosan/oil/1MMT)	230	0	0
COM3 (Chitosan/oil/3MMT)	250	0	0
COM5 (Chitosan/oil/5MMT)	200	0	0

### 5.6. *In vitro* Cytotoxicity and Biocompatibility of Chitosan Microspheres and Cinnamon bark oil

Biocompatibility is a critical issue for decision the right biomaterials that are used in drug delivery, tissue engineering and biomedical applications. Although chitosan is known as biocompatible, antiinflammatory and approved as GRAS, it is required to evaluate the potential toxicity of the oil loaded chitosan and chitosan nanocomposite microspheres prepared in this study. For this reason, *in vitro* cytotoxicity and cytocompatibility of chitosan nanocomposite microspheres on NIH3T3 fibroblast cell line were investigated. NIH3T3 fibroblast cell line was used as a model cell line as recommended in ISO 10993 standard. The cytotoxic activity was measured by using MTT assay following indirect cytotoxicity ISO standard (10993-5) at 24, 48 and 72 hour time points. Cell viability of each formulation after 24 h, 48 h and 72 h of incubation period was given in Figure 5.38 and it was observed that chitosan microspheres showed proliferation effect on fibroblast cells. However, oil loaded chitosan microspheres at 1 mg/mL concentration showed cytotoxic effect around LD50. The reason could be due to the burst release of cinnamon bark oil from chitosan microspheres and could cause cell death. However, neat chitosan and oil loaded chitosan nanocomposite microspheres did not significantly reduce cell viability compared with oil loaded chitosan microspheres, indicating good cytocompatibility properties for these materials. Unloaded chitosan nanocomposite microspheres (CM1-CM3-CM5) showed 70-92% cell viability at the end of 24 h and 48 h time point. These formulations decreased percentage of cell viability at

the end of 72 hours incubation period. Since all tested formulations showed high cell viability greater than 70%, this result suggests that the prepared microspheres exhibited no cytotoxic effect on fibroblast cells.

The results states that the cell proliferation is not affected by the incorporation of nanoclay into chitosan. This may be due to the enhanced interactions between nanoclay and growing cells on the biopolymer matrix. According to Lavie et al., MMT (nanoclay) may develop London–van der Waals forces and hydrogen bonding with cells. As a result, oil loaded chitosan nanocomposite microspheres were proved to be biocompatible.

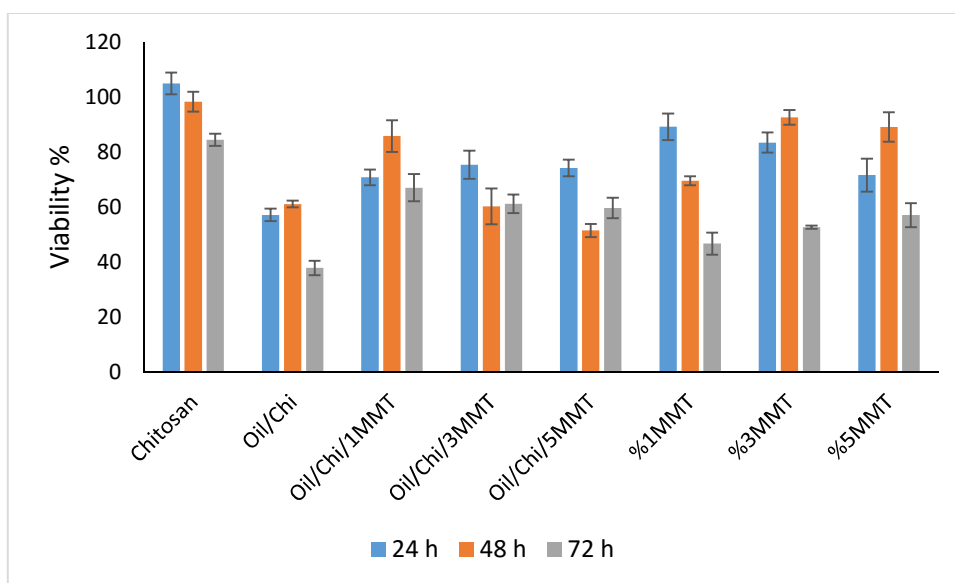


Figure 5. 38. *In vitro* cytotoxicity of chitosan microspheres on NIH3T3 cell line

Cell viability and cytotoxic effect of cinnamon bark oil on NIH3T3 cell line were also evaluated by MTT assay. *In vitro* cytotoxic activity was measured at 24, 48 and 72 hour time points. NIH3T3 fibroblast cells were treated with essential oil at different concentration range between 2 to 250  $\mu\text{g}/\text{mL}$ . Cinnamon bark oil concentrations were selected in accordance to MIC determination study against *H. pylori*. It was resulted that cinnamon bark oil significantly reduced cell viability of 3T3 cells in a dose-dependent manner starting 2 to 250  $\mu\text{g}/\text{mL}$  and cinnamon bark oil showed cytotoxic activity on NIH3T3 cell lines over 31  $\mu\text{g}/\text{mL}$  dose. Above this concentration, the cytotoxic effect of cinnamon bark oil was quite strong and therefore 31  $\mu\text{g}/\text{mL}$  of concentration could be defined as IC<sub>50</sub> value. The results showed that cinnamon bark oil has proliferative effect on NIH3T3 fibroblast cells up to 31  $\mu\text{g}/\text{mL}$  (Figure 5.39). This finding is valuable for safe use of chitosan microsphere in eradication therapy. MIC value against *H. pylori* was

found as 8  $\mu\text{g/ml}$ . Above 31  $\mu\text{g/mL}$ , cinnamon bark oil becomes toxic on NIH3T3 fibroblast cells. Direct contact of essential oil cause cell death. Essential oils are responsible for depolarization of the mitochondrial membranes by decreasing the membrane potential, affect ionic  $\text{Ca}^{++}$  cycling and other ionic channels. These along with reduction in the pH gradient and also affects the proton pump and the ATP pool. In addition, it was shown that essential oils increase the membrane fluidity, this results in leakage of ions, (calcium ions) proteins, thereby leading to cell death by apoptosis and necrosis (Bakkali et al., 2008). Based on our findings, it is concluded that the cinnamon bark oil can be used as a potential biotherapeutic agent in controlled release systems for *H. pylori* eradication therapy.

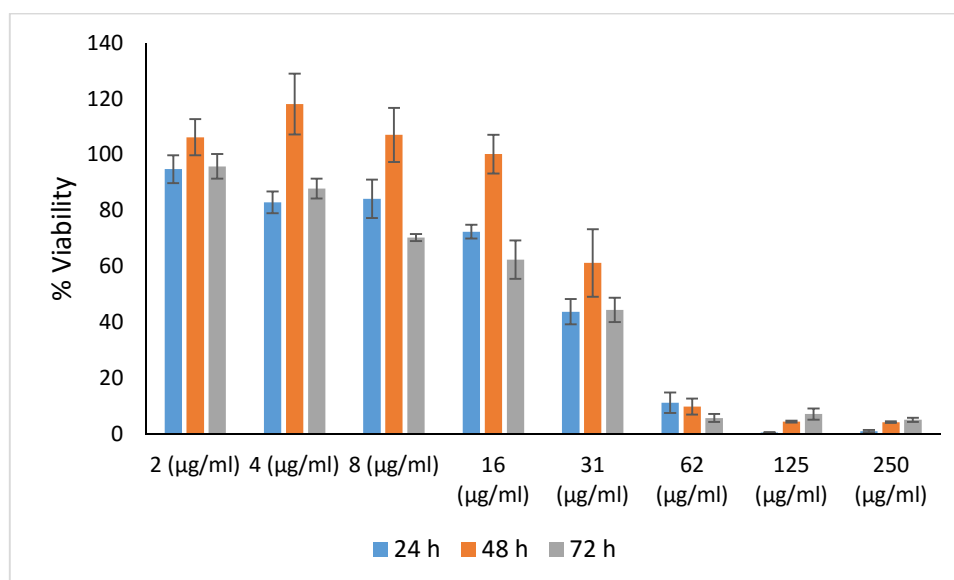


Figure 5. 39. *In vitro* cytotoxicity of cinnamon bark oil on NIH3T3 cell line

### 5.7. *In vitro* Cell Viability and Interaction of MKN45 Cells with Chitosan Microspheres and Cinnamon bark oil

*In vitro* cell viability and proliferation studies of oil loaded and unloaded chitosan microspheres were also evaluated by WST-1 assay using MKN45 cell line (poorly differentiated gastric carcinoma). Figure 5.40 shows *in vitro* cell viability performed by in direct cytotoxicity assay adopting ISO 10993-5 standart. MKN45 cell line was selected as model cell line in order to evaluate the biocompatibility of microspheres in gastrointestinal system. Results showed that chitosan microspheres have no cytotoxic

effects on MKN45 cells. However only 5% nanoclay incorporated microsphere demonstrated cell viability lower than 80% and reduced to 57% cell viability after 72 hours treatment. As a result, cinnamon bark oil loaded and unloaded chitosan microspheres were found as biocompatible for gastrointestinal (GI) system and a good candidate for gastroretentive drug carrier.

To investigate the effects of microspheres on MKN45 cell line, cells were treated with microspheres directly. 1 mg/mL of microspheres were added into growth medium and cells were treated for 24, 48 and 72 hours. At the end of the incubation period, cell viability and proliferation was evaluated by WST-1 cell proliferation assay and investigate the effect on gastric cells. The results were depicted in Figure 5.41. Microspheres did not show any cytotoxic effects when interacted with MKN45 cells.

Neat chitosan and oil loaded (CO) chitosan microspheres showed proliferative effect on MKN45 gastric epithelial cells. Nanoclay incorporation into chitosan matrix did not cause any significant effect on cell viability. Although the cell viability profiles of chitosan microspheres were comparable to each other (Figure 5.41), the 80% cell viability was obtained in all formulations. However, cell viability reduced from 130% to 81% after 24 h treatment with increased nanoclay concentration when cells were treated with oil loaded chitosan nanocomposite microspheres. Cytotoxic effect could be controlled by prolonged release of essential oil, particle size and surface charge of the wall material. Positive surface charge of chitosan nanocomposites leads to interact with epithelial cells. Lemieux et al. 2015 found a similar results with carboxymethyl starch (CMS) microspheres on human gastric NCI-N87 (CRL-5822). The cellular viability of NCI-N87 and Caco-2 cells were exposed to CMS microspheres at 10 mg/mL concentration and they found that the microspheres did not induce any cell mortality. AGS cell line is one of the human gastric carcinoma cell line. Chang et al. (2011) developed berberin loaded chitosan/heparin nanoparticles. They investigated antimicrobial activity against *H. pylori* and cell viability of AGS cells treated with berberine and nanoparticles. Cell viability reduced when cells were treated with nanoparticles higher than 12 mg/L berberine concentration. Cell viability was not affected by treatment of berberine at lower concentrations which have antimicrobial activity against *H. pylori*. Berberine loaded nanoparticles reduced the cytotoxic effects of *H. pylori* infection to the cells.

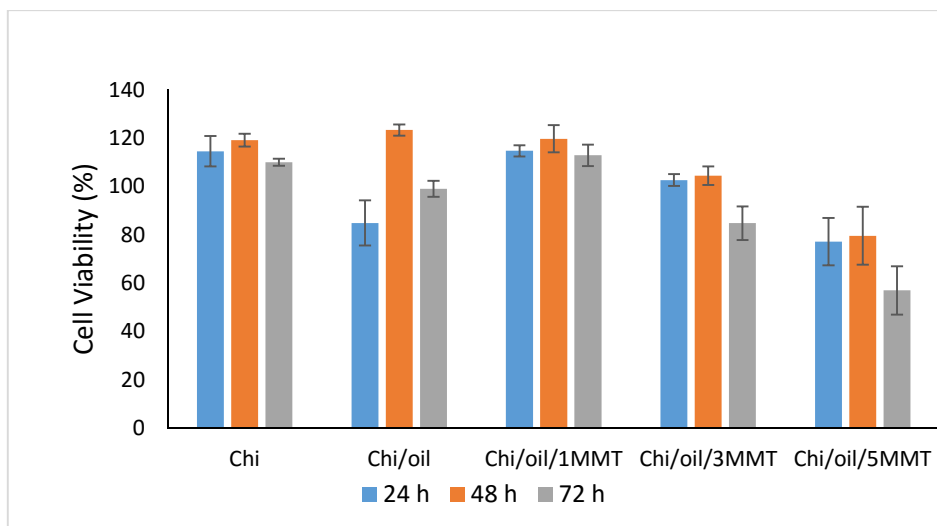


Figure 5. 40. *In vitro* in direct cytotoxicity of chitosan microspheres on MKN45 cell line

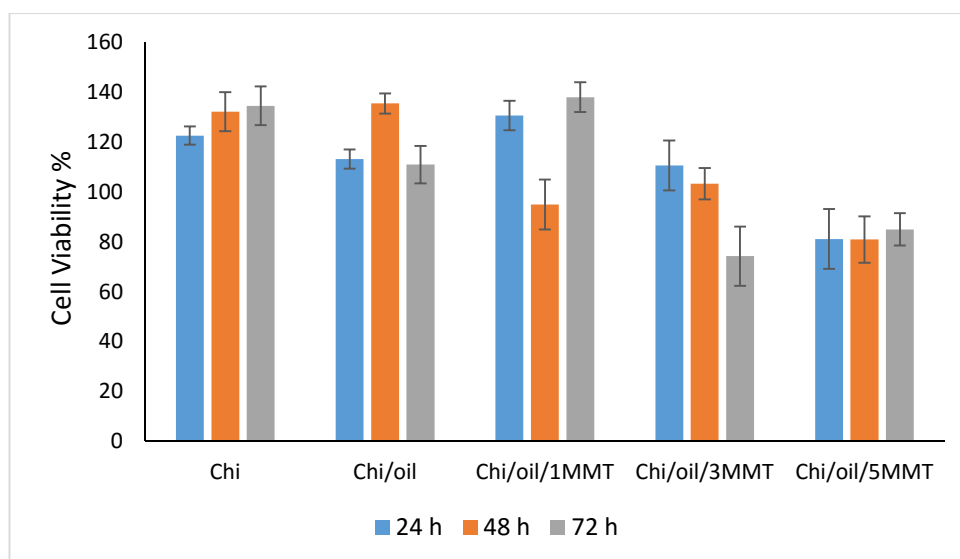


Figure 5. 41. *In vitro* cell viability of chitosan microspheres treated MKN45 cells

In addition, cell viability of MKN45 cells treated with different concentrations of cinnamon bark oil was also evaluated. As depicted in Figure 5.342, at concentrations higher than 31  $\mu\text{g/mL}$ , cinnamon bark oil exhibited cytotoxic activity on gastric epithelial cells. The same threshold value was already obtained for NIH3T3 fibroblast cell line by Muhammad et al. (2015). Antiinflammatory and anti-cytotoxic activity of *Cinnamomum cassia* on *H. pylori* infected gastric epithelial cells were evaluated (Muhammad et al., 2015). The effect of cinnamaldehyde on AGS and MKN cells (gastric carcinoma cell lines) was determined by DNA fragmentation assay up to 500  $\mu\text{M}$  concentration. They found that *C. cassia* at  $\leq 125$   $\mu\text{M}$  concentration was non-toxic for AGS and MKN cells

and suppressed the inflammation by down regulation of *H. pylori*-induced IL-8 expressions by inhibiting NF- $\kappa$ B activation in AGS cells.

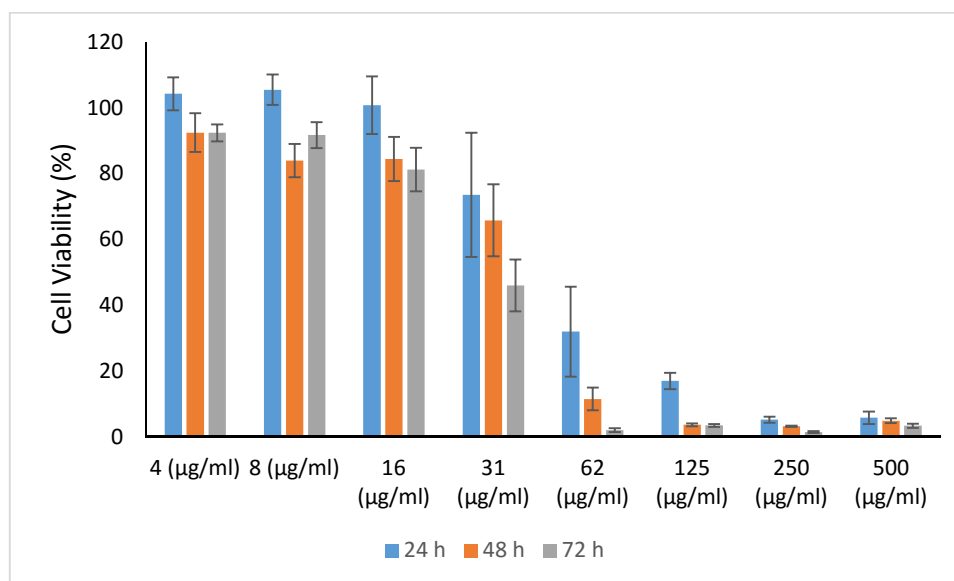


Figure 5. 42. *In vitro* cell viability of MKN45 cells treated with cinnamon bark oil

## 5.8. *In Vitro* Cellular Uptake

To investigate cellular uptake of chitosan microspheres, MKN45 cells were treated with 1mg/mL rhodamine fluorescent microspheres for 5 and 24 hours. After incubation period, the cells were fixed with 3.7% paraformaldehyde solution and washed with PBS. Fixed cells were stained with DAPI which binds specifically to nucleus at 5 h and 24 h treatment. The stained cells were examined and visualized by fluorescent microscopy.

In the experiment, neat chitosan and oil loaded chitosan nanocomposite microspheres were incubated with MKN45 cells for 2 h and 4 h. To track the internalization and examine the allocation of microspheres and oil in MKN45 cells, nucleus was stained with DAPI after treatment and the distribution of microspheres (red) and nucleus (DAPI) was determined by fluorescence microscopy. The fluorescent images of internalized fluorescent microspheres and cinnamon oil were presented in Figure 5.43. Cellular uptake resulted in strong fluorescence in the cell and fluorescence microscopy results showed that both oil loaded and unloaded chitosan microspheres were able to get internalized into the cells with reasonable amounts.

It has been reported that internalization was promoted by the electrostatic interaction between positively charged particle surface and negatively charged cell membrane. Main factors that influence cellular uptake are size, shape, material, surface charge, and surface hydrophobicity as well as cell type. Several studies related with effect of surface charge on cellular uptake have been conducted. Generally, cells are able to take up positively charged particles such as lipid particles, poly(lactic acid), chitosan, polymeric particles in comparison to negatively charged particles (Fröhlich, 2012). For example, PLGA particles coated with chitosan and coating process resulted in higher cellular uptake efficiency. This result could be attributed to surface modification of PLGA because its negative surface charge changed into positive with chitosan coating (Alqahtani et al., 2015; Chronopoulou et al., 2013). This result was also important for site-specific *H. pylori* infection treatment at stomach. Chang et al. (2010) prepared amoxicillin loaded chitosan nanoparticles and they showed cellular internalization of particles by AGS cells. This finding showed that amoxicillin could interact with intercellular spaces or cytoplasm as well as the site of *H. pylori* infection.

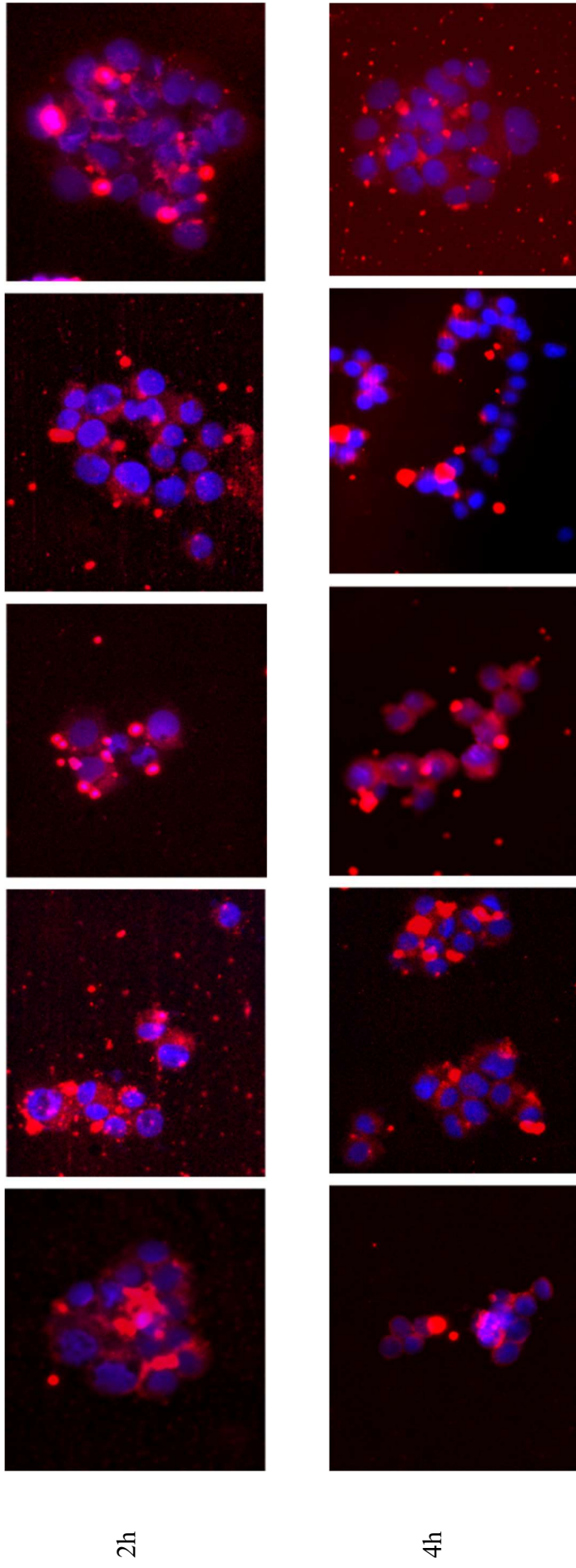


Figure 5. 43. Fluorescent images of MKN45 cells incubated with chitosan microspheres for 2 and 4 hours; Chi; CO; COM1; COM3; COM5 treated cells (red color shows internalized microspheres and blue color shows nucleus stained with DAPI) (Scale bar=10  $\mu\text{m}$ )



## 5.9. Radiolabeling and *In vitro* Cell Binding Study

### 5.9.1. Radiolabeling Studies

#### Labeling Efficiency (%)

Labeling efficiency of the  $^{99m}\text{Tc}$ -chitosan microspheres was evaluated by Dose calibrator. All tested microspheres exhibited more than 95% labelling efficiency when microspheres were labeled with  $^{99m}\text{Tc}$  (Table 5.11). Chitosan microspheres was labelled with  $^{99m}\text{Tc}$  with high labelling efficiency (Patil et al., 2010).

Table 5. 10. Percentage of radioactivity of microsphere formulations after labeling

Formulation	Labeling Efficiency (%)
<b>CO</b>	99.8
<b>COM1</b>	99.5
<b>COM3</b>	96.7
<b>COM5</b>	99.4

#### Radiochemical Purity (RP)

Radiochemical purity and stability of the product were evaluated successfully by TLC method. The results showed that oil loaded chitosan microspheres were radiolabeled by  $^{99m}\text{Tc}$  with high labeling efficiency (>90%) (Table 5.12).

Table 5. 11. Radiochemical purity of labeled microspheres

Formulation	RP (%)
<b>CO</b>	97,4
<b>COM1</b>	99,2
<b>COM3</b>	99,9
<b>COM5</b>	99,8

### 5.9.2. *In vitro* Cell Binding Study

*In vitro* binding of chitosan microspheres to MKN45 gastric cells was represented in Figure 5.44. The cell incorporation percentage after the application of radiolabeled with  $^{99m}\text{Tc}$ -chitosan microspheres was found to be between 93 % and 97 % for MKN45 cells during 2 hours exposure. All tested formulations showed significant high uptake (>90%). Although there was a slight decrease in oil loaded chitosan microsphere at the end of the 4 h incubation (from 93% to 86%), it was not observed any changes in COM5 formulation which contains 5% of nanoclay (w/w) (Table 5.12). This result demonstrated that chitosan/nanoclay formulations have greater stability and incorporation activity on gastric epithelial cells. Since nanoclay minerals have cation exchange and mucoadhesion property, chitosan/nanoclay formulations improved cellular binding and thus higher cell binding efficiency was observed. This significant results were also supported by *in vitro* mucoadhesion study with high mucoadhesion of microspheres. Bio/mucoadhesive systems bind to the gastric epithelial cell surface, or mucin, and increase the GRT by increasing the intimacy and duration of contact between the dosage form and the biological membrane.

Gundogdu et al. (2015) and Ekinici et al. (2015) performed cell binding of chitosan nanoparticles with different cell lines (H209, U2OS, MCF-7, HaCaT). They reported that  $^{99m}\text{Tc}$  labeled chitosan nanoparticles were incorporated into cells. Tested formulations showed slightly higher incorporation in cancer cell lines concluding  $^{99m}\text{Tc}$  labeled formulations could be a good candidate for both cancer diagnosis and treatment without harming normal cell.

Due to the increasing complications in the conventional eradication triple therapy, based on antibiotic drug, researchers are seeking to develop new non-antibiotic antibacterial agents against *H. pylori* infection that are safe, effective and have specific cellular targets. *In vitro* cell incorporation (binding) studies revealed that  $^{99m}\text{Tc}$ -chitosan microspheres have a great incorporation activity which is crucial for gastroretentive dosage formulations on MKN45 cells. This result was also confirmed by *in vitro* cellular uptake study which was evaluated by fluorescence micrographs.

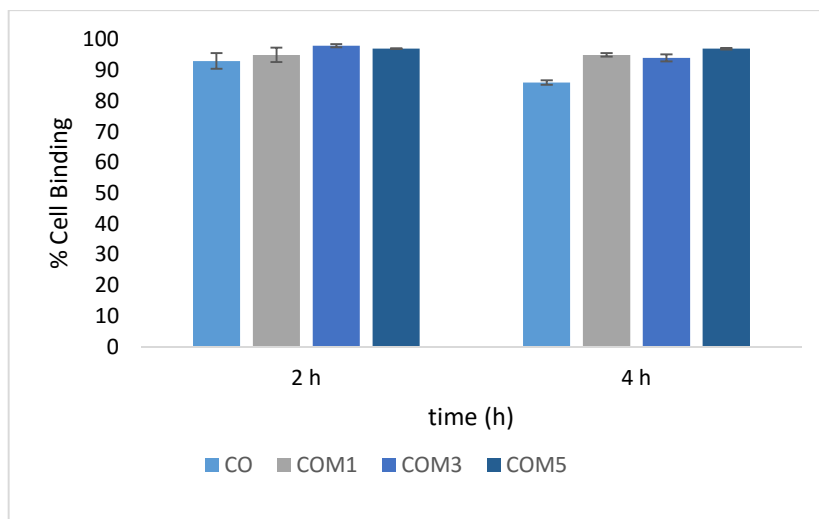


Figure 5. 44. *In vitro* cell binding of chitosan microspheres to MKN45 gastric cells (n=3)

Table 5. 12. Cell binding of chitosan microspheres during 2 h and 4 h exposure (n=3)

Formulation	2 h	4 h
	Cell Binding (%)	Cell Binding (%)
<b>CO</b>	93	86
<b>COM1</b>	95	95
<b>COM3</b>	98	94
<b>COM5</b>	97	97

## CHAPTER 6

### CONCLUSIONS

*Helicobacter pylori* (*H. pylori*) infection is one of the worldwide problem which induces chronic gastritis, peptic ulcer and risk factor in mucosal related lymphoid tissue lymphoma (MALT) and gastric cancer. Currently used treatment protocols in *H. pylori* eradication could not be achieved complete success because of poor permeability of antibiotic to mucus layer, poor stability of antibiotics in gastric conditions and antibiotic resistance. Therefore, studies on alternative drugs and therapeutic approaches with enhanced action and reduced side effects are being continued for better eradication of the organism. The use of essential oils in combination with antibiotics or as an alternative to antibiotics in *H. pylori* treatment is an innovative approach.

The main objective of this dissertation was to develop a novel drug delivery systems containing cinnamon bark oil as an active substance which release in a controlled manner and provide more efficient eradication therapy by prolonging the retention time and improving stability in stomach. Therefore, this dissertation comprises the encapsulation of cinnamon bark oil which is active against *H. pylori* and development a gastroretentive, controlled release composition that is retained in the stomach and releases the essential oil for an extended period of time for *H. pylori* eradication therapy as an alternative or complementary to conventional antibiotic treatment for patients having antibiotic allergy and resistance. For this purpose, cinnamon bark oil was encapsulated in chitosan nanocomposites. Nanoclay was introduced into chitosan matrix to improve stability, protect the bioactive substance and provide controlled release in stomach conditions.

Firstly, MIC value of cinnamon bark oil was determined against *H. pylori*. After determination MIC value, the microspheres containing cinnamon oil were prepared by spray drying. In order to determine the optimum process parameters for spray drying, different temperatures and pump rates were evaluated. The morphological and chemical characterization of the microspheres were investigated by scanning electron microscopy, FT-IR, Raman and NMR spectroscopies. Swelling property and biodegradation of prepared microspheres were examined in SGF and phosphate buffer solution at pH 4.5 at 37°C. *In vitro* drug release studies were carried in SGF and phosphate buffer solution at

pH 4.5 at 37°C to mimic the stomach conditions. *In vitro* mucoadhesion property and antimicrobial activity of the microspheres against *H. pylori* were investigated. *In vitro* cell viability and proliferation assays of cinnamon bark oil and chitosan nanocomposite microspheres on NIH3T3 and MKN45 cells were performed. *In vitro* cellular uptake studies and cellular binding capacity of prepared microspheres were investigated on MKN45 cell line.

The optimum conditions for production of cinnamon bark oil loaded microspheres by spray drying were determined as 190°C for inlet air temperature, 6 mL/min for pump rate taking into account particle size, humidity and process yield. Particle size of chitosan microspheres was found between 1-3 µm. Microspheres have wrinkled and spherical morphology. All formulations had positive zeta potential which causes electrostatic interaction between the negatively charged mucus. The excellent mucoadhesion properties of prepared microspheres between 55-70% were proved by their significant adsorption to the mucin solution mainly due to the electrostatic attraction between the positively charged amino groups of chitosan and the negatively charged mucin. Intercalation of nanoclay in chitosan matrix decreased percentage of biodegradation and enhance stability of microspheres in gastric conditions. Percentage of biodegradation of chitosan nanocomposite microspheres decreased up to 18.8% when compared neat chitosan. This result showed that nanoclay improved stability of microspheres in gastric conditions. Chemical characterization analysis indicated strong interaction between chitosan and cinnamon bark oil and imine bond formation between aldehyde group of cinnamon bark oil and amino group of chitosan. It was found that nanoclay incorporated microspheres decreased the drug release from 85 % to 43-40% in SGF in 6 h indicating improvement in drug release behaviour. Zero-order, First-order, Higuchi, Korsmeyer-Peppas and Hixson-Crowell kinetic models were applied to explain drug release mechanism and Kopcha equation was used to determine which mechanism was dominant. Higuchi and Korsmeyer-Peppas models fitted to our release data according to R<sup>2</sup> values. The release exponent, n, in Kosmeyer- Peppas well explained the release mechanism. Based on this model, drug release mechanism was found to be anomalous diffusion which means that release occurred from microspheres both diffusion and erosion controlled. However, when our experimental data were fitted to Kopcha equation, the results indicated the predominance of diffusion on controlled release.

MIC value of cinnamon bark oil was found as 8 µg/mL. MIC value gives information about the required essential oil amount to inhibit bacteria *in vivo* and aids to

measure the minimum amount which is required for patients. The chitosan nanocomposite microspheres developed in this work, exhibited excellent mucoadhesive property as well as controlled release profile for incorporated cinnamon bark oil by inhibiting the growth of *H. pylori*. *In vitro* cell viability results showed that cinnamon bark oil reduced cell viability of NIH3T3 cells in a dose-dependent manner starting 2 to 250 µg/mL and cinnamon bark oil showed cytotoxic activity on NIH3T3 cell lines over 31 µg/mL dose. Both chitosan and chitosan nanocomposites did not show any cytotoxic effects on both fibroblast and gastric epithelial cells. The prepared microspheres were able to get internalized into the cell. *In vitro* cell binding studies showed that chitosan nanocomposite formulations have greater incorporation activity on gastric epithelial cells. Since nanoclay minerals have cation exchange and mucoadhesion property, chitosan nanocomposite formulations improved cellular binding and thus higher cell binding efficiency was observed. As a result, chitosan microspheres were found as cytocompatible for safety use in gastrointestinal system. In the light of these findings, it can be proposed that cinnamon bark oil loaded chitosan nanocomposites developed in the thesis is useful for improving drug delivery and stability by prolonging residence time and mucoadhesion. Therefore, this carrier system could be used a promising biotherapeutic candidate as a safe and efficient carrier in treatment of *H. pylori* infection suggesting the potential of the released oil to act locally on *H. pylori* at a complete bactericidal clearance effect and the absorption enhancing action of the chitosan.

The advantages of the developed delivery system are not only eradication of *H.pylori* by controlled release but also prevention the adhesion/colonization of *H. pylori* to gastric mucosa. This system could also aid wound healing. However, further studies are needed for prove adhesion/colonization of *H. pylori* to gastric mucosa as proposed action. In addition to MIC, minimum bactericidal concentration (MBC) which is the lowest concentration of required essential oil to kill bacteria is recommended in this study. The MBC is complementary to the MIC. The MBC demonstrates the lowest level of essential oil that results in microbial death, whereas the MIC test determined as the lowest concentration of essential oil that inhibits growth. It is known that certain *H. pylori* strains can form biofilm. Due to the fact that bacterial biofilm formation is one of the important factors of eradication failure, anti-biofilm ability of cinnamon bark oil loaded chitosan nanocomposite microspheres for inhibiting the biofilm formation of *H. pylori* should be investigated. Also permeabilization study of gastric epithelial cells with oil loaded chitosan microspheres and interaction of *H. pylori* with this cell line is required for

cellular permeation enhancement property of chitosan. For this purpose, co-culture studies with *H. pylori* and gastric epithelial cells are needed. *In vivo* studies are recommended as further studies to determine the pharmacokinetic and pharmacodynamics behaviour. Moreover, *in vivo* product stability and tissue response and bioavailability should be evaluated.

## REFERENCES

- Abdollahi, M., Rezaei, M., Farzi, G. (2012). A novel active bionanocomposite film incorporating rosemary essential oil and nanoclay into chitosan. *Journal of Food Engineering*, 111(2), 343–350.
- Adebisi, A., Conway, B. R. (2011). Gastroretentive microparticles for drug delivery applications. *Journal of Microencapsulation*, 28(8), 689–708.
- Adebisi, A. O., Conway, B. R. (2014). Lectin-conjugated microspheres for eradication of *Helicobacter pylori* infection and interaction with mucus. *International Journal of Pharmaceutics*, 470(1-2), 28–40.
- Agnihotri, S. a., Mallikarjuna, N. N., Aminabhavi, T. M. (2004). Recent advances on chitosan-based micro- and nanoparticles in drug delivery. *Journal of Controlled Release*, 100(1), 5–28.
- Agudo, S., Pérez-Pérez, G., Alarcón, T., López-Brea, M. (2010). High prevalence of clarithromycin-resistant *Helicobacter pylori* strains and risk factors associated with resistance in Madrid, Spain. *Journal of Clinical Microbiology*, 48(10), 3703–3707.
- Aguzzi, C., Capra, P., Bonferoni, C., Cerezo, P., Salcedo, I., Sánchez, R., Caramella, C., Viseras, C. (2010). Chitosan-silicate biocomposites to be used in modified drug release of 5-aminosalicylic acid (5-ASA). *Applied Clay Science*, 50(1), 106–111.
- Alexis, F. (2005). Factors affecting the degradation and drug-release mechanism of poly(lactic acid) and poly[(lactic acid)-co-(glycolic acid)]. *Polymer International*, 54(1), 36–46.
- Ali, S. M., Khan, A. a, Ahmed, I., Musaddiq, M., Ahmed, K. S., Polasa, H., Rao, L. V., Habibullah, C. M., Sechi, L. a, Ahmed, N. (2005). Antimicrobial activities of Eugenol and Cinnamaldehyde against the human gastric pathogen *Helicobacter pylori*. *Annals of Clinical Microbiology and Antimicrobials*, 4, 20.
- Alqahtani, S., Simon, L., Astete, C. E., Alayoubi, A., Sylvester, P. W., Nazzal, S., Shen, Y., Xu, Z., Kaddoumi, A., Sabliov, C. M. (2015). Cellular uptake, antioxidant and antiproliferative activity of entrapped  $\alpha$ -tocopherol and  $\gamma$ -tocotrienol in poly (lactic-co-glycolic) acid (PLGA) and chitosan covered PLGA nanoparticles (PLGA-Chi). *Journal of Colloid and Interface Science*, 445, 243–251.
- Altioek, D. (2011). Preparation and evaluation of chitosan microspheres for eradication of *Helicobacter pylori*. İzmir Institute of Technology.
- Arteche Pujana, M., Pérez-Álvarez, L., Cesteros Iturbe, L. C., Katime, I. (2013). Biodegradable chitosan nanogels crosslinked with genipin. *Carbohydrate Polymers*, 94(2), 836–842.



- Augustin, M. a., Sanguansri, L. (2008). Encapsulation of bioactives. *Food Materials Science: Principles and Practice*, 577–601.
- Avena, M. J., Cabrol, R., Pauli, C. P. D. E. (1990). Study of Some Physicochemical Properties of Pillared Montmorillonites : Acid-Base Potentiometric Titrations a N D Electrophoretic Measurements, 38(4), 356–362.
- Averous, L. (2013). Handbook of Biopolymers and Biodegradable Plastics. In *Handbook of Biopolymers and Biodegradable Plastics* (pp. 171–188).
- Bakkali, F., Averbeck, S., Averbeck, D., Idaomar, M. (2008). Biological effects of essential oils - A review. *Food and Chemical Toxicology*, 46(2), 446–475.
- Babu, A. J., Sundari, A. R., Indumathi, J., Srujan, R. V. N., Sravanthi, M. (2011). Study on the antimicrobial activity and minimum inhibitory concentration of essential oils of spices. *Vet. World*, 4(7), 311–316.
- Bardonnet, P. L., Faivre, V., Pugh, W. J., Piffaretti, J. C., Falson, F. (2006). Gastroretentive dosage forms: Overview and special case of *Helicobacter pylori*. *Journal of Controlled Release*, 111(1-2), 1–18.
- Bassolé, I. H. N., Juliani, H. R. (2012). Essential oils in combination and their antimicrobial properties. *Molecules*, 17(4), 3989–4006.
- Baysal, K., Aroguz, A. Z., Adiguzel, Z., Baysal, B. M. (2013). Chitosan/alginate crosslinked hydrogels: Preparation, characterization and application for cell growth purposes. *International Journal of Biological Macromolecules*, 59, 342–348.
- Berger, J., Reist, M., Mayer, J. M., Felt, O., Peppas, N. a., Gurny, R. (2004). Structure and interactions in covalently and ionically crosslinked chitosan hydrogels for biomedical applications. *European Journal of Pharmaceutics and Biopharmaceutics*, 57(1), 19–34.
- Bergonzelli, G. E., Donnicola, D., Porta, N., Corthe, I. E. (2003). Essential Oils as Components of a Diet-Based Approach to Management of *Helicobacter* Infection. *Society*, 47(10), 3240–3246.
- Berthold, a., Cremer, K., Kreuter, J. (1996). Preparation and characterization of chitosan microspheres as drug carrier for prednisolone sodium phosphate as model for antiinflammatory drugs. *Journal of Controlled Release*, 39(1), 17–25.
- Bhattacharai, N., Gunn, J., Zhang, M. (2010). Chitosan-based hydrogels for controlled, localized drug delivery. *Advanced Drug Delivery Reviews*.
- Bilia, A. R., Guccione, C., Isacchi, B., Righeschi, C., Firenzuoli, F., Bergonzi, M. C. (2014). Essential oils loaded in nanosystems: A developing strategy for a successful therapeutic approach. *Evidence-Based Complementary and Alternative Medicine*, 2014.

- Chan, E. S. (2011). Preparation of Ca-alginate beads containing high oil content: Influence of process variables on encapsulation efficiency and bead properties. *Carbohydrate Polymers*, 84(4), 1267–1275.
- Chang, C. H., Huang, W. Y., Lai, C. H., Hsu, Y. M., Yao, Y. H., Chen, T. Y., Wu, J. Y., Peng, S. F., Lin, Y. H. (2011). Development of novel nanoparticles shelled with heparin for berberine delivery to treat *Helicobacter pylori*. *Acta Biomaterialia*, 7(2), 593–603.
- Chellat, F., Tabrizian, M., Dumitriu, S., Chornet, E., Rivard, C. H., Yahia, L. (2000). Study of biodegradation behavior of Chitosan-Xanthan microspheres in simulated physiological media. *Journal of Biomedical Materials Research*, 53(5), 592–599.
- Chevalier, E., Viana, M., Artaud, a, Haddouchi, S., Chulia, D. (2009). A novel application of the T-cell for flow-through dissolution: the case of bioceramics used as ibuprofen carrier. *Talanta*, 77(4), 1545–8.
- Chronopoulou, L., Massimi, M., Giardi, M. F., Cametti, C., Devirgiliis, L. C., Dentini, M., Palocci, C. (2013). Chitosan-coated PLGA nanoparticles: A sustained drug release strategy for cell cultures. *Colloids and Surfaces B: Biointerfaces*, 103, 310–317.
- Cojocariu, A., Profire, L., Aflori, M., Vasile, C. (2012). In vitro drug release from chitosan/Cloisite 15A hydrogels. *Applied Clay Science*, 57, 1–9.
- Cuppoletti, J. (2011). *Nanocomposites and Polymers with Analytical Methods*.
- D'Souza, S. S., DeLuca, P. P. (2006). Methods to assess in Vitro drug release from injectable polymeric particulate systems. *Pharmaceutical Research*, 23(3), 460–474.
- Datta, S. M. (2013). Clay-polymer nanocomposites as a novel drug carrier: Synthesis, characterization and controlled release study of Propranolol Hydrochloride. *Applied Clay Science*, 80-81, 85–92.
- de Francesco, V., Zullo, A., Ierardi, E., Giorgio, F., Perna, F., Hassan, C., Morini, S., Panella, C., Vaira, D. (2009). Phenotypic and genotypic *Helicobacter pylori* clarithromycin resistance and therapeutic outcome: Benefits and limits. *Journal of Antimicrobial Chemotherapy*, 65(2), 327–332.
- Depan, D., Kumar, A. P., Singh, R. P. (2009). Cell proliferation and controlled drug release studies of nanohybrids based on chitosan-g-lactic acid and montmorillonite. *Acta Biomaterialia*, 5(1), 93–100.
- Desai, K. G. H., Park, H. J. (2005). Preparation and characterization of drug-loaded chitosan-tripolyphosphate microspheres by spray drying. *Drug Development Research*, 64(2), 114–128.
- Desai, K. G., Liu, C., Park, H. J. (2006). Characteristics of vitamin C encapsulated tripolyphosphate-chitosan microspheres as affected by chitosan molecular weight. *Journal of Microencapsulation*, 23(1), 79–90.

- Desai, K. G., Park, H. J. (2006). Effect of manufacturing parameters on the characteristics of vitamin C encapsulated tripolyphosphate-chitosan microspheres prepared by spray-drying. *Journal of Microencapsulation*, 23(1), 91–103.
- Devrim, B., Canefe, K. (2006). Midede kalış süresini uzatan ilaç şekilleri. *Journal Faculty Pharmacology, Ankara*, 35(1), 69–94.
- Dhakar, R. C., Maurya, S. D., Sagar, B. P. S., Bhagat, S., Prajapati, S. K., Jain, C. P. (2010). Variables Influencing the Drug Entrapment Efficiency of Microspheres : A Pharmaceutical Review. *Der Pharmacia Lettre*, 2(5), 102–116.
- Donsì, F., Annunziata, M., Sessa, M., Ferrari, G. (2011). Nanoencapsulation of essential oils to enhance their antimicrobial activity in foods. *LWT - Food Science and Technology*, 44(9), 1908–1914.
- Escamilla-Garcia, M., Calderon-Dominguez, G., Chanona-Perez, J. J., Farrera-Rebollo, R. R., Andraca-Adame, J. A., Arzate-Vazquez, I., Mendez-Mendez, J. V., Moreno-Ruiz, L. A. (2013). Physical and structural characterisation of zein and chitosan edible films using nanotechnology tools. *International Journal of Biological Macromolecules*, 61, 196–203.
- Flávia Chiva Carvalho, Marcos Luciano Bruschi, Raul Cesar Evangelista, M. P. D. G. (2011). Mucoadhesive drug delivery systems, 3(1), 89–100.
- Forano, C. (2004). *Clay Surfaces - Fundamentals and Applications. Interface Science and Technology* (Vol. 1).
- Freiberg, S., Zhu, X. X. (2004). Polymer microspheres for controlled drug release. *International Journal of Pharmaceutics*, 282(1-2), 1–18.
- Fröhlich, E. (2012). The role of surface charge in cellular uptake and cytotoxicity of medical nanoparticles. *International Journal of Nanomedicine*, 7, 5577–91.
- Gautam, N., Mantha, A. K., Mittal, S. (2014). Essential oils and their constituents as anticancer agents: a mechanistic view. *BioMed Research International*, 2014, 154106.
- Geng, S., Cui, Z., Huang, X., Chen, Y., Xu, D., Xiong, P. (2011). Variations in essential oil yield and composition during *Cinnamomum cassia* bark growth. *Industrial Crops and Products*, 33(1), 248–252.
- Ha, J. U., Xanthos, M. (2011). Drug release characteristics from nanoclay hybrids and their dispersions in organic polymers. *International Journal of Pharmaceutics*, 414(1-2), 321–331.
- Harris, R., Lecumberri, E., Heras, A. (2010). Chitosan-genipin microspheres for the controlled release of drugs: Clarithromycin, tramadol and heparin. *Marine Drugs*, 8(6), 1750–1762.

- He, P. E. Al. (1998). In vitro evaluation of the mucoadhesive properties of chitosan microspheres. *International Journal of Pharmaceutics*, 166(1), 75–88.
- He, P., Davis, S. S., Illum, L. (1999). Chitosan microspheres prepared by spray drying. *International Journal of Pharmaceutics*, 187(1), 53–65.
- Hejazi, R., Amiji, M. (2003b). Chitosan-based gastrointestinal delivery systems. *Journal of Controlled Release*, 89(2), 151–165.
- Hejazi, R., Amiji, M. (2004). Stomach-specific anti-H. pylori therapy. Part III: Effect of chitosan microspheres crosslinking on the gastric residence and local tetracycline concentrations in fasted gerbils. *International Journal of Pharmaceutics*, 272(1-2), 99–108.
- Honary, S., Zahir, F. (2013). Effect of Zeta Potential on the Properties of Nano-Drug Delivery Systems - A Review (Part 2). *Tropical Journal of Pharmaceutical Research*, 12(2), 265–273.
- Hooda, A., Nanda, A., Jain, M., Kumar, V., Rathee, P. (2012). Optimization and evaluation of gastroretentive ranitidine HCl microspheres by using design expert software. *International Journal of Biological Macromolecules*, 51(5), 691–700.
- Hosseini, S. F., Zandi, M., Rezaei, M., Farahmandghavi, F. (2013). Two-step method for encapsulation of oregano essential oil in chitosan nanoparticles: Preparation, characterization and in vitro release study. *Carbohydrate Polymers*, 95(1), 50–56.
- Hua, S., Yang, H., Wang, A. (2010). A pH-sensitive nanocomposite microsphere based on chitosan and montmorillonite with in vitro reduction of the burst release effect. *Drug Development and Industrial Pharmacy*, 36(9), 1106–1114.
- Hua, S., Yang, H., Wang, W., Wang, A. (2010). Controlled release of ofloxacin from chitosan-montmorillonite hydrogel. *Applied Clay Science*, 50(1), 112–117.
- Jentzsch P. V., C. V. (2014). Raman spectroscopy as an analytical tool for analysis of vegetable and essential oils. *Flavour and Fragrance Journal*, 39(5), 636–645.
- Jin, M., Zhong, Q. (2012). Structure modification of montmorillonite nanoclay by surface coating with soy protein. *Journal of Agricultural and Food Chemistry*, 60(48), 11965–11971.
- Jin, Q., Schexnailder, P., Gaharwar, A. K., Schmidt, G. (2009). Silicate cross-linked bio-nanocomposite hydrogels from PEO and chitosan. *Macromolecular Bioscience*, 9(10), 1028–1038.
- Karczewska, E., Wojtas-Bonior, I., Sito, E., Zwolińska-Wcisło, M., Budak, A. (2011). Primary and secondary clarithromycin, metronidazole, amoxicillin and levofloxacin resistance to *Helicobacter pylori* in southern Poland. *Pharmacological Reports*, 63(3), 799–807.

- Ke, Y. C., Stroeve, P. (2005). *Polymer-Layered Silicate and Silica Nanocomposites*.
- Kevadiya, B. D., Bajaj, H. C. (2013). The Layered Silicate, Montmorillonite (MMT) as a Drug Delivery Carrier. *Key Engineering Materials*, 571, 111–132.
- Kharia, A. A., Singhai, A. K. (2013). Controlled Release Drug Delivery System with Stomach Specific Mucoadhesive Nanoparticles. *Indian Journal of Nanoscience*, 1(February), 36–52.
- Khunawattanakul, W., Puttipipatkachorn, S., Rades, T., Pongjanyakul, T. (2008). Chitosan-magnesium aluminum silicate composite dispersions: Characterization of rheology, flocculate size and zeta potential. *International Journal of Pharmaceutics*, 351(1-2), 227–235.
- Klose, D., Siepmann, F., Elkharraz, K., Krenzlin, S., Siepmann, J. (2006). How porosity and size affect the drug release mechanisms from PLGA-based microparticles. *International Journal of Pharmaceutics*, 314(2), 198–206.
- Ko, J. a., Park, H. J., Hwang, S. J., Park, J. B., Lee, J. S. (2002). Preparation and characterization of chitosan microparticles intended for controlled drug delivery. *International Journal of Pharmaceutics*, 249(1-2), 165–174.
- Kulkarni, S. a., Feng, S.-S. (2013). Effects of Particle Size and Surface Modification on Cellular Uptake and Biodistribution of Polymeric Nanoparticles for Drug Delivery. *Pharmaceutical Research*, 30(10), 2512–2522.
- Kumirska, J., Weinhold, M. X., Thöming, J., Stepnowski, P. (2011). Biomedical activity of chitin/chitosan based materials- influence of physicochemical properties apart from molecular weight and degree of N-Acetylation. *Polymers*, 3(4), 1875–1901.
- Lai, S. K., Wang, Y. Y., Hanes, J. (2009). Mucus-penetrating nanoparticles for drug and gene delivery to mucosal tissues. *Advanced Drug Delivery Reviews*, 61(2), 158–171.
- Lambert, R. J. W., Skandamis, P. N., Coote, P. J., Nychas, G. J. (2001). A study of the minimum inhibitory concentration and mode of action of oregano essential oil, thymol and carvacrol. *Journal of applied microbiology*, 91(3), 453-462.
- Lin, Y. H., Tsai, S. C., Lai, C. H., Lee, C. H., He, Z. S., Tseng, G. C. (2013). Genipin-cross-linked fucose-chitosan/heparin nanoparticles for the eradication of *Helicobacter pylori*. *Biomaterials*, 34(18), 4466–4479.
- Liu, K. H., Liu, T. Y., Chen, S. Y., Liu, D. M. (2008). Drug release behavior of chitosan-montmorillonite nanocomposite hydrogels following electrostimulation. *Acta Biomaterialia*, 4(4), 1038–1045.
- Lu, F., Ding, Y. C., Ye, X. Q., Ding, Y. T. (2011). Antibacterial effect of cinnamon oil combined with thyme or clove oil. *Agricultural Sciences in China*, 10(9), 1482–1487.

- Luo, Y., Teng, Z., Li, Y., Wang, Q. (2015). Solid lipid nanoparticles for oral drug delivery: Chitosan coating improves stability, controlled delivery, mucoadhesion and cellular uptake. *Carbohydrate Polymers*, 122, 221–229.
- Magdalena Gierszewska-Drużyńska, J. O.-C. (2012). Mechanism of water diffusion into noncrosslinked and ionically crosslinked chitosan membranes. *Prog. Chem. Appl. Chitin Deriv.*, XVII(17), 59–66.
- Malfertheiner, P., Megraud, F., O'Morain, C. a., Atherton, J., Axon, a. T., Bazzoli, F., Gensini, G. F., Gisbert, J. P., Graham, D. Y., Rokkas, T., El-Omar, E. M., Kuipers, E. J., Group., E. H. S. (2012). Management of Helicobacter pylori infection-the Maastricht IV/Florence Consensus Report.
- Maniruzzaman, M., Douroumis, D., Boateng, J. S., Snowden, M. J., Russo, P., Santoro, A., Prota, L., Stigliani, M., Aquino, R. P., Momoh, M. a, Builders, P. F., Bucak, S., Yavuztürk, B., Sezer, A. D., Escobar-chávez, J., Rodríguez-cruz, I. M., Domínguez-delgado, C. L., Torres, R. D.-, Revilla-vázquez, A. L., Aléncaster, N. C., Blanco, M. D., Teijón, C., Olmo, R. M., Teijón, J. M., Elsayed, A. M., Anand, U., Feridooni, T. (2012). *RECENT ADVANCES IN NOVEL DRUG CARRIER SYSTEMS Edited by Ali Demir Sezer.*
- Maryan, A. S., Montazer, M., Rashidi, A., Rahimi, M. K. (2013). Antibacterial properties of clay layers silicate: A special study of montmorillonite on cotton fiber. *Asian Journal of Chemistry*, 25(5), 2889–2892.
- McClements, D. J., Decker, E. A., Park, Y., Weiss, J. (2009). *Structural design principles for delivery of bioactive components in nutraceuticals and functional foods. Critical reviews in food science and nutrition* (Vol. 49).
- Mi, F., Wong, T., Shyu, S., Chang, S. (1998). Chitosan Microspheres : Modification of Polymeric Chem- Physical Properties of Spray-Dried Microspheres. *Journal of Applied Polymer Science*, 71, 747–759.
- Miguel, M. G. (2010). Antioxidant and anti-inflammatory activities of essential oils: A short review. *Molecules*, 15(12), 9252–9287.
- Muhammad, J. S., Zaidi, S. F., Shaharyar, S., Refaat, A., Usmanghani, K., Saiki, I., Sugiyama, T. (2015). Anti-inflammatory effect of cinnamaldehyde in Helicobacter pylori induced gastric inflammation. *Biological and Pharmaceutical Bulletin*, 38(1), 109–115.
- Muzzarelli, R. a a. (2009). Genipin-crosslinked chitosan hydrogels as biomedical and pharmaceutical aids. *Carbohydrate Polymers*, 77(1), 1–9.
- Mythri, G., Kavitha, K., Rupesh, K., Jagadeesh, S. (2011). Novel mucoadhesive polymers—a review. *J. Appl. Pharm. Sci*, 01(08), 37–42.
- Negi, H., Agarwal, T., Zaidi, M. G. H., Kapri, A., Goel, R. (2011). Antimicrobial organophilic montmorillonite nanoparticles: Screening and detection assay.

*Biotechnology Journal*, 6(1), 107–112.

- Nunthanid, J., Laungтана-Anan, M., Sriamornsak, P., Limmatvapirat, S., Puttipipatkachorn, S., Lim, L. Y., Khor, E. (2004). Characterization of chitosan acetate as a binder for sustained release tablets. *Journal of Controlled Release*, 99(1), 15–26.
- Oguzlu, H., Tihminlioglu, F. (2010). Preparation and barrier properties of chitosan-layered silicate nanocomposite films. *Macromolecular Symposia*, 298(1), 91–98.
- Ohno, T., Kita, M., Yamaoka, Y., Imamura, S., Yamamoto, T., Mitsufuji, S., Kodama, T., Kashima, K., Imanishi, J. (2003). Antimicrobial activity of essential oils against *Helicobacter pylori*. *Helicobacter*, 8(3), 207–215.
- Oleastro, M., Me, A., Santos, A., Monteiro, L., Barthe, P., Bordeaux, V. S. (2003). Real-Time PCR Assay for Rapid and Accurate Detection of Point Mutations Conferring Resistance to Clarithromycin in *Helicobacter pylori*. *Journal of Clinical Microbiology*, 41(1), 397–402.
- Ooi, L. S. M., Li, Y., Kam, S.-L., Wang, H., Wong, E. Y. L., Ooi, V. E. C. (2006). Antimicrobial activities of cinnamon oil and cinnamaldehyde from the Chinese medicinal herb *Cinnamomum cassia* Blume. *The American Journal of Chinese Medicine*, 34(3), 511–522.
- Paluszkiwicz, C., Stodolak, E., Hasik, M., Blazewicz, M. (2011). FT-IR study of montmorillonite-chitosan nanocomposite materials. *Spectrochimica Acta - Part A: Molecular and Biomolecular Spectroscopy*, 79(4), 784–788.
- Pandey, S., Mishra, S. B. (2011). Organic-inorganic hybrid of chitosan/organoclay bionanocomposites for hexavalent chromium uptake. *Journal of Colloid and Interface Science*, 361(2), 509–520.
- Panee, C., Wacharee, L., Chandhane, I. (2014). Antiinflammatory effects of essential oil from the leaves of *Cinnamomum cassia* and cinnamaldehyde on lipopolysaccharide-stimulated J774A.1 cells. *Journal of Advanced Pharmaceutical Technology & Research*, 5(4), 164.
- Paños, I., Acosta, N., Heras, A. (2008). New drug delivery systems based on chitosan. *Current Drug Discovery Technologies*, 5(4), 333–341.
- Patel, J. K., Patel, M. M. (2007). Stomach specific anti-helicobacter pylori therapy: preparation and evaluation of amoxicillin-loaded chitosan mucoadhesive microspheres. *Current Drug Delivery*, 4(1), 41–50.
- Patel, R. P., Baria, a. H., Pandya, N. B. (2009). Stomach-specific drug delivery of famotidine using floating alginate beads. *International Journal of PharmTech Research*, 1(2), 288–291.
- Patil, S., Babbar, A., Mathur, R., Mishra, A., Sawant, K. (2010). Mucoadhesive chitosan microspheres of carvedilol for nasal administration. *Journal of Drug Targeting*,

18(4), 321–331.

- Paul, D. R., Robeson, L. M. (2008). Polymer nanotechnology: Nanocomposites. *Polymer*, 49(15), 3187–3204.
- Pedro, a S., Santo, I. E., Silva, C. V, Detoni, C., Albuquerque, E. (2013). The use of nanotechnology as an approach for essential oil-based formulations with antimicrobial activity, 1364–1374.
- Pongjanyakul, T., Suksri, H. (2009). Alginate-magnesium aluminum silicate films for buccal delivery of nicotine. *Colloids and Surfaces B: Biointerfaces*, 74(1), 103–113.
- Prabuseenivasan, S., Jayakumar, M., Ignacimuthu, S. (2006). In vitro antibacterial activity of some plant essential oils. *BMC Complementary and Alternative Medicine*, 6, 39.
- Qi, L.-F., Xu, Z.-R., Li, Y., Jiang, X., Han, X.-Y. (2005). In vitro effects of chitosan nanoparticles on proliferation of human gastric carcinoma cell line MGC803 cells. *World Journal of Gastroenterology : WJG*, 11(33), 5136–5141.
- Ramteke, S., Ganesh, N., Bhattacharya, S., Jain, N. K. (2009). Amoxicillin, clarithromycin, and omeprazole based targeted nanoparticles for the treatment of H. pylori. *Journal of Drug Targeting*, 17(3), 225–234.
- Raval, a., Parikh, J., Engineer, C. (2010). Mechanism of controlled release kinetics from medical devices. *Brazilian Journal of Chemical Engineering*, 27(2), 211–225.
- Raval, J. a, Patel, J. K., Patel, M. M. (2010). Formulation and in vitro characterization of spray dried microspheres of amoxicillin. *Acta Pharmaceutica (Zagreb, Croatia)*, 60(4), 455–465.
- Rinaudo, M. (2006). Chitin and chitosan: Properties and applications. *Prog. Polym. Sci.*, 31(7), 603–632.
- Rokstad, A. M. a, Lacík, I., de Vos, P., Strand, B. L. (2014). Advances in biocompatibility and physico-chemical characterization of microspheres for cell encapsulation. *Advanced Drug Delivery Reviews*, 67-68, 111–130.
- Sahasathian, T., Praphairaksit, N., Muangsin, N. (2010). Mucoadhesive and floating chitosan-coated alginate beads for the controlled gastric release of amoxicillin. *Archives of Pharmacal Research*, 33(6), 889–899.
- Sahil, K., Akanksha, M., Premjeet, S., Bilandi, A., Kapoor, B. (2011). Microsphere : a Review. *INTERNATIONAL JOURNAL OF RESEARCH IN PHARMACY AND CHEMISTRY Available*, 1(4), 1184–1198.
- Salcedo, I., Aguzzi, C., Sandri, G., Bonferoni, M. C., Mori, M., Cerezo, P., Sánchez, R., Viseras, C., Caramella, C. (2012). In vitro biocompatibility and mucoadhesion of montmorillonite chitosan nanocomposite: A new drug delivery. *Applied Clay*



*Science*, 55, 131–137.

- Samie, A., Tanih, N. F., Ndip, R. N. (2014). Helicobacter pylori Infection — Challenges of Antimicrobial Chemotherapy and Emergence of Alternative Treatments. In *Trends in Helicobacter pylori Infection* (pp. 243–277).
- Sarmah, M., Banik, N., Hussain, A., Ramteke, A., Sharma, H. K., Maji, T. K. (2015). Study on crosslinked gelatin–montmorillonite nanoparticles for controlled drug delivery applications. *Journal of Materials Science*, 50(22), 7303–7313.
- Sarmiento, B., Pedro, A. S., Ferreira, D. (2008). Chitosan particles as new essential oil carrier for antimicrobial application, 4–7.
- Selomulya, C., Liu, W., Wu, W. D., Chen, X. D. (2011). Uniform chitosan microparticles prepared by a novel spray-drying technique. *International Journal of Chemical Engineering*, 2011.
- Shaaban, H. a. E., El-Ghorab, A. H., Shibamoto, T. (2012). Bioactivity of essential oils and their volatile aroma components: Review. *Journal of Essential Oil Research*, 24(2), 203–212.
- Shah, S., Qaqish, R., Patel, V., Amiji, M. (1999). Evaluation of the factors influencing stomach-specific delivery of antibacterial agents for Helicobacter pylori infection. *The Journal of Pharmacy and Pharmacology*, 51(6), 667–672.
- Shweta, A., Sonia, P. (2013). Pharmaceutical relevance of crosslinked chitosan in microparticulate drug delivery. *International Research Journal of Pharmacy*, 4(2), 45–51.
- Siepmann, J., Faisant, N., Akiki, J., Richard, J., Benoit, J. P. (2004). Effect of the size of biodegradable microparticles on drug release: Experiment and theory. *Journal of Controlled Release*, 96(1), 123–134.
- Siewert, M., Dressman, J., Brown, C. K., Shah, V. P. (2003). FIP/AAPS guidelines for dissolution/in vitro release testing of novel/special dosage forms. *Pharmazeutische Industrie*, 65(2), 129–134.
- Singhvi, G., Singh, M. (2011). Review: in vitro drug release characterization models. *Int J Pharm Stud Res*, II(I), 77–84.
- Sinha, V. R., Singla, a. K., Wadhawan, S., Kaushik, R., Kumria, R., Bansal, K., Dhawan, S. (2004). Chitosan microspheres as a potential carrier for drugs. *International Journal of Pharmaceutics*, 274(1-2), 1–33.
- Stumm, W. (1992). *Chemistry of the Interface Processes at the Mineral-Water*. New York.
- Suresh, R., Borkar, S. N., Sawant, V. a, Shende, V. S., Dimble, S. K. (2010). Nanoclay Drug Delivery System. *International Journal of Pharmaceutical Sciences and Nanotechnology*, 3(2), 901–905.

- Theng, B. K. G. (1970). Interactions of clay minerals with organic polymers. Some practical applications. *Clays and Clay Minerals*, 18, 257–362.
- Tombácz, E., Szekeres, M. (2006). Surface charge heterogeneity of kaolinite in aqueous suspension in comparison with montmorillonite. *Applied Clay Science*, 34(1-4), 105–124.
- Touitou, E., Barry, B. W. (2007). *Enhancement in Drug Delivery*.
- Uddin, F. (2008). Clays, nanoclays, and montmorillonite minerals. *Metallurgical and Materials Transactions A: Physical Metallurgy and Materials Science*, 39(12), 2804–2814.
- Unlu, M., Ergene, E., Unlu, G. V., Zeytinoglu, H. S., Vural, N. (2010). Composition, antimicrobial activity and in vitro cytotoxicity of essential oil from *Cinnamomum zeylanicum* Blume (Lauraceae). *Food and Chemical Toxicology*, 48(11), 3274–3280.
- Utracki, L. a. (2004). *Clay-Containing Polymeric Nanocomposites Volume 1* (Vol. 1).
- Waché, R., Klopffer, M.-H., Gonzalez, S. (2015). Characterization of Polymer Layered Silicate Nanocomposites by Rheology and Permeability Methods: Impact of the Interface Quality. *Oil & Gas Science and Technology – Revue d'IFP Energies Nouvelles*, 70(2), 267–277.
- Wang, A. N., Wu, L. G., Jia, L. L., Li, X. L., Sun, Y. D. (2010). Alginate-Chitosan Microspheres for Controlled Release of Tea Polyphenol. *Advanced Materials Research*, 152-153, 1726–1729.
- Wang, S. F., Shen, L., Tong, Y. J., Chen, L., Phang, I. Y., Lim, P. Q., Liu, T. X. (2005). Biopolymer chitosan/montmorillonite nanocomposites: Preparation and characterization. *Polymer Degradation and Stability*, 90(1), 123–131.
- Wang, X., Du, Y., Luo, J. (2008). Biopolymer/montmorillonite nanocomposite: preparation, drug-controlled release property and cytotoxicity. *Nanotechnology*, 19(6), 065707.
- Xia, Y., Pack, D. W. (2014). Uniform biodegradable microparticle systems for controlled release. *Chemical Engineering Science*, 125, 129–143.
- Yao Fu, W. J. K. (2010). Drug Release Kinetics and Transport Mechanisms of Nondegradable and Degradable Polymeric Delivery Systems. *Expert Opin Drug Deliv.*
- Yeo, Y., Park, K. (2004). Control of encapsulation efficiency and initial burst in polymeric microparticle systems. *Archives of Pharmacal Research*, 27(1), 1–12.
- Yilmaz, L. (1984). Anomalous Diffusion of Liquids in Glassy Polymers. *Mathematical Modelling*, 4, 535–543.

- Yuan, Q., Shah, J., Hein, S., Misra, R. D. K. (2010). Controlled and extended drug release behavior of chitosan-based nanoparticle carrier. *Acta Biomaterialia*, 6(3), 1140–1148.
- Yuan, Y., Chesnutt, B. M., Utturkar, G., Haggard, W. O., Yang, Y., Ong, J. L., Bumgardner, J. D. (2007). The effect of cross-linking of chitosan microspheres with genipin on protein release. *Carbohydrate Polymers*, 68(3), 561–567.
- Yu-shan, X. I. E., Shao-zao, T. A. N., Ma-hua, L., Ren-fu, L. I. U. (2009). Structure and Antibacterial Activity of Modified Montmorillonite, 26(4), 509–513.
- Zhang, J., Xia, W., Liu, P., Cheng, Q., Tahi, T., Gu, W., Li, B. (2010). Chitosan Modification and Pharmaceutical/Biomedical Applications. *Marine Drugs*, 8(7), 1962–1987.
- Zhang, Y., Yu, Y. F., Shi, X. X., Zhao, S. C., Chen, A. B., Huang, D. W., Niu, D. J., Qin, Z. (2013). Study on the preparation of genipin crosslinked chitosan microspheres of resveratrol and in vitro release. *Journal of Polymer Research*, 20(7).
- Zhou, J., Cui, Y. L., Qi, Y. (2014). A Preliminary Study of Crosslinked Alginate-Chitosan Microspheres for Delivery System. *Advanced Materials Research*, 887-888, 520–523.

## CURRICULUM VITAE

### GENERAL INFORMATION

Suna Seda GÜNEŞ

Telephone: +90 5324968043

E-mail: [ssedagunes@gmail.com](mailto:ssedagunes@gmail.com)

### EDUCATION:

**PhD** in Bioengineering 2009-2016  
Izmir Institute of Technology, Izmir, Turkey

**MSc** in Bioengineering 2006-2009  
Ege University, Izmir, Turkey

**B.S.** in Bioengineering 2002-2006  
Ege University, İzmir, Turkey



### Research experience:

**PhD.** Development of Novel Chitosan Nanocomposites as a Controlled Drug Release System for *Helicobacter pylori* Treatment, Supervisor, Prof. Dr. Funda TIHMINLIOĞLU, Izmir Institute of Technology, Izmir, Turkey

**M.Sci.** Development of Skin Cream Including *Spirulina platensis* Extracts and Investigation of Effects on *In Vitro* Cell Culture (SAN-TEZ Project), Supervisor: Prof. Dr. Meltem CONK DALAY, Ege University, Izmir, Turkey

### Experiences:

2013-2015: Research Assistant, Izmir Institute of Technology, Izmir, Turkey

2012-2013: R&D Project Specialist, Zentiva Health Product, Turkey

### Publications:

- S Gunes, S Tamburacı, F Tihminlioglu. Zein Based Bilayer Composites for Wound Healing, Regenerative Medicine, 2015, 10(7), S96-S296.
- Gunes S, Tamburacı S, Imamoglu E, Conk Dalay M. Determination of Superoxide Dismutase Activities in Different Cyanobacteria for Scavenging of Reactive Oxygen Species, TBAP 5(1): 25-32.
- Gunes, S., Becerikli, T., Tihminlioglu, F., Yilmaz O. Investigation Of Antimicrobial Activity To Determine Mic Value Of Cinnamon Bark Oil Against Helicobacter Pylori, HELICOBACTER Volume: 19 Special Issue: SI Supplement: 1 Pages: 153-153 Meeting Abstract: P13.28. Published: SEP 2014

### Presentations:

- 21-23 October.2015- World Conference on Regenerative Medicine Congress 2015, “Zein Based Bilayer Composites for Wound Healing”
- 8-11 July.2015- 11th Frontiers in Biomedical Polymers Symposium, “Chitosan Based Bioactive Films for Wound Healing Applications”
- 12-14 March.2015- International Biomedical Engineering Congress 2015, “Development of Spirulina Extract Incorporated Skin Creams and Its Effect on In Vitro Cell Cultures”
- 14-17 October.2014- 7th International Conference and Exhibition on Nutraceuticals and Functional Foods, “Development of a novel chitosan nanocomposites as food supplement for gastrointestinal system”
- 17-19 April.2014- 2nd International Bahçeşehir University (BAU) Drug Design Congress, “Development of a Novel Controlled Drug Delivery System: Chitosan Nanocomposite Microspheres”
- 12-15 November.2013- 19th International Biomedical Science and Technology Symposium (BIOMED2013), “Chitosan Nanocomposite Microspheres as a Controlled Drug Delivery System”
- 16-19 September.2013- Advanced Materials World Congress, “Preparation and Characterization of Essential Oil Loaded Chitosan Nanoclay Microspheres”
- 17-19 Kasım.2011- I. Ulusal Ege Kompozit Malzemeler Sempozyumu, “Esnek PVC Kabak Lifi Kompozitlerinin Hazırlanması ve Karakterizasyonu”
- 16-19 June.2010- V.International Bioengineering Congress, “Determination and Comparison of Cytotoxic Effects of Spirulina platensis and Pseudanabaena sp. on Animal Cell Cultures”
- 15-18 October.2008- IVth National Congress of Bioengineering, “Studies on Microalgae For Cosmetic Application”
- 4-7 May.2008- 14th Biomedical Science and Technology Symposium, “In vitro Animal Cell Culture Tests For Determination of The Cytotoxic and Genotoxic Effects of Microalgal Products”